LC - ^{13}C NMR

UTILIZING DYNAMIC NUCLEAR POLARIZATION (DNP)

FOR SIGNAL ENHANCEMENT

by

Steven Alan Stevenson

Thesis submitted to the Faculty of the
Virginia Polytechnic Institute and State University
in partial fulfillment of the requirements
for the degree of

MASTER OF SCIENCE
in
Analytical Chemistry

APPROVED:

Harry C. Dorn

H.C. Dorn, Chairman

M.R. Anderson

L.T. Taylor

c.2

LC - ^{13}C NMR
UTILIZING DYNAMIC NUCLEAR POLARIZATION (DNP) FOR SIGNAL ENHANCEMENT

by

Steven Alan Stevenson

Committee Chairman: H.C. Dorn

Chemistry

(ABSTRACT)

The primary difficulty for successful LC -^{13}C NMR (whether ^{1}H or ^{13}C) is overcoming the relatively low sensitivity of NMR as a chromatographic detector. For the ^{1}H nuclide this is much less of a problem; the sensitivity is approximately 6000 times more sensitive than that of ^{13}C nuclei. For this reason, much of the literature focuses on LC -^{1}H NMR. To ever successfully realize LC -^{13}C NMR, it is mandatory that an augmentation of ^{13}C signal intensity must be effectuated to overcome this sensitivity deficit (~ three orders of magnitude). To satisfy this requirement, our laboratory has utilized dynamic nuclear polarization (DNP) to ameliorate these otherwise weak or non-existent signals. For favorable molecules, sensitivity recoveries of up to two orders of magnitude have been developed. This improvement (relative to ^{1}H) narrows the sensitivity gap between ^{1}H and ^{13}C NMR detection of chromatographically separated analytes. Despite the fact that relatively large injection volumes were required in most LC experiments, the wealth of structural information inherent to ^{13}C NMR justifies any attempt to successfully couple nuclear magnetic resonance to liquid chromatography.

In addition, DNP was utilized in a series of SLIT and LLIT experiments where a test mixture was recycled through a NMR spectrometer. Results indicate that ^{13}C spectra were obtained with a significantly higher signal-to-noise ratio in a shorter amount of analysis time relative to experiments where DNP was not employed for signal enhancement.

THIS THESIS IS DEDICATED

TO THE MEMORY OF

GEORGE NATTRASS

ACKNOWLEDGEMENTS

At this time, I would like to express my gratitude toward several individuals without whom would have made the production of this thesis more difficult. First, I extend my thanks to my research advisor, Dr. Harry C. Dorn, for his continual support and never-ending committment toward my progress in Analytical Chemistry despite the inundation of trials and tribulations which we have both undergone here at Virginia Tech.

From Analytical Services, I thank Mr. Bill Bebout for his time and expertise on NMR spectrometry and its instrumental aspect. In addition, Mr. Tom Glass was also helpful from a NMR standpoint. From previous graduate students who worked for Dr. Dorn, acknowledgement is given to Rossi Gitti for her synthesis of the SPIN samples. Also, Juan Gu provided her insight on the use of our flow NMR instrumentation and on the variables which must be considered in successfully performing both SLIT and LLIT DNP experiments. Acknowledgement is also given to the Glass Shop for construction of the NMR flow cell, and financial assistance from Eastman Kodak was also appreciated.

TABLE OF CONTENTS

LIST OF FIGURES

LIST OF TABLES

CHAPTER 1: INTRODUCTION

1.1 Sensitivity.

The primary difficulty for successfully implementing LC-NMR (^{1}H or ^{13}C) is overcoming the relatively low sensitivity of NMR as a chromatographic detector. For the ^{1}H nuclide this is much less of a problem; but the sensitivity of ^{13}C is orders of magnitude lower than the ^{1}H nuclide. One reason for the lower sensitivity of ^{13}C NMR is the low natural abundance (1.13 %) for non-labelled carbon samples. Furthermore, the magnetogyric ratio (γ) of ^{1}H is $\approx$ 4 times that of ^{13}C. Since the signal intensity in NMR is proportional to γ^3, it can be calculated that ^{13}C NMR is $\approx$ 6,000 times less sensitive than ^{1}H based on these two arguments. For this reason, most of the literature has focused on LC -^{1}H NMR. To ever realize LC -^{13}C NMR on a successful basis, it is mandatory that an augmentation of ^{13}C signal intensity **must be effectuated** to regain this sensitivity deficit of three to four orders of magnitude. In our laboratory, dynamic nuclear polarization (DNP) is utilized to ameliorate the otherwise weak or non-existent

^{13}C NMR signals. In reality, a recovery of up to two orders of magnitude has been attained. This improvement relative to the ^{1}H nuclide **narrows** the sensitivity gap between ^{1}H and ^{13}C NMR detection of chromatographically separated analytes.

1.2 Research Objectives.

Based on the preliminary discussion, it appears that at least prep-scale LC -^{13}C NMR would now be feasible, and this is one of the objectives of this thesis. Research objectives include the following:

1. Demonstrate that the sensitivity gap between ^{13}C and ^{1}H NMR can been reduced to the extent that LC -^{13}C NMR (DNP) on a prep-scale basis is now possible - at least for favorable classes of compounds.

2. Demonstrate that ^{13}C NMR structural information can be obtained from a chromatographically separated mixture.

3. To utilize DNP for signal enhancement in ^{13}C NMR recycle experiments with the intent of reducing analysis time via improvements in sensitivity.

CHAPTER 2: BACKGROUND

2.1 General Remarks.

The interest in NMR monitoring of a flowing system has been piqued since Suryan's discovery[1] in 1951 that the intensity of a NMR signal was enhanced when compared to the signal of a stationary sample. Suryan detected a ^{1}H enhancement of a factor of five. In 1969, Forsen and Rupprecht[2] also investigated the relationship between flow rate and signal intensity and demonstrated that there was an increase in ^{13}C NMR signals for a flowing sample relative to a stationary one. Since then, nuclear magnetic resonance has been utilized to probe into flow dynamics,[3-6] to measure flow rates,[7-9] to modify relaxation rates (T_1,T_2),[10-12] to monitor intermediates of kinetic reactions,[13-16] and to investigate the **in vivo** metabolism of chemicals in blood.[17]

2.2 Feasibility.

2.2.1 LC - ^{1}H NMR

The foundation and mathematics of flow NMR described by previous scientists **coupled with** improvements in NMR design

and instrumentation **combined with** the advent of Fourier transform (FT) NMR, chemists realized the potential significance of merging the separation power of liquid chromatography with the wealth of structural information inherent in nuclear magnetic resonance (NMR) detection.

In 1978, Watanabe[18] provided the scientific community with the first report describing the direct coupling of LC - ^{1}H NMR. Chromatography and detection were accomplished on-line with a ferromagnet NMR system operating at 60 MHz, and UV detection was employed to trigger stopped-flow acquisition. This enabled sensitivity increases via time-averaging but required longer analysis times.

In 1979, Bayer et al[19] successfully accomplished for the first time LC - ^{1}H NMR on-line (90 MHz) with detection in the continuous-flow mode, which permitted a large reduction in analysis time since measurements were taken with a continuously flowing liquid.

LC - ^{1}H NMR experiments in the early 1980's were characterized by sensitivity increases arising from the following:

1. The transition from electromagnets to the higher field strengths of superconducting magnets since signal intensity in NMR is

directly proportional to $(B)^{7/4}$, where B is the magnetic field strength.

2. Sensitivity improvements arising from flow cell design.

3. Reduction of dead volume between the chromatographic column and the NMR flow cell.

4. Placement of the chromatographic column directly inside the bore of a superconducting magnet. This strategic column placement yielded sensitivity increases due to a full build-up of the Boltzmann distribution before sampling the magnetization with a r.f. pulse in the flow cell. Since full magnetization of ^1H spins occurred while analytes were still inside the column, a reduction of dead volume from the column to the detector (reduced to a few microliters) was successfully accomplished since the necessity of maintaining a large, dead-volume, premagnetization region was obviated.

By the mid-1980's, LC - ^{1}H NMR had been extended to both normal- and reverse-phase chromatographic separations with detection limits reduced to 50-100 μg injections for analytes in the molecular weight region of 100 - 300 Daltons. In terms of resolution, spectral linewidths for ^{1}H signals in the continous-flow mode were decreased to less than 1.0 Hz for favorable situations. From 1980 to 1985, researchers - including those of Dorn et al,[20-25] Bayer & Albert,[26-27]and Buddrus et al[28-29] - contributed to the development of LC - ^{1}H NMR as a potential analytical tool.

From 1985 to present,[30-32] further reductions in dead volume as well as improvements in design and instrumentation have reduced minimum detectable quantities to yet lower limits. However, future reductions in minimum detectable quantities (MDQ's) are constrained by sensitivity limitations inherent to NMR.

2.2.2 LC - ^{13}C NMR.

In contrast, the development of continuous-flow, on-line, LC - ^{13}C NMR has not yet been successfully established. The primary hindrance to on-line LC - ^{13}C NMR as a viable technique is the extremely low sensitivity of ^{13}C nuclei. Unfortunately, the abundant isotope of carbon,

^{12}C, is not magnetically active. Only the less abundant ^{13}C (1.1% of ^{12}C) is responsive in a magnetic field. Thus, the probability of finding a ^{13}C in the molecular skeleton is significantly reduced when compared to hydrogen - where virtually all nuclei are magnetically active. Already hampered with a factor of ≈ 100 reduction in signal intensity arising from these natural abundance considerations, the sensitivity of ^{13}C NMR is further reduced. The intensity of a NMR signal is directly proportional to a nuclei's magnetic moment, which in turn is proportional to the magnetogyric ratio, gamma (γ). Since signal intensity is proportional to γ^3 ($\gamma_H/\gamma_C \approx 4$), the sensitivity of ^{13}C NMR is further decreased by an additional factor of ≈ 64 relative to ^{1}H NMR.

In summary, ^{13}C nuclear magnetic resonance experiments are approximately 6,000 times less sensitive than ^{1}H NMR (for natural abundance samples). This immense reduction in sensitivity must be overcome (at least in part) before on-line LC - ^{13}C NMR can be successfully achieved.

The mere suggestion of LC - ^{13}C NMR immediately implies that several potential difficulties must be overcome. First, an increase in sample injection volumes would be required to overcome sensitivity limitations as previously discussed. Second, the large volume of sample injections would mandate a transition from an analytical-scale

chromatographic column to at least a semi-preparatory column which would be more amenable to overloading.

2.3 Advantages.

The advantages of successfully performing continuous-flow, on-line LC - ^{13}C NMR are self-evident. A merger of the liquid chromatography portion to the wealth of structural information intrinsic in ^{13}C nuclear magnetic resonance could arguably justify increases in injection volumes and column capacity.

LC-NMR offers several advantages for the scientist. First, individual components in a mixture could be separated by LC and valuable structural information of those components would be provided with ^{13}C NMR detection. Second, the on-line detection permits the NMR investigation of air- and UV-sensitive analytes. Furthermore, the elimination of the transfer step which is typical of performing off-line analysis is obviated with continous-flow LC-NMR. In addition, there is a reduction in analysis time, and the potential of sample contamination is significantly reduced. Another advantage of NMR as a liquid chromatography detector is the fact that nuclear magnetic

resonance is a non-invasive technique. Therefore, sample recovery beyond the detection element is permissible.

NMR as a detector is arguably more amenable to coupling with LC from a technical viewpoint. With LC-NMR the analyte remains in the liquid phase throughout the entire chromatographic run. The conversion of a compound from the liquid state to the vapor state (typical in LC-MS) is not necessary.

Another important advantage which NMR possesses is the lack of a sample volatility constraint - which is a potential concern for other LC detection schemes. An example is LC-MS which requires sample heating to produce the liquid to vapor state transition. Suppose the analyte of interest is non-volatile? What if the high temperatures required in LC-MS create irreparable structural modification of the analyte? LC-NMR avoids these potential difficulties. The possible derivatization step to achieve sample volatility is not necessary, and a savings in experimental time is possible. Moreover, since the entire LC-NMR experiment is performed at ambient temperature, molecular degradation due to thermal effects can be suppressed. Although fluorescence, ultraviolet, and refractive index detectors typically possess much lower minimum detectable quantities than NMR, they are unable to approach NMR in terms of yielding structural information.

Finally, LC - ^{13}C NMR has the potential to detect molecules which are transparent in the UV. It is also able to detect the presence of molecules with quaternary carbon atoms in which there are no protons attached. In contrast, with LC - ^{1}H NMR these latter molecules with quaternary carbon atoms would not be detectable.

2.4 Disadvantages.

The primary disadvantage of LC - ^{13}C NMR (or even LC - ^{1}H NMR) is the poor sensitivity and relatively large injection volumes which are necessary to obtain a NMR signal with a satisfactory signal-to-noise ratio. Thus, the minimum detectable quantities are orders of magnitude higher for NMR compared to other LC detectors. For this reason, LC - ^{13}C NMR is not suitable for analytical-scale trace analysis **at the present time.**

Another potential difficulty of any LC-NMR experiment is a dynamic range problem. The presence of a strong NMR signal (^{1}H or ^{13}C) in the midst of weaker signals can distort the shape of the free-induction decay (FID) and therefore affect the resulting NMR spectra. The presence of a dynamic range problem is not likely to be a factor in the LC - ^{13}C NMR experiment. These weaker signals (typical of analytes)

can be permanently lost in the presence of an intense solvent signal. Thus, the LC-NMR experiment mandates a sufficient number of data points in the noise to digitize in order to detect these weaker NMR signals. To remedy this potential problem, there are several solvent suppression techniques (r.f. pulse sequences)[33a,b] which are capable of reducing intense solvent signals by several orders of magnitude to more acceptable limits.

The number of papers involving the technical aspect of LC - ^{1}H NMR and experimental design are very few when compared to the progress and development of other detectors for LC experiments. To our knowledge, there are no published reports for on-line, continuous-flow LC - ^{13}C NMR experiments. Thus, valuable information which can sometimes be drawn from the literature is very limited. This dearth of literature on LC-NMR can be construed as a lack of development of this technique by the analytical community - who have utilized more acceptable techniques to obtain necessary information.

2.5 Previous Attempts of LC - ^{13}C NMR.

Previous attempts at merging NMR with liquid chromatography have involved separation of mixtures followed by off-line collection of the sample. These fractions are

then placed in a NMR spectrometer and a spectrum for each of the collection vials is then obtained. However, experimental time is increased due to the necessity of taking a large number of scans to obtain a sufficient signal-to-noise ratio. The problem is further exacerbated by the requirement of relatively long time delays between each scan. This delay is mandatory because the excited ^{13}C nuclei must "relax" and return to their Boltzmann distribution before the next pulse (scan) should occur. These experimental delays are typically on the order of five times the T_1 value. For ^{13}C nuclei, the relaxation times (T_1) range from seconds to minutes and waiting a period of 5 x T_1 further increases the delay. For ^{1}H nuclei, this has generally not been a problem since relaxation times are much shorter than those for ^{13}C. T_1 values for ^{1}H are typically on the order of seconds.

Previous attempts to accomplish continuous-flow, on-line LC - ^{13}C NMR have been stifled in part due to the short residence time of the analyte in the NMR detection cell. Assuming a simple plug flow model, mathematics reveal that at a flow rate of 2.3 mL/min, a flow cell of 150 μL is flushed every 3.9 seconds. Thus, the analyte is in the detection region for only a few seconds, and a **sufficient signal-to-noise ratio (S/N) must be generated in that time frame.**

In conclusion, a literature search has revealed no published data pertaining to continuous-flow, on-line LC - ^{13}C NMR for natural abundant carbon samples.

The primary stumbling block to hurdle in successfully achieving continuous-flow, on-line LC - ^{13}C NMR is an improvement in sensitivity for this low abundant nucleus. Any increase in ^{13}C NMR sensitivity must be dramatic (i.e. at least one or two orders of magnitude). Improvements by factors less than one order of magnitude (<10) are not sufficient to practically couple ^{13}C NMR detection with liquid chromatography.

CHAPTER 3: NMR IN FLOWING LIQUIDS

3.1 General Considerations.

In order to understand the LC - ^{13}C DNP experiment, it is imperative to understand the advantages and limitations of the usual flow NMR experiment. Experiments involving NMR in flowing liquids[34] involve the consideration of several factors relative to nuclear magnetic resonance where no flow (static) is involved. For example, the intensity of a NMR signal is a function of the flow rate. Signal height decreases as flow rate increases - with the following exception. If a sample has a residence time, τ, of 3-5 T_1 (i.e. a sufficient time to reach the Boltzmann distribution) within a magnetic field **before** sampling a volume element in the detector cell with a r.f. pulse, there will be an observable **increase** in intensity of the NMR signal relative to that in a stationary NMR experiment for repetitive experiments. However, if the flow rate is too rapid (i.e. τ is very short) and if the Boltzmann distribution has not been attained, then the signal intensity will thereupon **decrease** with increasing flow rate and will experience a concomitant increase in linewidth (i.e. line broadening).

Another factor to consider is broadening of the NMR signal when flow is involved. Line broadening is dependent on the following: [33c]

1. magnetic field homogeneity
2. residence time of a sample in the flow cell.

In LC-NMR, the flow rate and residence time of the analyte in the detector cell are the predominant sources of line broadening.

3.2. Mathematical Description.

A mathematical model has been reported to describe the relationship of flow rate and its effect on experimental NMR parameters.[34-43] (Ref. 34 is a detailed treatise of flow NMR by Zhernovoi while Ref's. 35-43 are less comprehensive, and all subsequent equations and information in this chapter originate from a composite of these references). As stated earlier, the sample should reside in a magnetic field for a period of 3 - 5 times the T_1 value before a scan is taken to ensure full premagnetization and to avoid a concomitant reduction in signal intensity. This value of 3 T_1 arises from Equation 3.1[34]

$$M_t = M_o (1 - e^{-\tau/T1}) \qquad \textbf{Eq. 3.1}$$

where M_t = the magnetization at time (t), M_o is the magnetization at an infinite time, τ is the time in the detector cell, and T_1 is the spin-lattice relaxation time. The parameter T_1 is the time for the excited nuclei to "relax" and to recover their Boltzmann distribution before applying the next r.f. pulse (scan). When $t = 3T_1$, M_t will have recovered 95% of its equilibrium magnetization (M_o). At a period of $5T_1$, an equilibrium magnetization would then be equal to 99.3%.

The following equation relates the relaxation time (T_1) to flow:

$$1/T_{1\ flow} = 1/T_{1\ static} + 1/\tau \qquad \textbf{Eq. 3.2}$$

where $T_{1\ flow}$ is equal to the spin-lattice relaxation time in a flowing stream, and likewise $T_{1\ static}$ is the spin-lattice relaxation time under static conditions. The parameter, τ, is the residence time of a sample bolus in the detector cell

region and is given by the subsequent equation for a plug flow model.

$$\tau = V_{cell} / \upsilon \qquad \textbf{Eq. 3.3}$$

where V_{cell} is equal to the volume of the flow cell, and υ is the mean velocity of the flow rate.

From Eq. 3.2, the NMR parameter $T_{1\ flow}$ is reduced due to a decreased residence time, τ, in the detector coil region. As a result, the delay period $3T_1$ is likewise reduced. Since the effective T_1 is now shorter, a sample in the detector cell can absorb more r.f. power before saturation occurs, and thus a potential for signal enhancement now exists.

Unfortunately, broadening of NMR signals and hence a loss in resolution occurs in conjunction with too high a flow rate as depicted by the following equations:

$$1 / T_{2\ flow} = 1 / T_{2\ static} + 1 / \tau \qquad \textbf{Eq. 3.4}$$

$$\Delta\omega_{1/2} = 2 / T_{2\ flow} \qquad \textbf{Eq. 3.5}$$

$$\Delta\omega_{1/2\ flow} = \Delta\omega_{1/2\ static} + 1 / \tau \qquad \textbf{Eq. 3.6}$$

where $T_{2\ flow}$ and $T_{2\ static}$ are spin-spin relaxation times under flowing and non-flowing conditions, respectively, and $\Delta\omega_{1/2}$ is the width of the signal at half-height.

These equations suggest that as the residence time, τ, in the flow cell region decreases, the term $1/T_{2\ flow}$ increases, and therefore the value of $T_{2\ flow}$ decreases. Substitution of a reduced value of $T_{2\ flow}$ into Eq. 3.5 results in an increase in the term $2/T_{2\ flow}$ - which corresponds to an increase in the width of an NMR signal at half-height, $\Delta\omega_{1/2}$.

Another consideration in flow NMR is the potential loss of the nuclear Overhauser effect (NOE) and subsequent signal enhancement. The NOE can be suppressed if the flow rate is rapid (i.e. the residence time is too short to permit

sufficient time for NOE build-up). Thus a reduction in ^{13}C signal-to-noise by a factor of 2 - 3 is possible.

3.3 Summary.

In summary, signal intensity and peak width in a LC-NMR experiment are primarily affected by flow rate, premagnetization volume, flow cell volume, NMR detector coil design, residence time of the analyte, and on NMR acquisition parameters - such as the flip angle (pulse width) and the time between scans (pulse delay).

CHAPTER 4: FUNDAMENTALS OF DNP IN LIQUIDS

4.1 Mathematical Models

4.1.1 Classical DNP Equations.

Signal enhancements arising from dynamic nuclear polarization (DNP) can be described mathematically according to the following equations.[45-50] Classic DNP equations express the observed enhancement, A_{obs}, as

$$A_{obs} = (\langle I_z \rangle - I_o) / I_o = -\rho f s (\gamma_s/\gamma_i) \qquad \textbf{Eq. 4.1}$$

where $\langle I_z \rangle$ is equal to the nuclear spin operator, I_o is the value of $\langle I_z \rangle$ at thermal equilibrium, ρ is the coupling factor, f is the leakage factor, s is the saturation factor, and γ_s/γ_i are the magnetogyric ratios of the two spins (e.g. ^{13}C and ^{1}H). The DNP enhancement is maximized when ρ, f, and s are optimized.

The coupling factor, ρ, is a parameter which reflects the extent of nuclear-electron interactions and can be defined by[45-50]

$$\rho = (W_2^D - W_o^D - W_o^{Sc}) / (W_o^D + W_o^{Sc} + 2W_1^D + W_2^D) \qquad \textbf{Eq. 4.2}$$

where electron transition probabilities are denoted by W_i, and where W_2^D, W_o^D, W_1^D refer to relaxation transitions for a nuclear-electron coupled spin system dominated by dipolar interactions. Likewise, the W_o^{Sc} trasition arises from a scalar dominated interaction. The maximum theoretical values of ρ are +1/2 and -1 for dipolar ($W_o^{Sc} = 0$) and scalar dominated transitions ($W_o^D = W_1^D = W_2^D = 0$). Figure 4.1 reveals the energy level diagram showing the transition probabilities for the combined spin states of an electron spin ($S = \frac{1}{2}$) to a nuclear spin ($I = \frac{1}{2}$) where W_{1o} and W_s refer to the relaxation probabilities of nuclear-electron and electron-electron transitions, respectively.

The leakage factor, f, is a parameter whose value is a measure of the percentage of the total relaxation rate that can be attributed to the influence of electron-nuclear interactions. This parameter, f, can be expressed in terms

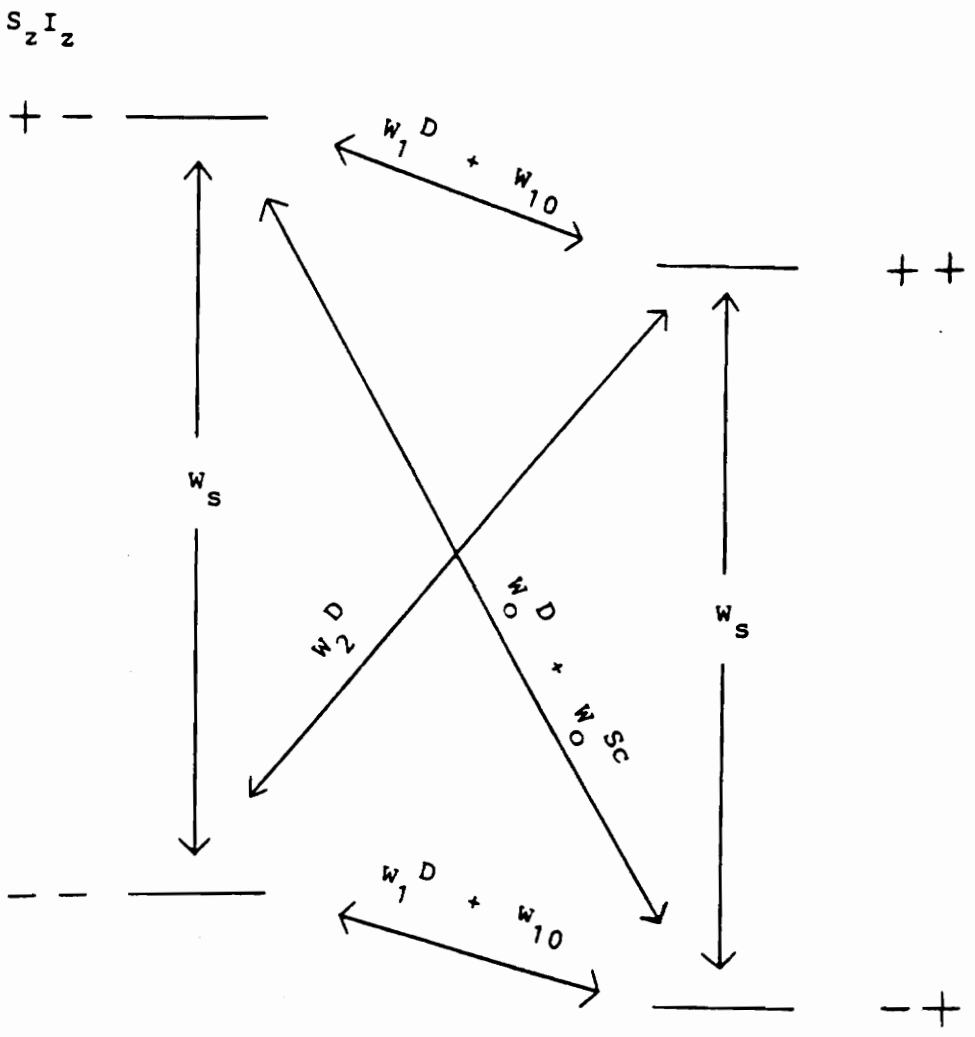

Figure 4.1 Energy level diagram showing transition probabilities for combined spin states of an electron spin (S = ½) to a nuclear spin (I = ½).

of transition probabilities by[45-50]

$$f = (W_o^D+2W_1^D+W_2^D+W_o^{Sc}) / (W_o^D+W_o^{Sc}+2W_1^D+W_2^D)+2W_{1o} \quad \textbf{Eq. 4.3}$$

where T_{1no} is the spin-lattice relaxation time in the absence of electron spins. The term $(W_o^D+W_o^{Sc}+2W_1^D+W_2^D)$ is representative of the fraction of the nuclear relaxation rate emanating from interactions with electrons.

The maximum value for the parameter, f, is 1 and occurs when $T_{1o} << T_{1no}$, where T_{1o} is the nuclear relaxation time when the radical is present, and T_{1no} is the spin-lattice relaxation time in the absence of electron spins, S. Optimum values for the leakage factor are obtained when high radical concentrations are utilized.

The saturation factor, s, reveals the extent of saturation of the electron spin resonance transition, and is defined by[48-50]

$$s = (S_o - \langle S_z \rangle) / S_o \quad \textbf{Eq. 4.4}$$

where $\langle S_z \rangle$ is equal to the expectation value for the electron spin operator, S, where

$$S = S_o / (1 + \gamma^2 B^2_{1s} T_{1s} T_{2s}) \quad \textbf{Eq. 4.5}$$

in which γ is the magnetogyric ratio of a given nucleus, and T_{1s} and T_{2s} are the electron spin-lattice and spin-spin relaxation times, respectively. For an ideal case of complete saturation, the value of s = 1. To maximize the DNP enhancement, high microwave power, P ($P \propto B_{1s}$, where B_{1s} is the field strength) as well as narrow EPR lines of the electron-bearing radical are desired.

4.1.2 Summary.

In summary, it is experimentally difficult to simultaneously obtain the maximum theoretical values for the coupling factor (ρ), the saturation factor (s), and the leakage factor (f). For this reason, the maximum theoretical DNP enhancements are difficult to attain. Since the DNP enhancement is proportional to γ_e/γ_n (γ_e, γ_n are the magnetogyric ratios for the electron and nucleus, respectively) and since γ_e is typically greater than γ_n by several orders of magnitude, a potential for large NMR signals for a given nuclide are predicted. The ultimate DNP enhancements for ^{13}C nuclei are -1310 and +2620 for dipolar and scalar dominated signals, respectively.[48]

4.1.3 Flow DNP Equations.

In our laboratory, where DNP is attained in one region and transferred to a separate region for NMR detection, these aforementioned classical DNP equations require slight modifications. A thorough mathematical model for the low to high field DNP transfer experiment has previously been described by Tsai and Dorn[46] which relates the effect of flow DNP to the enhancement, A_{obs}, by [45-46,48-50]

$$A_{obs} = A/K \left(1 - E_{1a} \right) E_{1b} E_{1c} \qquad \textbf{Eq. 4.6}$$

where $E_{1a} = e^{-ta/T1a}$, $E_{1b} = e^{-tb/T1b}$, $E_{1c} = e^{-tc/T1c}$, K is equal to the ratio of the high to low field magnets (4.7/0.33 Tesla), and t_a, t_b, t_c are residence times of a polarized bolus in regions a,b,c, respectively. T_{1a}, T_{1b}, T_{1c} are spin-lattice relaxation times in regions a,b,c respectively, and E_{1a}, E_{1b}, E_{1c} represent the magnetization in these regions.

Region a is the location of polarization build-up, region c is where NMR detection of this polarized bolus occurs, and region b is the dead volume connecting the spatially isolated regions a and c. Figure 4.2 illustrates the apparatus utilized by our laboratory for the low to high field DNP experiment.

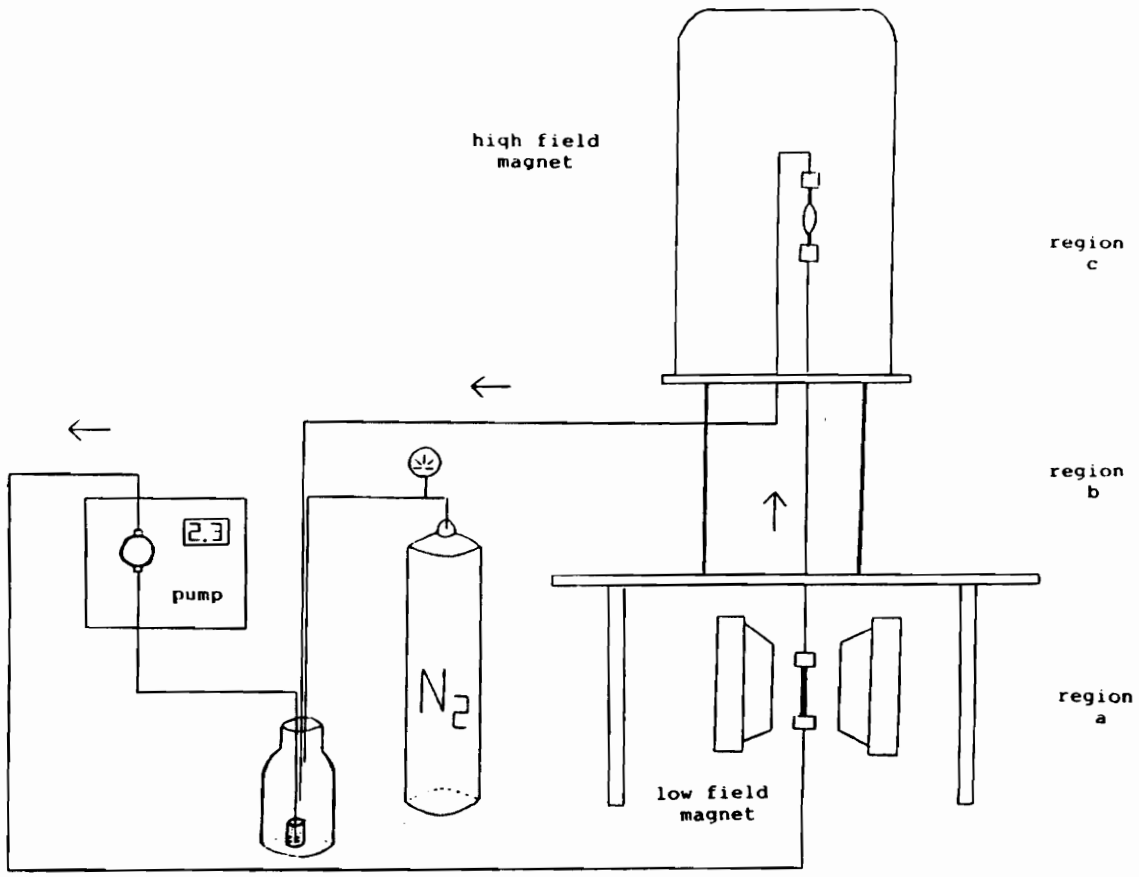

Figure 4.2 Apparatus for the low to high field transfer DNP experiment utilized for both ^{13}C SLIT and LLIT experiments.

4.2 Build-up Loss.[48]

The improper choice of flow rate in the low field can have a detrimental effect on the magnitude of the subsequent DNP enhancement. A sufficient residence time (3-5 T_1) of a sample in region a (t_a) is necessary for complete polarization build-up and interaction with a radical whose electronic transitions have been saturated by an oscillating microwave field, B_{1s}. Thus, a reduction in signal intensity will occur for a given nuclei if the flow rate is too rapid to ensure complete build-up of the polarization.

4.3 Transfer Loss.[48]

Transfer losses result in a reduction of the DNP enhancement if there is a long residence time in regions b and c. Once dynamic nuclear polarization has occured in region a, the sample must transfer that polarization to region b and detector region c. This is a time, $t = t_b+t_c$. To ensure optimum enhancements, the amount of time spent in region a should typically be long relative to T_{1a} whereas

the amount of time spent in regions b and c should be short relative to T_{1b} and T_{1c}.

An explanation for this requirement can be addressed with a discussion of relaxation times. Upon interaction with the radical in region a, the relaxation time of the sample is reduced due to an alternative mechanism of relaxation - in this case, a nuclear-electron relaxation process. Detection in the high field (region c) with a r.f. pulse must occur **before** relaxation due to polarization (T_{1a}). If a nucleus relaxes to equilibium before detection, then the DNP enhancement and corresponding augmentation in signal will be lost.

4.4 Three-spin Effect.[48-49]

Another important factor to consider in a DNP experiment is the three-spin effect and its potential influence on the intensity of the resulting NMR signal. Thus far, only the interaction of a two spin system (the electron of a radical with a ^{13}C nuclide) has been assumed in previous equations. However, there are situations where a third spin (e.g. ^{1}H) can become involved and interrupt the pure polarization transfer from the electron to the ^{13}C atom. In this scenario, the resulting ^{13}C polarization would then be influenced by both the presence of the

electron **and** the proton. Thus, the ^{13}C nuclear spin would receive magnetization from the unpaired electron spin in the usual (direct) transfer step in addition to magnetization contributions from the electron spin via the polarized ^{1}H spin (indirect transfer). The effect of this three-spin interaction on the DNP enhancement can either augment or degrade the signal intensity - depending on several factors (i.e. the predominant relaxation mechanism of a nuclear spin and/or the concentration of radical in solution). For ^{13}C dipolar dominated relaxation mechanisms, the resulting ^{13}C NMR signal will be negative (an emission signal). However, the presence of a three-spin effect will add a positive (+) component to the otherwise negative signal. The potential effect is to reduce the DNP enhancement due to both (+) and (-) contributions to the signal intensity.

In contrast, scalar dominated ^{13}C relaxation mechanisms in the absence of a three-spin effect are positive (+) signals. The effect of a three-spin interaction is to provide an additional positive (+) component to the DNP enhancement, and the intensity of the NMR signal would then always be positive.

An equation which relates the three-spin effect to the magnitude of an observed DNP enhancement (A) is given by[45-46,48-50]

$$A = (\rho_c^s f_c^s - \rho_c^H f_c^H \rho_H^s f_H^s)(\gamma_s/\gamma_c) \qquad \textbf{Eq. 4.7}$$

where ρ_c^s and ρ_s^H are carbon-electron and hydrogen-electron coupling factors, respectively, and where f_c^s and f_H^s are the carbon and hydrogen leakage factors, respectively. ρ_c^H is equal to 1/2 for interactions where dipolar ^{13}C-^1H coupling is dominant, and f_c^H is the fraction of carbon relaxation arising from the third spin, ^1H. Finally, γ_s, γ_c are the magnetogyric ratios of the electron and nuclear spin (^{13}C), respectively.

For LLIT (liquid-liquid intermolecular transfer) DNP experiments, high radical concentrations will eliminate the three-spin effect since the fraction of carbon relaxation from the third spin, ^1H (f_c^H) will approach zero.

There are several techniques which can be employed in the DNP experiment to alleviate the potential influence of a three-spin effect. In addition to the aforementioned employment of high radical concentrations (LLIT), a second method utilizes strong irradiation[51-54] at the low field ^1H Larmor frequency to saturate the proton spin transitions. This latter technique could be useful for SLIT (solid-liquid intermolecular transfer) experiments.

4.5 SLIT Experiments.

In the SLIT experiment, the radical is immobilized on a given surface and placed in a field of low magnetic field strength (region a). Microwave power is then applied to irradiate the electron spin transitions. Upon flowing through the bed of immobilized radical and experiencing a nuclear-electron interaction to receive polarization, the analyte flows through the transfer region b and eventually to region c, where the NMR signal of the analyte is obtained.

In our laboratory, a system for observing flow DNP enhancements from low to high field[48-50] has already been established. Figure 4.2 is a representation of the experimental apparatus. The nitroxide radical immobilized on silica gel was prepared by Gitti.[49] SPIN #511 (Silica Phase Immobilized Nitroxide Radical) was selected for all SLIT experiments in this thesis.

An important factor to consider in the SLIT experiment is that the radical is **not** in solution and therefore remains in the low field (region a) throughout the entire DNP experiment. There are several ramifications of isolating the SPIN (radical) in region a. First, since the radical is therefore not present in the high field where NMR detection occurs), any problems associated with radical-induced line

broadening ($\Delta\omega_{1/2}$) of the NMR signal as well as possible contact chemical shifts are eliminated. Second, recovery of the sample is possible since the radical is not present in solution. Third, the SLIT experiment is more "forgiving" experimentally than the LLIT. The reduction in relaxation time, T_{1o}, induced by the electron-nuclear mechanism occurs in both the SLIT and LLIT experiments, but with the SLIT experiment, the ^{13}C relaxation time is not reduced during the transfer and observation in the high magnetic field. Since these relaxation times (T_{1b} and T_{1c}) are typically longer with the SLIT relative to the LLIT for these regions, the dynamic nuclear polarization transfer and observation times can be much longer. Therefore, the urgency to transfer the polarized bolus from the low to the high field (regions a - c) is not as stringent a demand on the experimental design. This translates into reduced transfer losses with the SLIT and therefore a larger potential enhancement, A.

Another advantage of the SLIT experiment at present when compared to the LLIT - at least in terms of a ^{13}C liquid chromatography detector - is the larger allowed detector volume in the flow cell because at this stage in the development of LC - ^{13}C NMR, larger detector cells are necessary to obtain a sufficient signal-to-noise ratio. At present, detection volumes of 100 - 200 μL must be used in

order to increase the amount of ^{13}C nuclei in the flow cell. This larger detector volume is required at the expense of some chromatographic resolution (peak mixing and dead volume near the flow cell region).

From a chromatographic standpoint, the SLIT offers another advantage over the LLIT. SLIT experiments typically obtain their maximum enhancements at flow rates of 1 - 5 mL/min and are therefore better suited as a ^{13}C NMR LC detector. In contrast, the LLIT requires flow rates of 5 - 10 ml/min to obtain maximum signal enhancements and therefore does not appear to be as suited for a ^{13}C NMR LC detector from a chromatographic viewpoint. These high flow rates are necessary in the LLIT experiment due to potentially significant large transfer losses resulting from too short a relaxation time of the analytes since the electron-nuclear relaxation mechanism is present in all regions (a,b,c).

SLIT possesses yet another potential advantage over the LLIT. In the LLIT, dipolar dominated ^{13}C enhancements (negative signals) are dependent on the concentration of radical in solution. At too low a concentration, the three-spin effect can dominate to the extent that a NMR signal might not be observed for a particular ^{13}C nuclide. However, low radical concentrations typically favor scalar dominated NMR signals - although at too low a radical

concentration, the DNP enhancement diminishes concomitantly, and signals can be weak to non-existent. If higher radical concentrations are employed to alleviate the three-spin effect and to increase DNP enhancements, the dipolar dominated ^{13}C signals can now be seen as negative peaks, but potentially only at the expense of scalar dominated ^{13}C signals - which typically are no longer observed at these high radical concentrations due to too high a transfer loss arising from too large a reduction in the relaxation times, T_{1a}, T_{1b}, T_{1c}. However, a disadvantage of the SLIT experiment is the lower ultimate enhancements even though transfers are more efficient.

4.6 LLIT Experiments.

In our laboratory, a liquid-liquid intermolecular transfer (LLIT) DNP experiment has been developed[45-50] in which a radical (in this thesis, TEMPO, 2,2,6,6 - tetramethylpiperidine-1-oxyl, Aldrich) is dissolved in a solution containing analytes. TEMPO is present in all regions (a,b,c) in the LLIT experiment. Since the radical is present in region c (where NMR detection occurs), broadening of the NMR signal, in addition to flow broadening

contributions, as well as movements in the chemical shift can become a concern at high concentrations.

An advantage of LLIT versus SLIT is that dipolar dominated ^{13}C signals (negative) are generally easier to obtain with the LLIT experiment - but this is typically achieved at the expense of employing high radical concentrations (TEMPO). At high concentrations of radical, relaxation times for some scalar dominated interactions are rendered very short (milliseconds for certain ^{13}C nuclei), and therefore the DNP "lifetime" is on the order of milliseconds. If transfer from low to high field is not accomplished during this time span, a DNP enhanced NMR signal will not be observed.

For this reason, transfer losses in LLIT flow DNP experiments are potentially very high. As a result, (1) small transfer volumes (region b), (2) small flow cell volumes in the detector cell (region c), and (3) high flow rates are typical in a LLIT experiment since NMR detection of the polarized bolus must be effectuated before full relaxation (T_{1_0}) occurs to avoid losing DNP enhancements.

4.7 Factors Influencing DNP Enhancements.

In summary, the extent of the DNP enhancement is a function of the magnitude of the free-radical induced

transition probabilities (W_o^{Sc}, W_o^D, W_1^D, W_2^D) as discussed earlier. Other factors which influence the enhancement in a DNP experiment are the ratios of scalar to dipolar coupling, transfer loss, polarization build-up loss, nature of the free radical, and the leakage, saturation, and coupling factors. In addition, the chemical environment of the nuclear spin, choice of nuclei (e.g. ^{13}C, ^{1}H, ^{15}N, ^{19}F) being monitored, field strength, temperature, viscosity, and instrumental considerations (e.g. NMR probe design, pre-amplifier performance, quality factor (Q) of the detection coil, flow cell design) influence the resulting DNP enhancements. Other factors include the selection of flow rate, NMR acquisition parameters, choice of SLIT or LLIT experiment, the extent of interaction between the analyte and radical, and the concentration of the electron spin system.

CHAPTER 5: EXPERIMENTAL DESIGN

5.1 Schematic.

A modification of the previously described low to high field flow DNP apparatus[48-50] was necessary due to the addition of a chromatographic column and an injection port. A diagram of the LC - ^{13}C NMR (DNP) chromatography apparatus is illustrated in Figure 5.1.

5.2 Pump.

A Waters SSI (Model 200) HPLC pump capable of mobile phase flow rates of up to 9.9 mL/min and capable of withstanding backpressures of up to 5000 p.s.i. was utilized. Typical backpressures during LC - ^{13}C NMR experiments were approximately 1200 - 2300 p.s.i. and originated from the large capacity column and from a 2 micron frit placed after the SPIN radical in the low field.

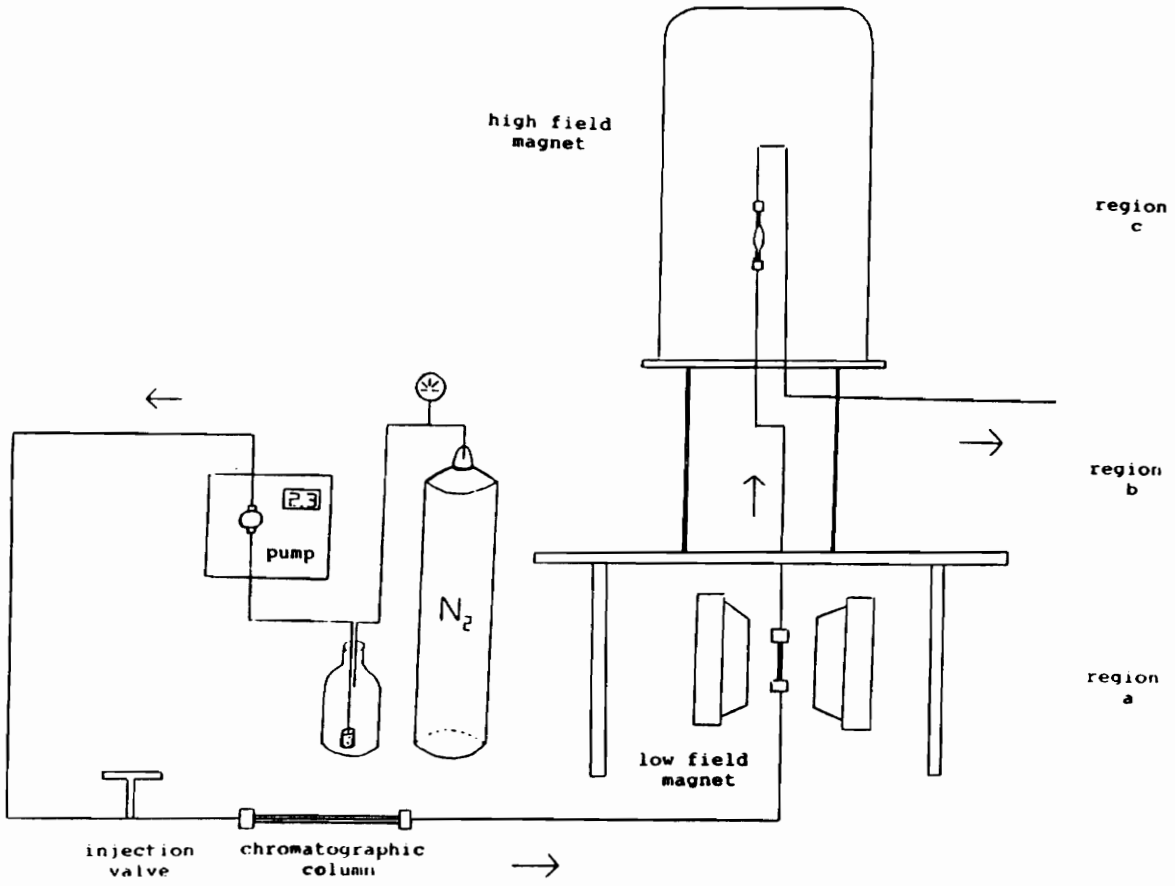

Figure 5.1 Illustration of the continuous-flow, on-line LC - ^{13}C NMR (DNP) apparatus utilized for chromatographic separations.

5.3 Chemicals.

HPLC grade mobile phase (CCl_4) was utilized, and all analytes were injected and utilized as received from the manufacturer without further purification. Degassing of the solvent was accomplished by bubbling N_2 prior to and during all experiments. Removal of dissolved O_2 is necessary to avoid a reduction in the DNP enhancement.

5.4 Injection Port.

The amount of sample injected into the column was dependent on the type of experiment. For mixtures containing a large number of components (5 - 10), a Valco injection loop of 10 mL was employed to assure sufficient loading capacities. Other experiments required only a 500 μL injection loop. Injection volumes for halogenated analytes range from 50 to 1500 μL (neat) depending on the magnitude of the DNP enhancement for a given analyte.

5.5 Column.

A preparative scale column capable of withstanding large injection volumes was necessary since ^{13}C NMR detection requires a relatively large amount of ^{13}C nuclei in the flow cell region to obtain a NMR signal with a satisfactory signal-to-noise ratio. A Whatman (Partisil PAC 10) x 250 mm was employed for all LC experiments performed for this thesis.

5.6 Mobile Phase.

Selection of the proper mobile phase in a LC -^{13}C NMR (DNP) experiment must not be overlooked. In this thesis, carbon tetrachloride (CCl_4) was used in lieu of other ^{1}H bearing solvents (e.g. cyclohexane) for several reasons. First, since CCl_4 contains no ^{1}H nuclei, the one concern for the potential influence of a three-spin effect is obviated. Second, since CCl_4 undergoes a relatively large scalar DNP enhancement (but not too large an enhancement to initiate concern for a dynamic range problem), the entire system can be optimized by monitoring the magnitude of the CCl_4 ^{13}C

free-induction decay (FID) prior to commencing a chromatographic run.

5.7 Low Field (Region A).

5.7.1 Introduction.

Tuning of the microwave cavity at ~9.3 GHz was performed to minimize the amount of reflected power in order to permit maximum forward microwave power and to minimize sample heating in the EPR flow cell. Selection of the flow rate for the LC experiments varied from 2.3 - 3.5 mL/min, whereas flow rates were increased to as high as 7.2 mL/min for recycle experiments. The magnitude of the low field (B_1) strength can be adjusted manually and was kept at ~0.3 T. The vertical positioning of the SPIN sample in the low field influences the tuning of the microwave cavity and the subsequent magnitude of DNP enhancements. An efficient tuning and matching of the NMR detection coil was performed at 50.10 MHz for ^{13}C nuclei to permit as high a signal-to-noise ratio as possible. In addition, the selection of NMR acquisition parameters also affects the magnitude of the FID and subsequent DNP enhancements for both the solvent and

analytes. These experimental variables can be optimized prior to sample injection. Selection of CCl_4 as the mobile phase allows for easier optimization of the LC - ^{13}C NMR apparatus since the DNP enhanced ^{13}C NMR signal is large enough to permit optimization of these variables while simultaneously monitoring the ^{13}C FID.

5.7.2 Packing of SPIN Samples.

The Silica Phase Immobilized Nitroxide (SPIN) radical #511 (80 - 100 mg) from Gitti[49] were packed into ceramic tubing and placed in the low field microwave cavity as illustrated in Figure 5.2.

5.7.3 Microwave Power/Cavity.

A variable low field magnet, B_o^L, at 0.33 T is located orthogonally to a high field magnet, B_o^H, at 4.7 T and separated by 1.2 meters - a distance which does not significantly alter homogeneity and resolution of the high magnetic field. Microwave frequency and power is transferred to a microwave TE_{102} cavity located in a modified Varian E-3 EPR spectrometer containing the SPIN radical via

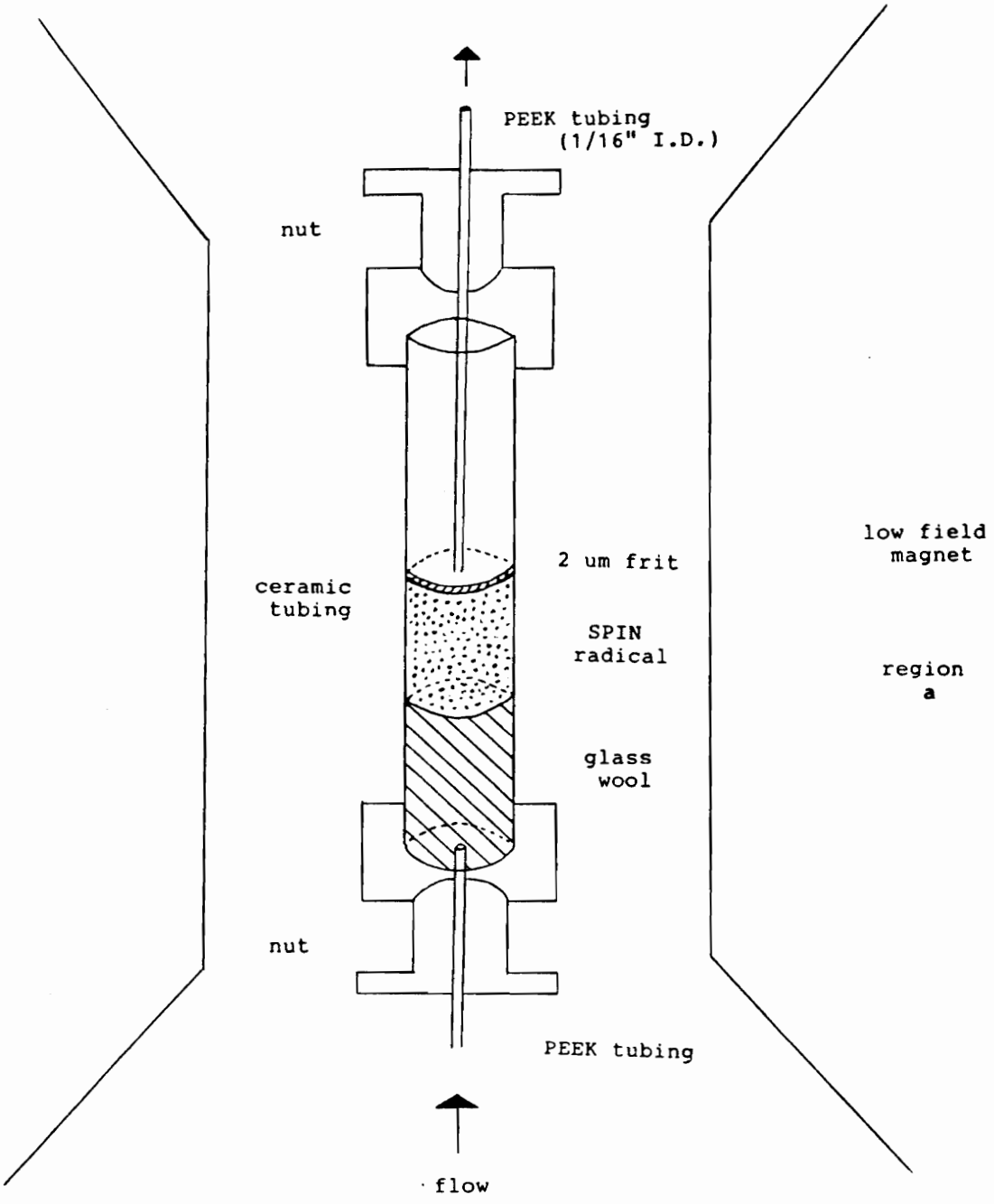

Figure 5.2 Diagram of the low field EPR flow cell containing Silica Phase Immobilized Nitroxide (SPIN) radical.

low loss cables originating from a klystron source of a Bruker microwave bridge. A Varian "K" series TWT amplifier capable of delivering up to 25 watts of power was employed. The amount of microwave power being delivered to the cavity can be controlled with an attenuator. Microwave frequencies required to saturate the electron spin transitions range from 9.29 to 9.33 GHz, and typical low field strengths vary from 3435 to 3455 Gauss. Ambient temperatures were employed in all experimental runs. The total volume in region a is approximately 160 μL (without the spin radical).

A diagram of the EPR flow cell which is located in the low field is shown in Figure 5.2.

5.8 Region B.

The connection of the low to the high field (region b) was accomplished with 1/16" OD x 0.005" ID PEEK tubing (Upchurch Scientific) and an approximate transfer volume of 40 μL can be estimated. It is essential that the residence time of the analyte be as brief as possible in this region to avoid a loss in polarization (i.e. reduced enhancements).

5.9 High Field (Region C).

Region c consists of a Jeol FX 200 (4.7 T) high field superconducting magnet. Exiting region b, the sample enters a 150 μL flow cell for NMR detection. A homebuilt flow NMR probe was employed using a standard tuning and match r.f. circuit. An additional fixed ceramic capacitor (10 pF) was placed on the tuning side of the ^{13}C observation channel in order to facilitate tuning in the high field magnet. Irradiation of ^{13}C nuclei was accomplished at 50.10 MHz and decoupling was performed at 199.5 MHz using a Helmholtz coil. It is important to note that a preequilibration volume on the order of only microliters existed prior to sampling with a r.f. pulse since optimum DNP enhancement in the flow experiment is maximized when the transfer volume between regions **a** and **c** is a minimum. In addition, a slight modification of the NMR flow cell was adopted. Instead of placing glass wool **before** and **after** the detection volume (to achieve a better flow pattern), a decision to only use glass wool after NMR detection was made. A diagram of the NMR flow cell is illustrated in Figure 5.3.

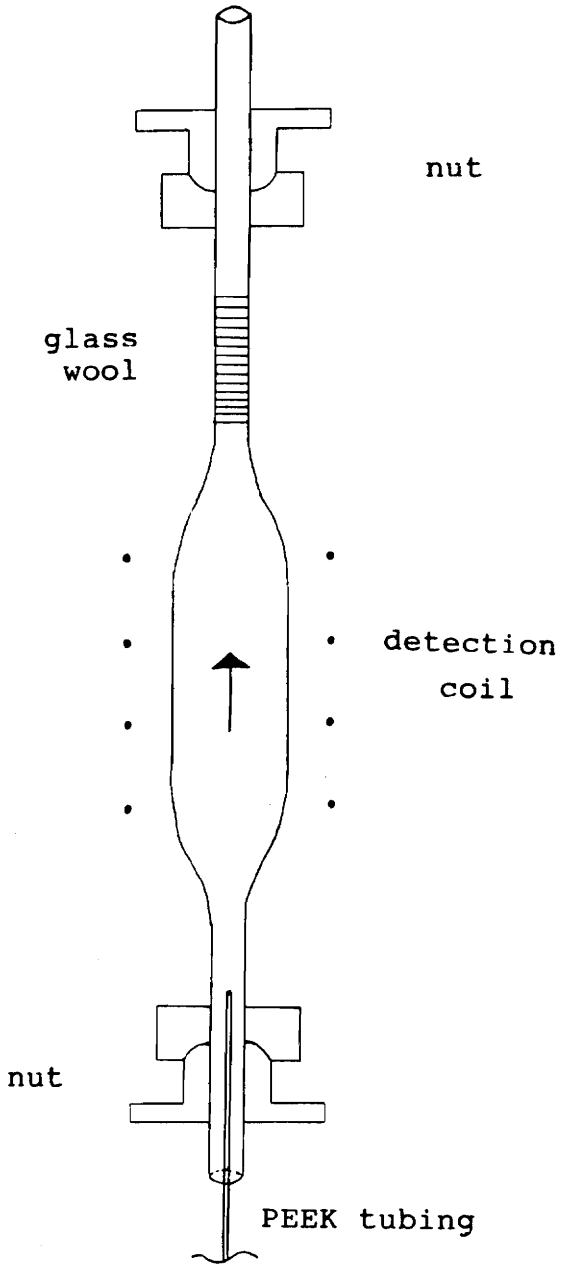

Figure 5.3 Diagram of the high field NMR flow cell with a detection volume of 150 μL.

CHAPTER 6: RESULTS AND DISCUSSION

6.1 Introduction.

As a prerequisite for successful LC separations with on-line, continuous-flow ^{13}C NMR detection, it must be demonstrated that a relatively significant improvement in ^{13}C sensitivity by factors of at least 10 - 100 must be realized. To illustrate that our laboratory has successfully satisfied this requirement, refer to Figure 6.0 - the free induction decay (FID) of only **1** scan of $CHCl_3$ with a detection volume of 150 μL. The FID is shown **prior** to any exponential multiplication with the corresponding ^{13}C NMR spectrum of $CHCl_3$ with DNP at 77.5 ppm as illustrated in Figure 6.1. Peak-to-peak S/N is ~ 80:1 with a root mean square (RMS) signal-to-noise ratio of ~ 200:1. As of today, we believe this is the largest ^{13}C NMR signal-to-noise ratio ever reported (per unit volume) for an unenriched flowing sample. For comparison, Figure 6.2 (**without DNP**) is representative of the static ^{13}C NMR signal from 150 μL $CHCl_3$ but with 64 scans. The

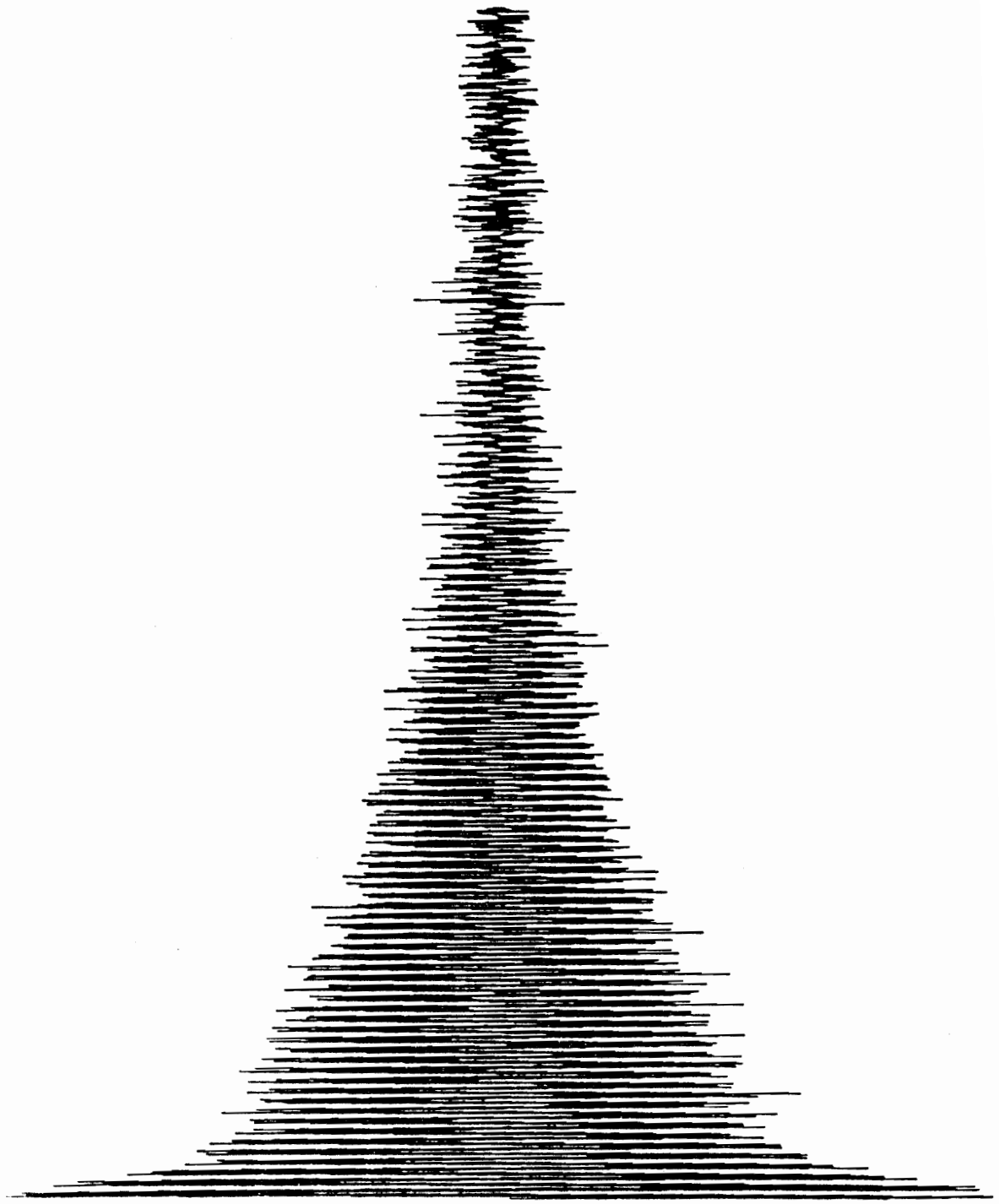

Figure 6.0 ^{13}C free induction decay (FID) with dynamic nuclear polarization (DNP) for signal enhancement shown **prior** to exponential multiplication for **only 1 scan** of $CHCl_3$ flowing at 2.3 ml/min with a detection volume of 150 μL.

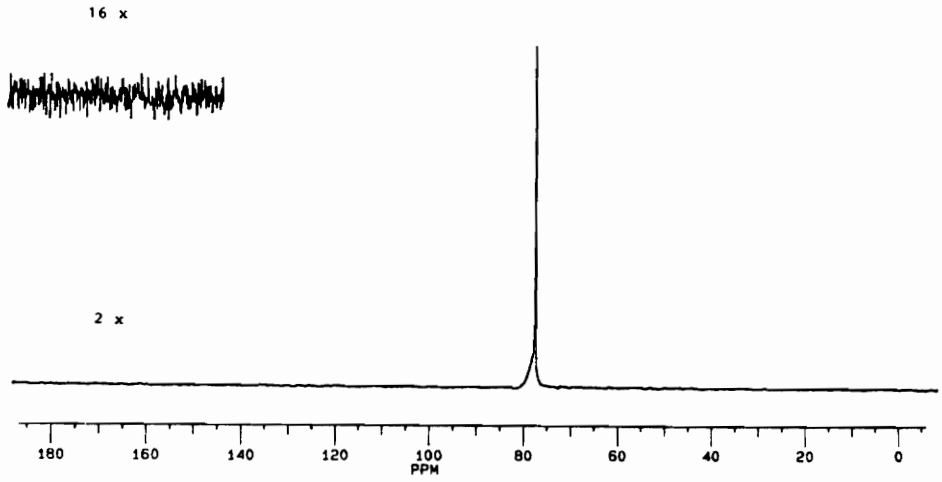

Figure 6.1 ^{13}C NMR signal with dynamic nuclear polarization (DNP) for signal enhancement shown for **only 1 scan** of $CHCl_3$ flowing at 2.3 ml/min with a detection volume of 150 μL.

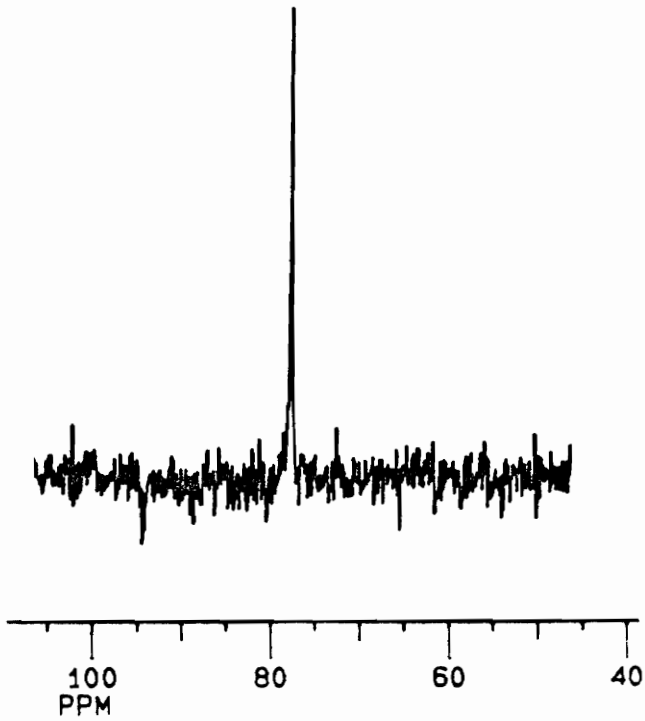

Figure 6.2 ^{13}C NMR signal **without dynamic nuclear polarization (DNP)** for 64 scans of $CHCl_3$ measured under static conditions with a detection volume of 150 μL.

signal-to-noise ratio remains poor (peak-to-peak ~ 10:1 with a RMS S/N ~ 25:1).

All LC - ^{13}C NMR (DNP) experiments utilized the SLIT technique with detection employing a home-built flow probe. The emphasis was placed on obtaining a sufficient S/N at the expense of other considerations (e.g. optimum flow cell volume for a LC experiment, optimum preequilibration volume prior to sampling with a r.f. pulse, and in some cases column overloading). Halogenated compounds were selected for LC - DNP (NMR) experiments due to (1) environmental interests and (2) typically large DNP enhancements for these molecules - some of which have previously been studied in our laboratory for their DNP enhancements.[48] A table listing the chemical shifts of all compounds utilized in this thesis is presented in Appendix I.

6.2 LC - ^{13}C NMR with DNP.

6.2.1 Injections of one compound.

The molecule $CHCl_3$ was expected to yield a large scalar DNP enhancement.[48] To obtain an estimate of the quantities of injection volumes necessary for the LC -

^{13}C NMR experiment, 500 μL of chloroform was injected into a semi-preparatory column with the resulting NMR spectra collected every 31 seconds as illustrated in Figure 6.3. In this way, the presence of chloroform in the detector cell could be monitored as a function of time. The mobile phase for all experiments was CCl_4, and the flow rate for this particular injection was 3.5 mL/min. For the chloroform LC experiment, each spectrum (or file) consists of 10 scans.

In comparison, a second chromatographic experiment was performed <u>without DNP</u> to illustrate the significant reduction in S/N when utilizing "classic" LC - ^{13}C NMR detection. Figure 6.4 shows the resulting spectra of a 500 μL $CHCl_3$ injection <u>without utilizing DNP</u>. All conditions between these two runs were identical (e.g. flow rate & NMR acquisition parameters) except for the absence of the microwave source.

Since halocarbon molecules typically exhibit large enhancements, chlorinated and fluorinated compounds (both partially and fully substituted) were thus selected for this study. A series of halogenated alkanes, alkenes, and aromatic compounds were next examined using the LC - ^{13}C DNP technique. These compounds were present in relatively large amounts in order to demonstrate whether or not the weak dipolar

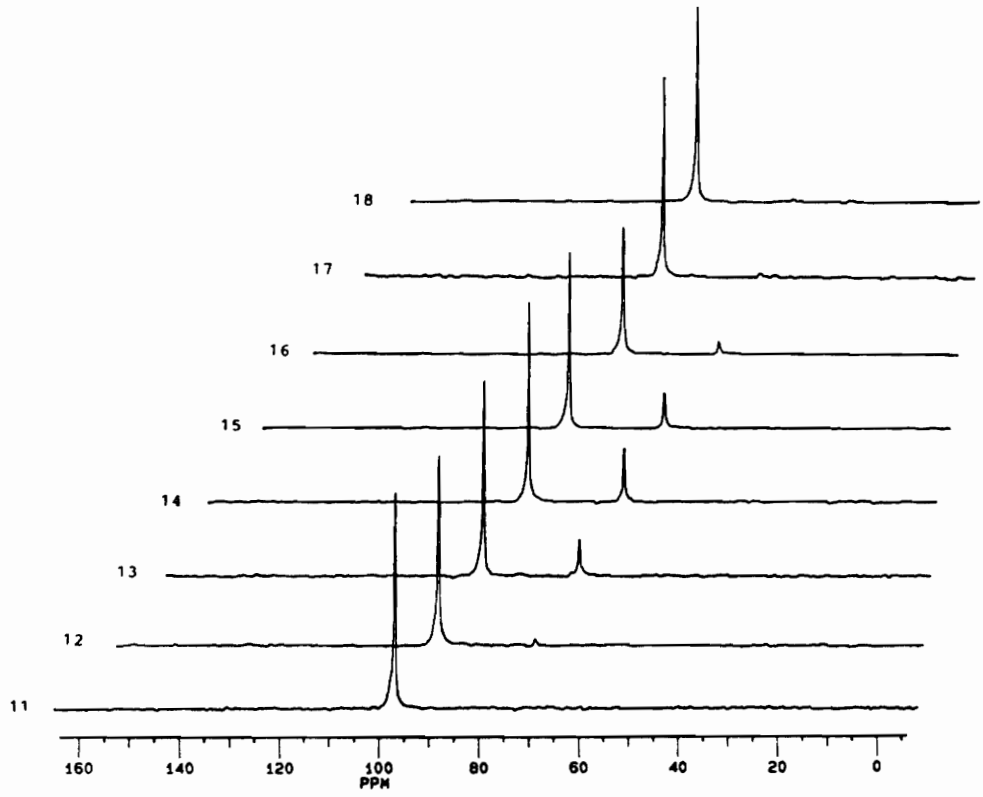

Figure 6.3 LC -^{13}C NMR (DNP), 500 μL chloroform, 3.5 mL/min, 10 scans/file, 31 sec/file, with CCl_4 as the mobile phase.

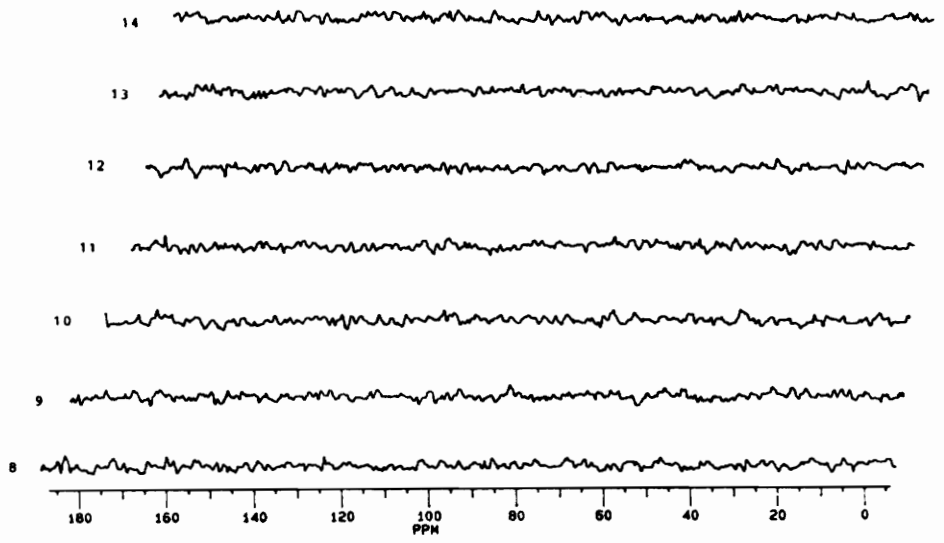

Figure 6.4 LC -^{13}C NMR **(without DNP)**, 500 μL chloroform, 3.5 mL/min, 10 scans/file, 31 sec/file, with CCl_4 as the mobile phase.

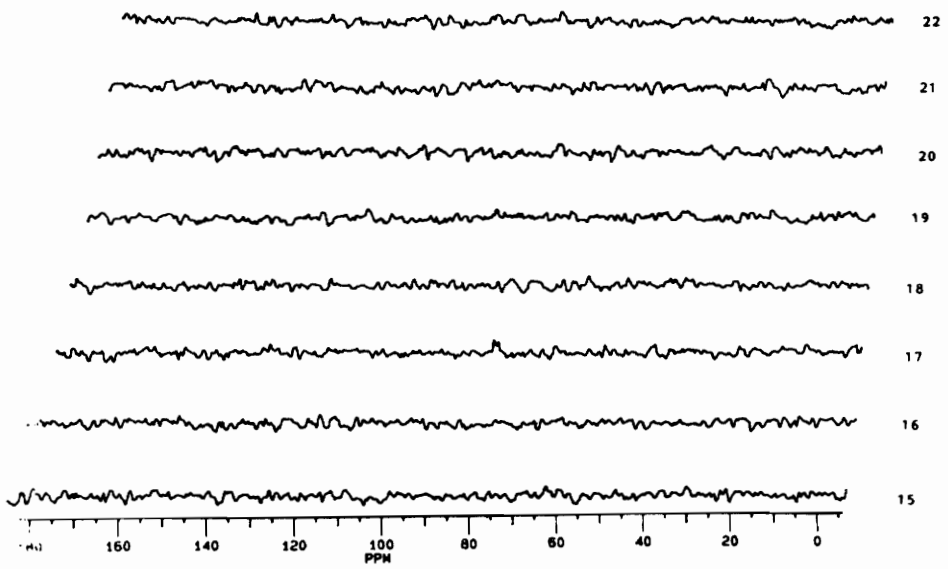

Figure 6.4 LC -^{13}C NMR **(without DNP)**, 500 μL chloroform, 3.5 mL/min, 10 scans/file, 31 sec/file, with CCl_4 as the mobile phase.

dominated and scalar dominated signals would be observed with DNP.

For example, a chromatographic experiment was performed by injecting 1400 μL 1,3,5-trichlorobenzene onto the column, and the resulting spectra are illustrated in Figure 6.5. Two distinct NMR signals are expected for this molecule[48]. In 1,3,5-trichlorobenzene, one carbon is dipolar dominated while the other carbon is scalar dominated.[48] However, only one ^{13}C NMR signal is observed. The signal arising from the carbon atoms attached at positions 2,4,6 is observed due to scalar interactions arising from H-bonding with the immobilized radical. In contrast, the NMR signal from the carbon atoms attached to the chlorine is not observed with a sufficient S/N.

Next, a transition from a trisubstituted to a monosubstituted aromatic was effectuated with an injection of 1300 μL of chlorobenzene, and the corresponding spectra are illustrated in Figure 6.6. Note that of the expected **four** ^{13}C signals for chlorobenzene, only the three scalar dominated signals are observed with a sufficient S/N. The carbon atom at position #1 (C - Cl) on the benzene ring exhibits the poorest signal-to-noise ratio and is dominated by a dipolar enhancement.[48] However, it should be noted

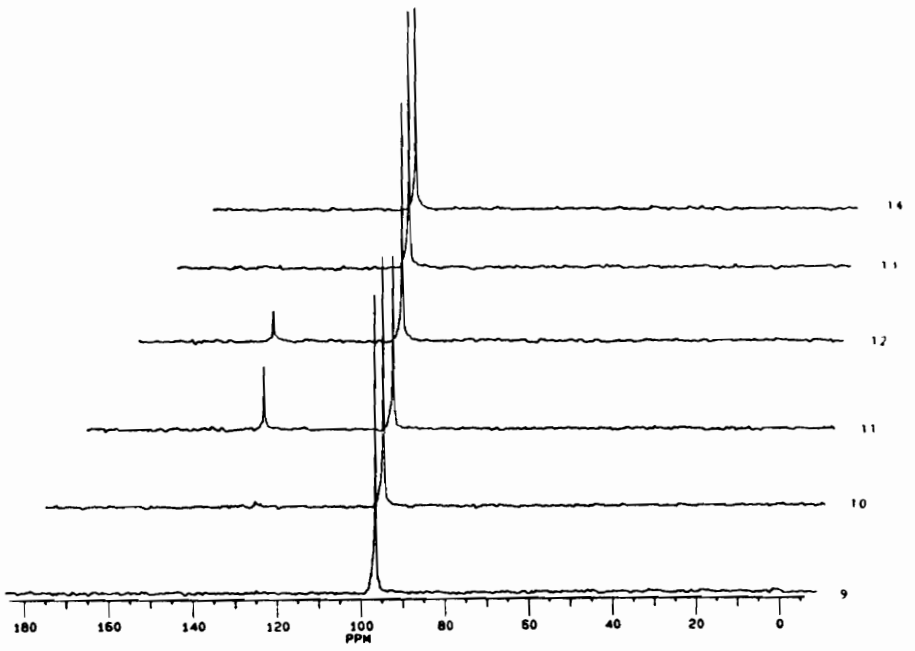

Figure 6.5 LC -^{13}C NMR (DNP), 1400 μL 1,3,5-trichlorobenzene, 2.3 mL/min, 8 scans/file, 31 sec/file, with CCl_4 as the mobile phase.

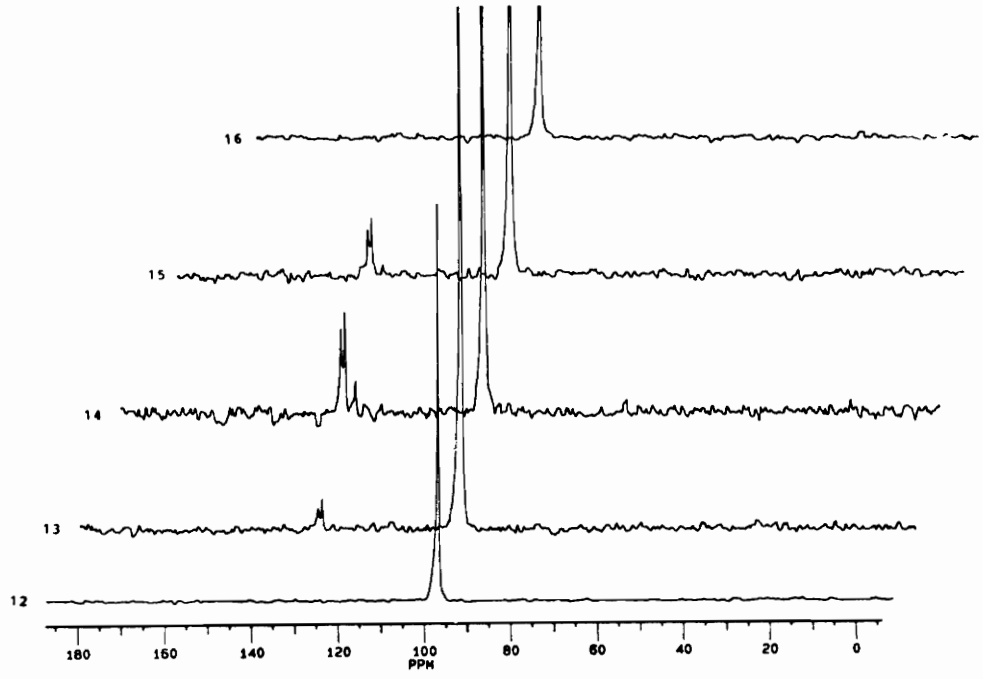

Figure 6.6 LC -^{13}C NMR (DNP), 1300 μL chlorobenzene, 3.3 mL/min, 10 scans/file, 31 sec/file, with CCl_4 as the mobile phase.

that aromatic carbon nuclei bonded to hydrogen atoms do not always possess scalar dominated DNP enhancements. For example, the carbon nuclei of benzene exhibit a dipolar dominated enhancement rather than the scalar dominated signals as in the aforementioned injection of chlorobenzene. It should also be noted that the presence of a three-spin effect would suppress the NMR signal for benzene (dipolar), but not for chlorobenzene (scalar).

Next, a fully substituted haloalkane (1250 μL hexachloroethane) was injected onto the column. It is expected that one NMR signal would be observed with an increase in intensity arising from six identical ^{13}C NMR signals coalescing into a larger singlet. Figure 6.7 does indeed reveal the signal for hexachloroethane, but the signal-to-noise ratio is only about 10:1 (RMS). Without DNP, the signal would not be observable, but the enhancement is much lower for hexachloroethane than for chloroform or trichloroethylene - where hydrogen bonding interactions with the radical can occur to yield larger increases in signal intensity.

Figure 6.8 reveals the ^{13}C NMR spectra arising from an injection of 1000 μL of hexafluorobenzene. From a detection standpoint, it is anticipated that a relatively large dipolar dominated NMR signal in the

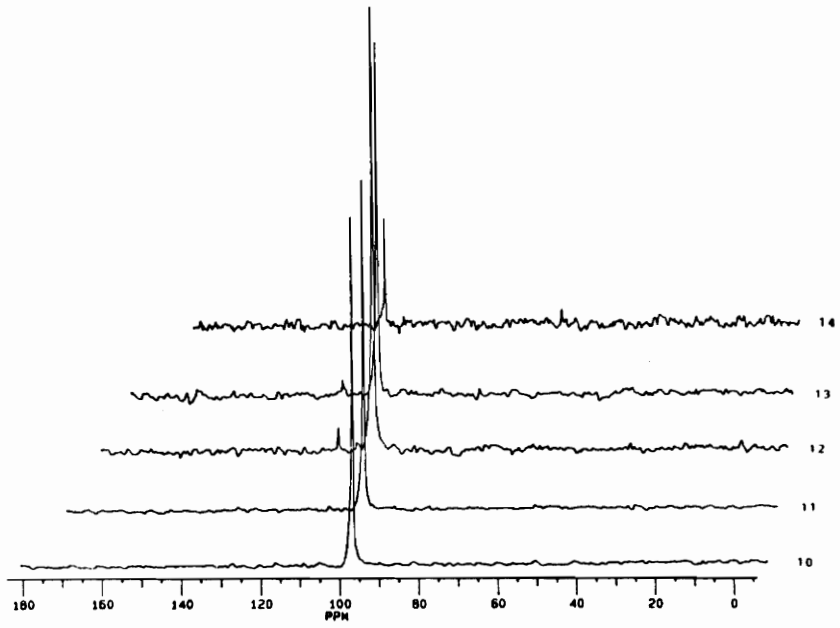

Figure 6.7 LC -^{13}C NMR (DNP), 1250 μL hexachloroethane, 2.3 mL/min, 8 scans/file, 31 sec/file, with CCl_4 as the mobile phase.

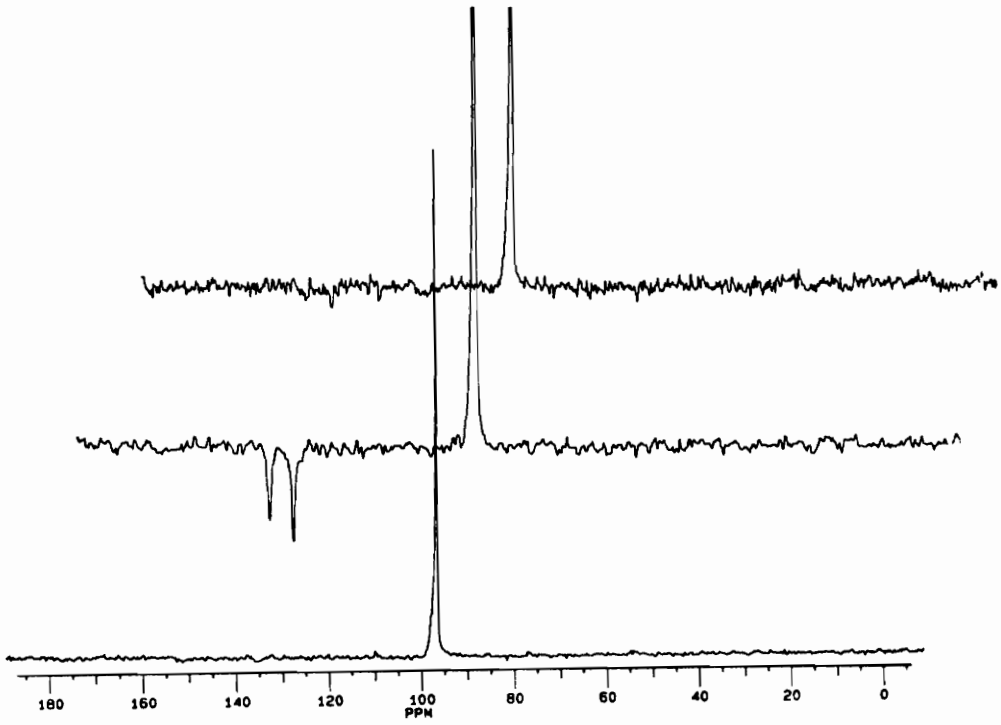

Figure 6.8 LC -^{13}C NMR (DNP), 1000 μL hexafluorobenzene, 3.3 mL/min, 10 scans/file, 31 sec/file, with CCl_4 as the mobile phase.

negative direction will be observed. As stated previously, dipolar dominated signals arising from SLIT DNP as a LC detector tend to be relatively weak in the present experiment, but now it can be seen that dipolar dominated signals arising from fluorine atoms (e.g. C - F) do exhibit **large** negative enhancements due to interactions of the lone pairs of electrons with the immobilized radical.[48-50] A doublet was observed for hexafluorobenzene since ^{19}F decoupling { ^{19}F } was not employed in the present study.

6.2.2 Injections of two or three compounds.

At this point, an investigation pertaining to the injection of two closely eluting compounds was explored. Figure 6.9 shows the resulting NMR spectra of an injection of 725 μL tetrachloroethylene and 725 μL trichloroethylene at a chromatographic flow rate of 2.3 mL/min. The increase and decrease in signal intensity of both compounds is observed. Note that although equal volumes of these compounds were injected, the signal intensity for trichloroethylene (^{13}C nuclei attached to Cl atoms) is much greater than that of the tetrachloroethylene molecule. The explanation for this phenomenum is as follows:

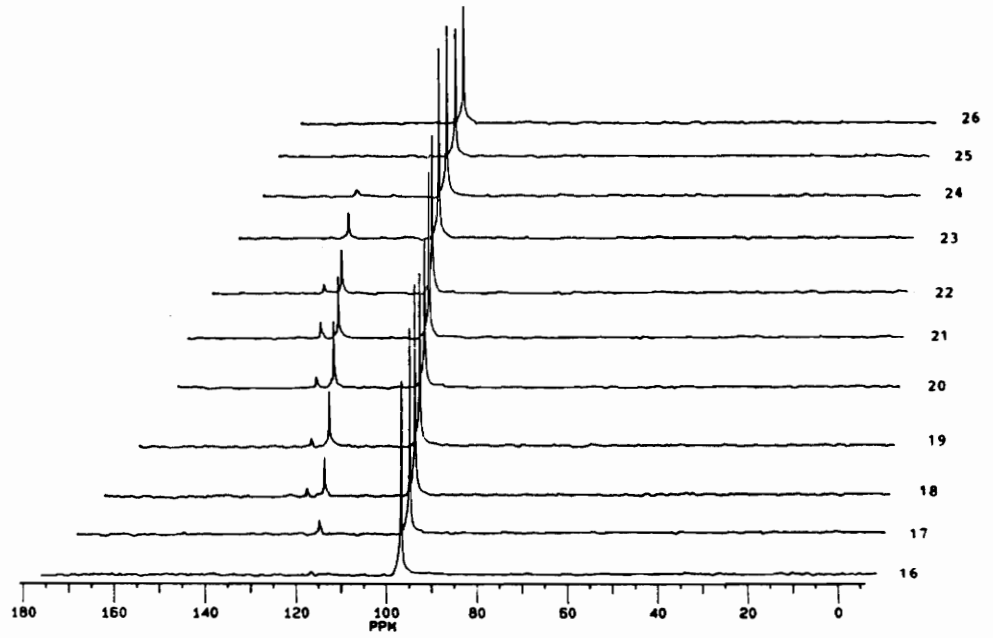

Figure 6.9 LC -^{13}C NMR (DNP), 725 μL tetrachloroethylene, 725 μL trichloroethylene, 2.3 mL/min, 5 scans/file, 19 sec/file, with CCl_4 as the mobile phase.

Without utilizing DNP, trichloroethylene would yield two distinct NMR signals - one from position C-1 and the other from position C-2. However, the ^{13}C signal from position C-2 (the carbon with two chlorine atoms attached) is not observed; instead only the ^{13}C signal from position C-1 (the carbon with the proton and one chlorine attached) is observed. As stated earlier, the enhancement is typically greater for those nuclei which have a more efficient interaction with the radical. Hydrogen bonding interactions with the radical (position C-1) as in trichloroethylene yield much larger scalar dominated signal enhancements than do interactions arising from ^{13}C nuclei which only contain lone pair elections like chlorine atoms C-2.[48] For this reason, interaction between the radical at position C-1 is much more pronounced than at position C-2.

Tetrachloroethylene exhibits one signal arising from two equivalent carbon atoms. Figure 6.9 reveals that the expected tetrachloroethylene signal is indeed observed (albeit relatively weak). No H-bonding with the radical can occur for this molecule whereas the ^{13}C NMR signal arising from position C-1 of trichloroethylene is scalar dominated and large due to

the hydrogen bonding considerations[48] with the immobilized radical as previously discussed.

The effect of an increase in injection volume is illustrated in Figure 6.10 where 1250 μL tetrachloroethylene and 1250 μL trichloroethylene were injected. At 19 seconds per file, the elution time of trichloroethylene is on the order of 4 minutes; however if sensitivity limits were improved even further, then tailing from column overloading would be more evident. In terms of the tetrachloroethylene molecule, the detection limits for this compound are much higher than that of the trichloroethylene molecule.

Next, a mixture of two halogenated aromatics was chromatographically separated. Figure 6.11 shows the resulting NMR spectra of injections of 725 μL chlorobenzene and 725 μL 1,3,5-trichlorobenzene. The flow rate was 2.3 mL/min with each file consisting of only 6 scans. From the data, it can be seen that 1,3,5-trichlorobenzene elutes slightly before chlorobenzene (file #15). By file #16, the NMR signal intensity of both compounds has increased, and by file #17 it can be seen that the trichlorobenzene signal intensity has diminished whereas the intensity of the chlorobenzene is still relatively strong. By file #18 the trichlorobenzene has almost vanished while the

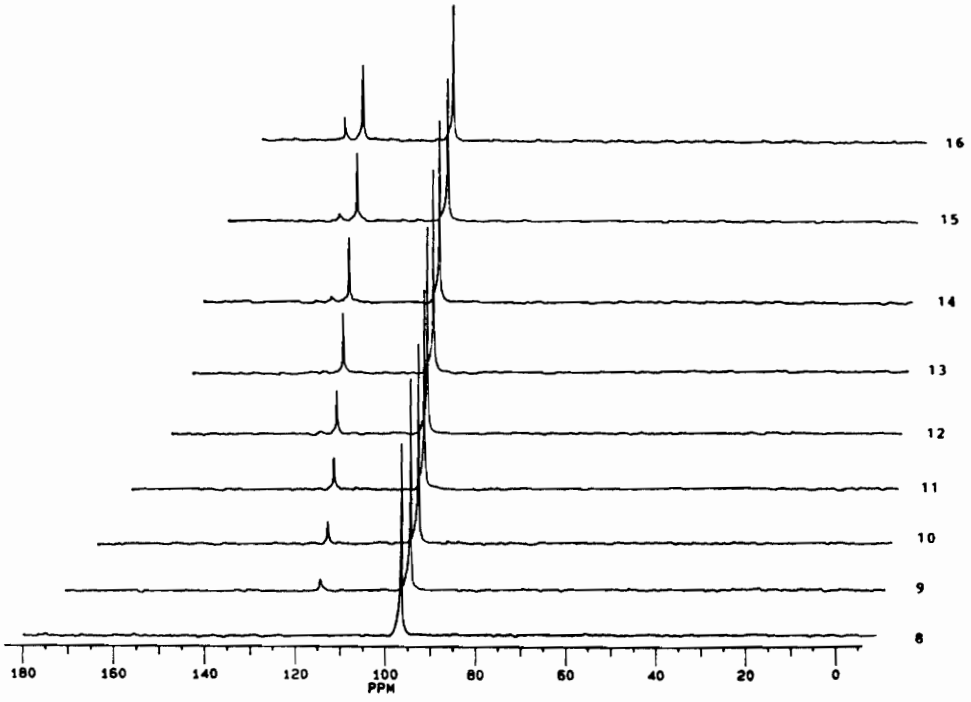

Figure 6.10 LC -^{13}C NMR (DNP), 1250 μL tetrachloroethylene, 1250 μL trichloroethylene, 2.3 mL/min, 5 scans/file, 19 sec/file, with CCl_4 as the mobile phase.

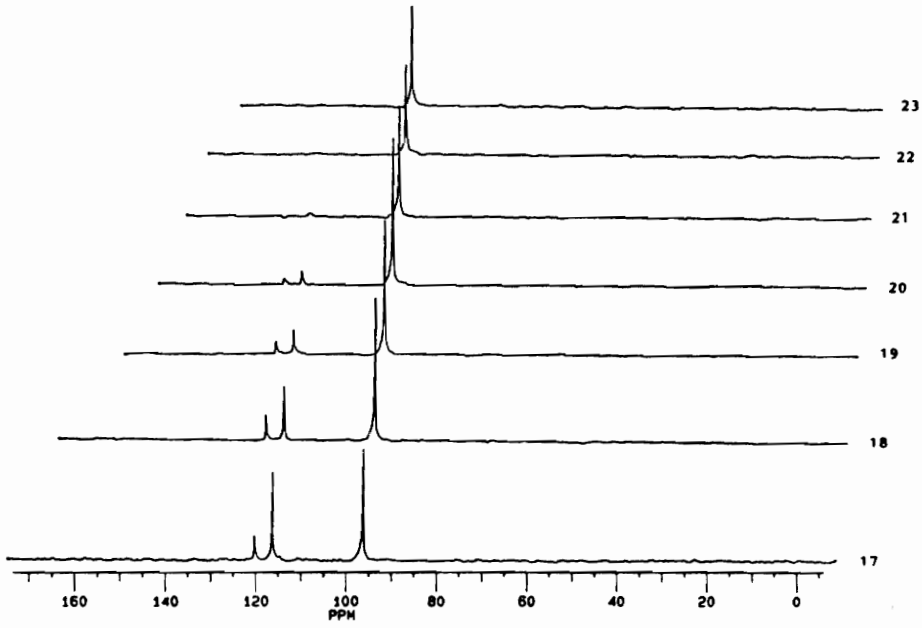

Figure 6.10 LC -^{13}C NMR (DNP), 1250 μL tetrachloroethylene, 1250 μL trichloroethylene, 2.3 mL/min, 5 scans/file, 19 sec/file, with CCl_4 as the mobile phase.

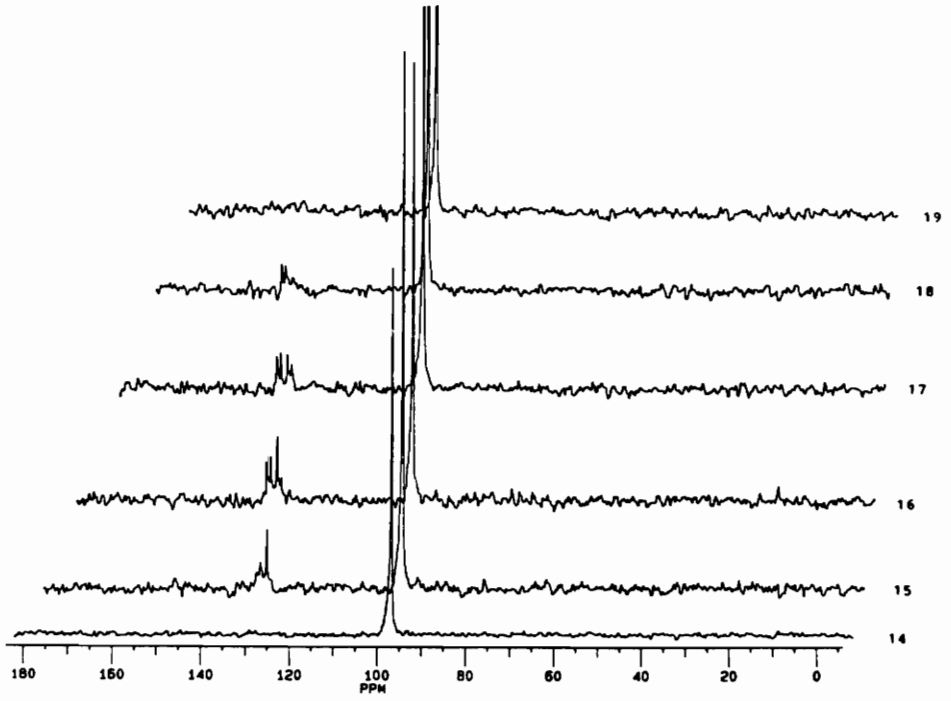

Figure 6.11 LC -^{13}C NMR (DNP), 725 μL chlorobenzene, 725 μL 1,3,5-trichlorobenzene, 2.3 mL/min, 5 scans/file, 23 sec/file, with CCl_4 as the mobile phase.

chlorobenzene signals remain, and by file #19, both compounds are no longer detectable in the flow cell. Thus, the elution order of these compounds is 1,3,5-trichlorobenzene followed by chlorobenzene. However it should be noted that although chromatographic resolution is lost for these two compounds, resolution is maintained in the chemical shift dimension.

Two NMR signals are expected to be observed for 1,3,5-trichlorobenzene whereas only the carbon atom bonded to the hydrogen is able to be observed. The carbon atom bonded to chlorine is not observed in the spectra (again the signal is suppressed due to the fact that the SLIT experiment is being utilized and therefore does not favor dipolar dominated signals unless irradiation of the ^{1}H frequency in the low magnetic field and/or utilization of LLIT DNP as the chromatographic detector would have been employed).

Likewise for the chlorobenzene molecule, **four** signals are expected to be observed in the resulting NMR spectra whereas only **three** signals are manifested. The carbon atom bonded to the chlorine is not detectable since it appears to possess a dipolar enhancement whose NMR signal is not favored by the SLIT experiment.

Figure 6.12 reveals the effect of employing too high a flow rate. At 3.5 mL/min with 10 scans/file and 31 sec/file, injections of 750 μL tetrachloroethylene and 500 μL chloroform result in similar elution times, and the separation is not efficient. The NMR signals from both compounds approach a maximum in file #14.

Also at 3.5 mL/min, a LC experiment was performed in which 250 μL tetrachloroethylene and 1000 μL chlorobenzene were injected on the column, and the resulting ^{13}C NMR spectra are presented in Figure 6.13.

6.2.3 Detection limits.

The next issue to address is the sensitivity and approximate detection limits for the present continuous-flow LC - ^{13}C NMR (DNP) apparatus. Figure 6.14 is the spectral profile when 98 μL chloroform and 975 μL trichloroethylene are introduced onto the column. Due to the aforementioned hydrogen bonding interactions with the immobilized SPIN radical, it was expected that these two compounds would possess the lowest minimum detectable quantities. At 77.5 ppm, the injection of only 98 μL of chloroform provides a DNP

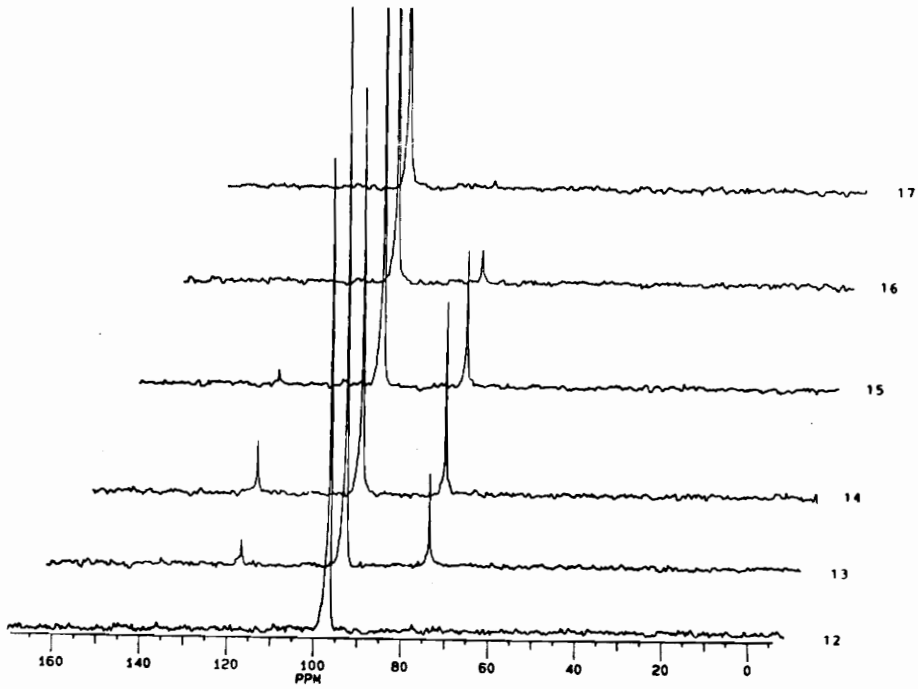

Figure 6.12 LC -^{13}C NMR (DNP), 750 μL tetrachloroethylene, 500 μL chloroform, 3.5 mL/min, 10 scans/file, 31 sec/file, with CCl_4 as the mobile phase.

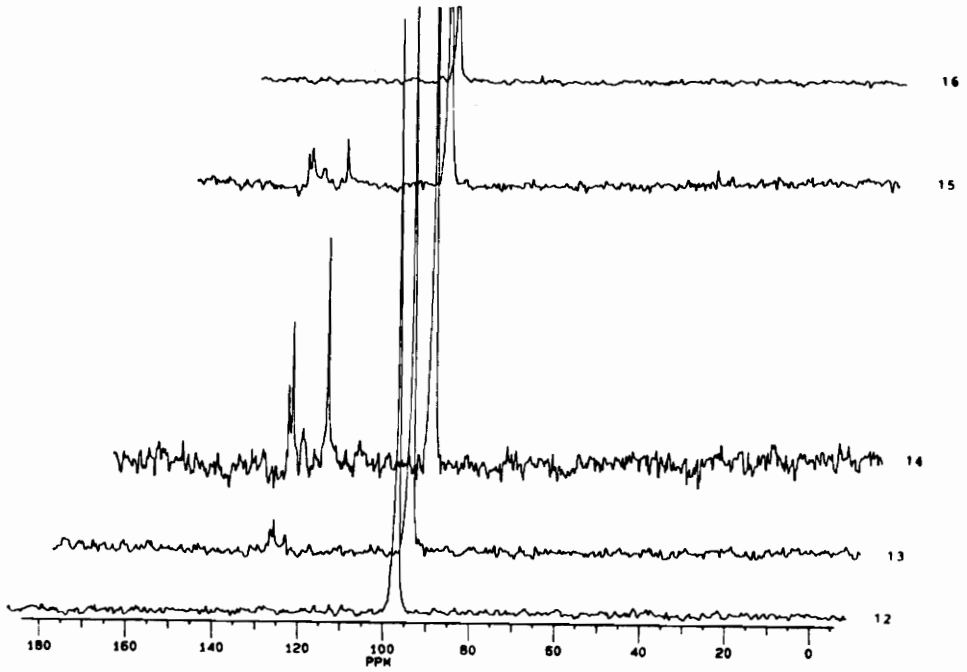

Figure 6.13 LC -^{13}C NMR (DNP), 250 μL tetrachloroethylene, 1000 μL chlorobenzene, 3.5 mL/min, 10 scans/file, 31 sec/file, with CCl_4 as the mobile phase.

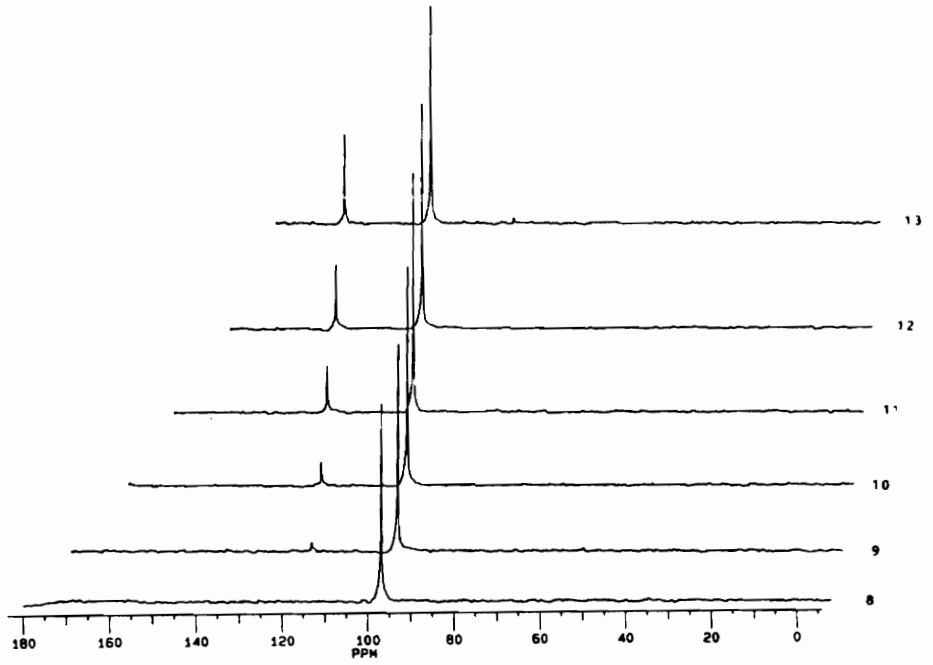

Figure 6.14 LC -^{13}C NMR (DNP), 98 μL chloroform, 975 μL trichloroethylene, 2.3 mL/min, 5 scans/file, 16 sec/file, with CCl_4 as the mobile phase.

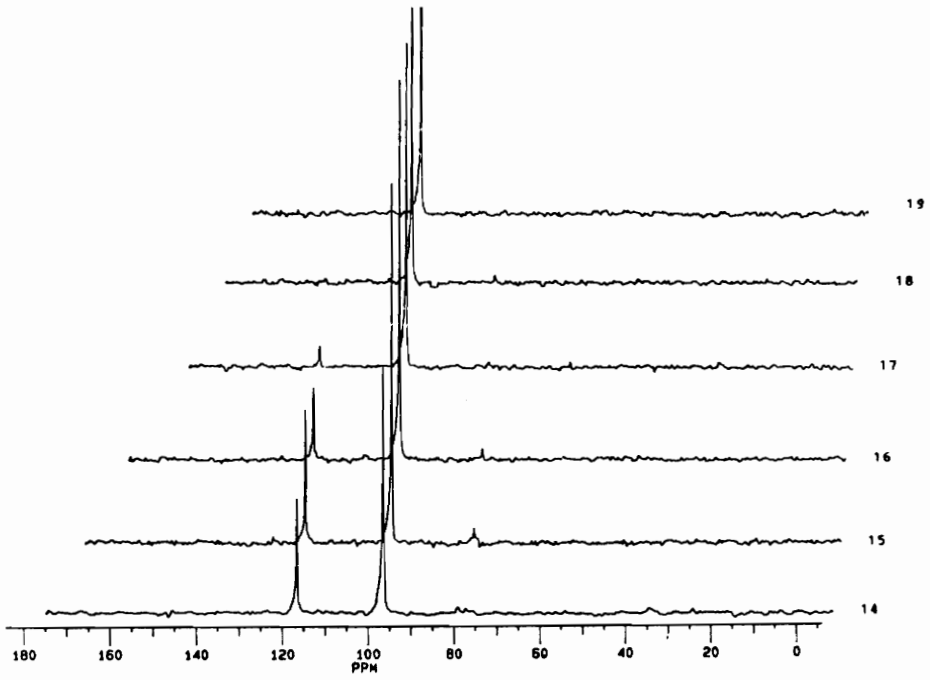

Figure 6.14 LC -^{13}C NMR (DNP), 98 μL chloroform, 975 μL trichloroethylene, 2.3 mL/min, 5 scans/file, 16 sec/file, with CCl_4 as the mobile phase.

enhanced NMR signal which can be observed in file #'s 13 - 18.

It was expected that 975 μL trichloroethylene would result in a large ^{13}C signal, which is indeed the case. At only 5 scans/file, it is incredible that ^{13}C NMR data with such a large a signal-to-noise ratio can be obtained.

Figure 6.15 shows the resulting ^{13}C NMR spectra from injections of 75 μL chloroform, 85 μL trichloroethylene, and 250 μL tetrachloroethylene. The purpose of this chromatographic run was to obtain approximate minimum detectable quantities for these compounds. Regarding the 75 μL chloroform injection, an insufficient signal-to-noise ratio was obtained to legitimately claim that the peak at 77.5 ppm is indeed representative of $CHCl_3$. This data combined with the NMR spectra previously obtained in Figure 6.14 suggest that the minimum detectable quantity lies in the range of 85 - 95 μL chloroform.

The injection of 85 μL trichloroethylene results in a NMR signal-to-noise ratio (peak-to-peak) of approximately 2:1 and a root mean square signal-to-noise of about 5:1. This relatively low minimum detectable quantity (high sensitivity) is a result of the efficient interaction between this analyte and the

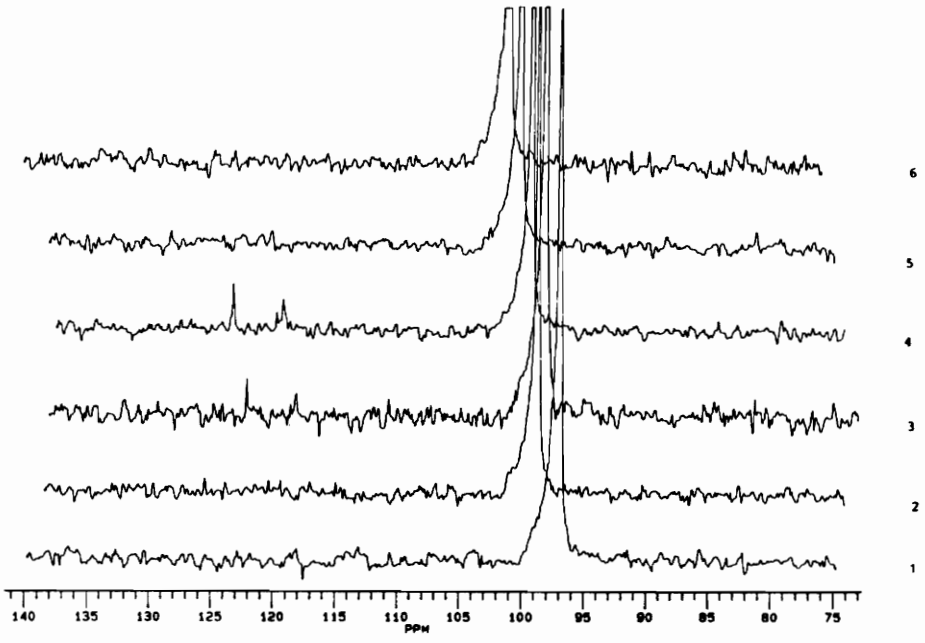

Figure 6.15 LC -^{13}C NMR (DNP), 75 μL chloroform, 85 μL trichloroethylene, 250 μL tetrachloroethylene, 2.8 mL/min, 10 scans/file, 35 sec/file, with CCl_4 as the mobile phase.

immobilized radical due to the hydrogen bonding which occurs and allows a more effective polarization build-up.

The injection of 250 μL tetrachloroethylene results in a peak-to-peak S/N of approximately 4 : 1 with a root mean square S/N of about 10 : 1. With this signal-to-noise ratio, it is estimated that injection volumes of 175 - 200 μL would still result in a detectable NMR signal. The minimum detectable quantity for tetrachloroethylene is higher than that for the chloroform and trichloroethylene molecules since the tetrachloroethylene contains no hydrogen atoms in its structure to interact with the immobilized radical, and hence lower enhancements are expected.

6.2.4 Injections of five or more compounds.

All future LC - ^{13}C NMR (DNP) experiments consist of a variety of injection mixtures which were

arbitrarily chosen. Thus the primary difference between each LC experiment was the selection of compounds to inject.

A more complex mixture consisting of seven compounds was next injected onto the column for the next ^{13}C LC - NMR (DNP) experiment. Figure 6.16 illustrates the resulting carbon NMR spectra of 400 μL chloroform, 400 μL trichloroethylene, 2000 μL hexafluorobenzene, 2000 μL chlorobenzene, 2000 μL benzene, 1200 μL tetrachloroethylene, and 1500 μL 1,3,5-trichlorobenzene at a flow rate of 2.3 mL/min of carbon tetrachloride. Each file consists of 10 scans with a time of 31 sec. At file #8, several of the compounds begin to elute from the column into the NMR detector flow cell. Hexafluorobenzene, 1,3,5-trichlorobenzene, and tetrachloroethylene elute with a strong S/N in file #8 with only traces of chlorobenzene and trichloroethylene being observed. In file #9, the chlorobenzene and trichloroethylene molecules exhibit a much higher signal-to-noise ratio and elute with much more prominence than in the preceding file. File #10 represents the beginning of the elution of chloroform - which can be detected over a span of seven files (approximately 3 minutes). The only molecule which was not observed was the injection of 2000 μL benzene. The

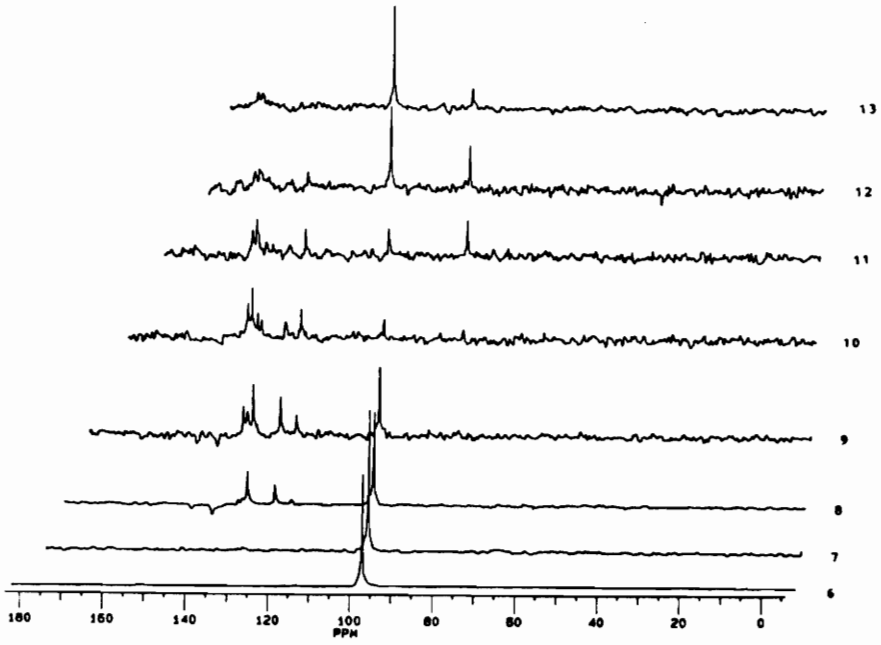

Figure 6.16 LC -^{13}C NMR (DNP), 400 μL chloroform, 400 μL trichloroethylene, 1200 μL tetrachloroethylene, 2000 μL hexafluorobenzene, 2000 μL benzene, 2000 μL chlorobenzene, 1500 μL 1,3,5-trichlorobenzene, 2.3 mL/min, 10 scans/file, 31 sec/file, with CCl_4 as the mobile phase.

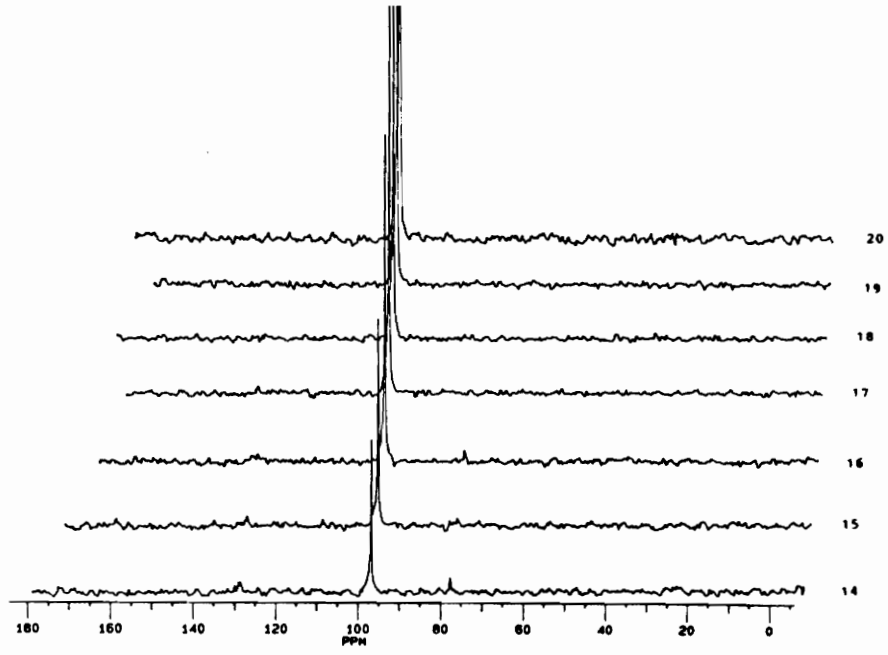

Figure 6.16 LC -^{13}C NMR (DNP), 400 μL chloroform, 400 μL trichloroethylene, 1200 μL tetrachloroethylene, 2000 μL hexafluorobenzene, 2000 μL benzene, 2000 μL chlorobenzene, 1500 μL 1,3,5-trichlorobenzene, 2.3 mL/min, 10 scans/file, 31 sec/file, with CCl_4 as the mobile phase.

reason for this lack of detection is most likely a result of a poor dipolar dominated DNP enhancement for benzene and/or the existence of a dominating three-spin effect which can reduce the intensity of the NMR signal to a null.

For the sake of comparison, an experiment was created which would demonstrate the effect of performing LC - ^{13}C NMR **without DNP.** Figure 6.17 is the resulting ^{13}C spectra for the next LC-NMR (without DNP) run which consists of an injection of an identical mix of 400 μL chloroform, 400 μL trichloroethylene, 2000 μL hexafluorobenzene, 2000 μL chlorobenzene, 2000 μL benzene, 1200 μL tetrachloroethylene, and 1500 μL 1,3,5-trichlorobenzene at a flow rate of 2.3 mL/min. All experimental conditions remained constant with the only difference between Figures 6.16 and 6.17 being the presence (DNP) or absence of the microwave source.

Figure 6.17 is respresentative of the LC experiment performed without DNP, and a rapid perusal of the resulting ^{13}C spectra reveals that only signals from three of the seven injected compounds are detectable. Thus the significance and potency of the DNP technique is established. Only the aromatic compounds of benzene, chlorobenzene, and 1,3,5-trichlorobenzene were detected. Benzene was observed

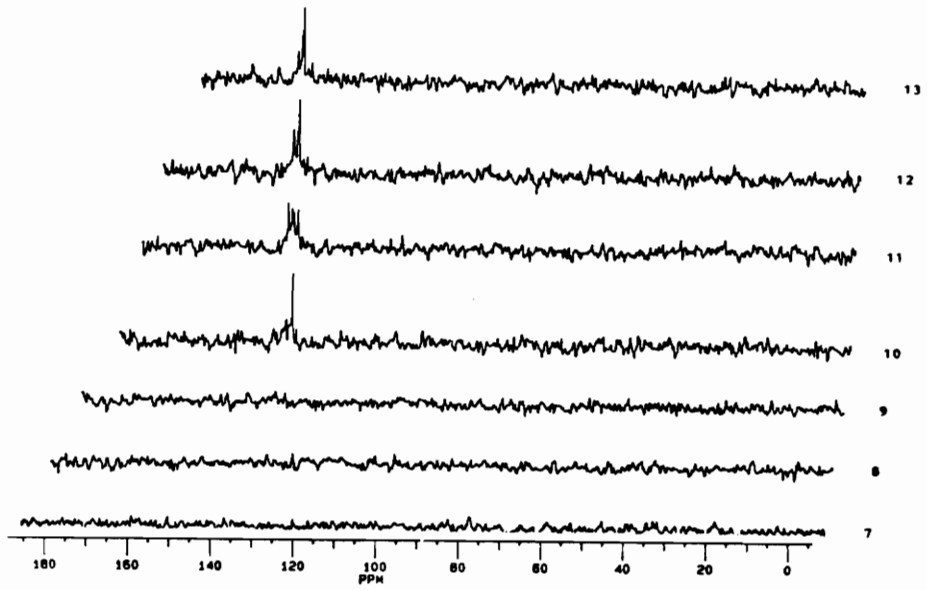

Figure 6.17 LC -^{13}C NMR **(without DNP)**, 400 μL chloroform, 400 μL trichloroethylene, 1200 μL tetrachloroethylene, 2000 μL hexafluorobenzene, 2000 μL benzene, 2000 μL chlorobenzene, 1500 μL 1,3,5-trichlorobenzene, 2.3 mL/min, 10 scans/file, 31 sec/file, with CCl_4 as the mobile phase.

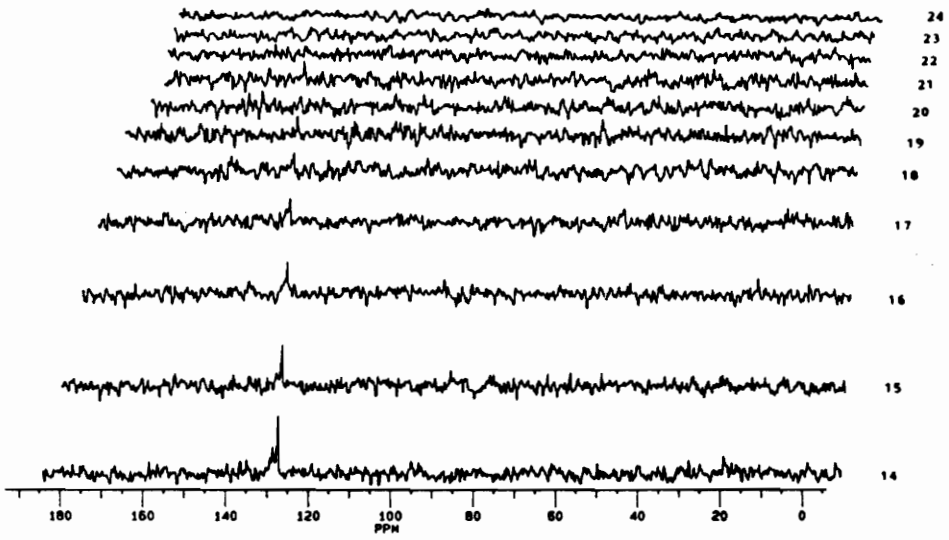

Figure 6.17 LC -^{13}C NMR (without DNP), 400 μL chloroform, 400 μL trichloroethylene, 1200 μL tetrachloroethylene, 2000 μL hexafluorobenzene, 2000 μL benzene, 2000 μL chlorobenzene, 1500 μL 1,3,5-trichlorobenzene, 2.3 mL/min, 10 scans/file, 31 sec/file, with CCl_4 as the mobile phase.

due to the large injection volume, a possible nuclear Overhauser effect (NOE), six equivalent carbons which coalesce into one strong NMR signal, and perhaps due to a better preequilibration build-up. Two of the carbon atoms in chlorobenzene were observed due to the large injection volume, the two equivalent carbons in positions 2 and 3 in the ring, and perhaps due to better polarization build-up before sampling the detector volume with a r.f. pulse (scan). Likewise, 1,3,5-trichlorobenzene was also observed due to a large injection volume and to the three equivalent carbons at position #'s 2,4,6. The remaining compounds which were present in relatively small amounts were not observed. Even more striking, the solvent (mobile phase) signal is not observed. This is probably due to a combination of several factors which contribute to the low signal intensity of the solvent. First, there is only one equivalent ^{13}C in carbon tetrachloride, and consequently increases in signal intensity arising from the possession of several equivalent nuclei in a given molecule can not occur. Second, there are no attached protons to the carbon atom to allow for an enhancement from NOE build-up. Third, CCl_4 contains a quaternary carbon - which bears no hydrogen atoms that can participate in relaxation mechanisms and can therefore

possess larger relaxation times. Since carbon tetrachloride fulfills these conditions, these nuclei require longer time delays between scans to avoid a potential reduction in signal intensity arising from sampling a detection volume with a r.f. pulse to previously excited ^{13}C nuclei which have not yet had sufficient time to relax and return to their equilibrium distribution before the next scan.

A comparison with and without DNP already performed with the previous two LC experiments, mixtures of different compositions were then injected onto the column. Figure 6.18 reveals the resulting ^{13}C spectra following an injection of 1000 μL chloroform, 1500 μL tetrachloroethylene, 2500 μL hexafluorobenzene, 1500 μL 1,1,1-trichlorotrifluoroethane, and 3000 μL benzene at a flow rate of 2.5 mL/min. Each file consists of only 5 scans with a time per file of 19 seconds. Signals from all five compounds are detected with chloroform eluting first in file #12 and continuing to file #23. Tetrachloroethylene is next to elute and can be seen in file #14 and continuing to file #20. Next, hexafluorobenzene elutes from file #'s 17 - 22. The 1,1,1-trichlorotrifluoroethane is detectable between file #'s 20 - 21 with the last compound to elute being benzene which can be observed

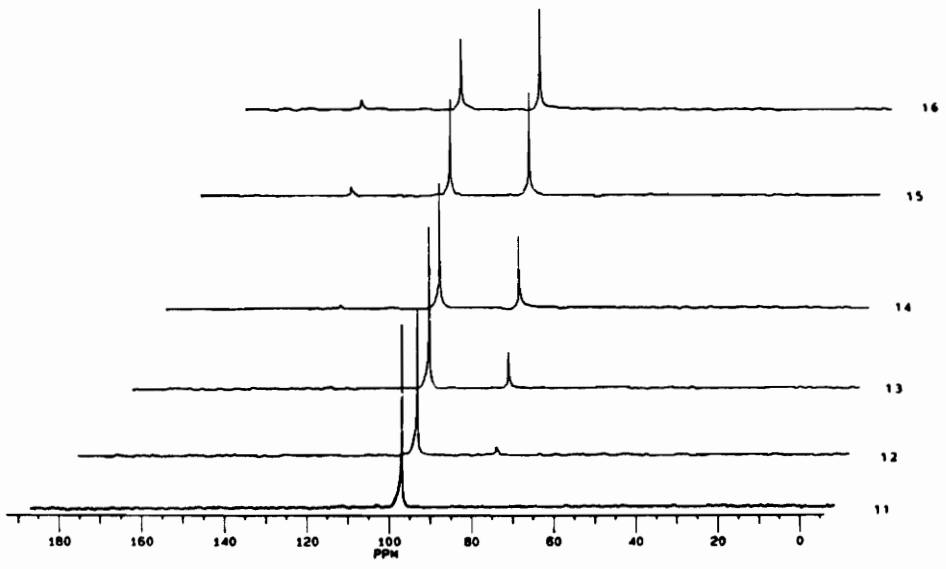

Figure 6.18 LC -^{13}C NMR (DNP), 1000 μL chloroform, 1500 μL tetrachloroethylene, 2500 hexafluorobenzene, 3000 μL benzene, 1500 hexachloroethane, 2.5 mL/min, 5 scans/file, 19 sec/file, with CCl_4 as the mobile phase.

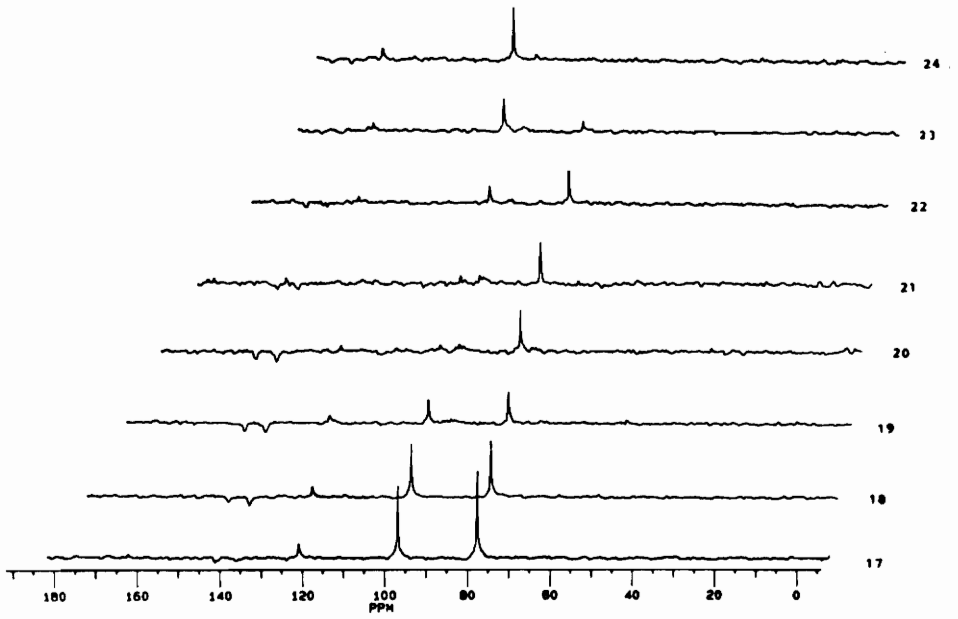

Figure 6.18 LC -^{13}C NMR (DNP), 1000 μL chloroform, 1500 μL tetrachloroethylene, 2500 hexafluorobenzene, 3000 μL benzene, 1500 hexachloroethane, 2.5 mL/min, 5 scans/file, 19 sec/file, with CCl_4 as the mobile phase.

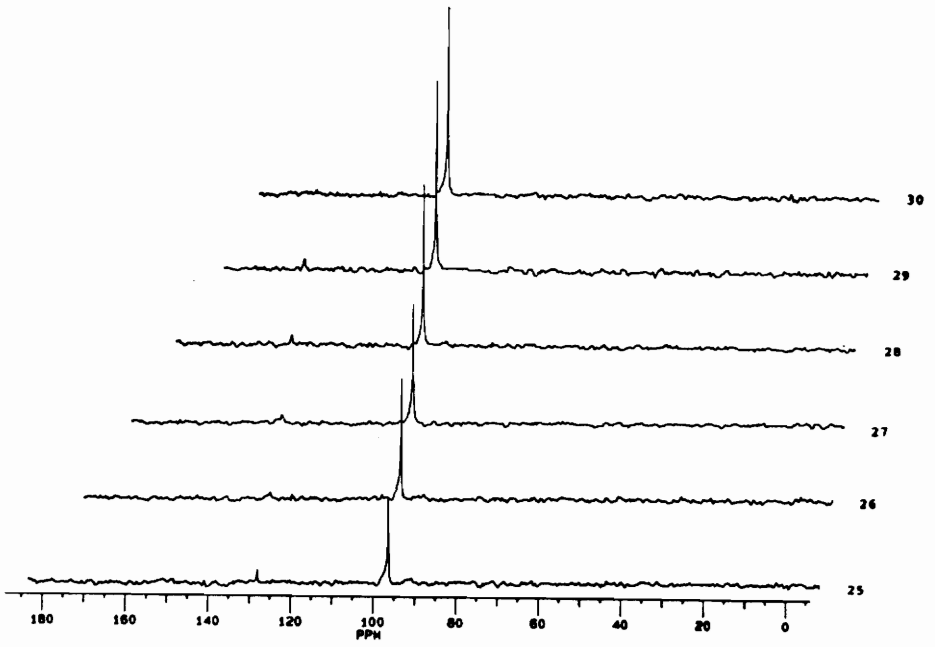

Figure 6.18 LC -^{13}C NMR (DNP), 1000 μL chloroform, 1500 μL tetrachloroethylene, 2500 hexafluorobenzene, 3000 μL benzene, 1500 hexachloroethane, 2.5 mL/min, 5 scans/file, 19 sec/file, with CCl_4 as the mobile phase.

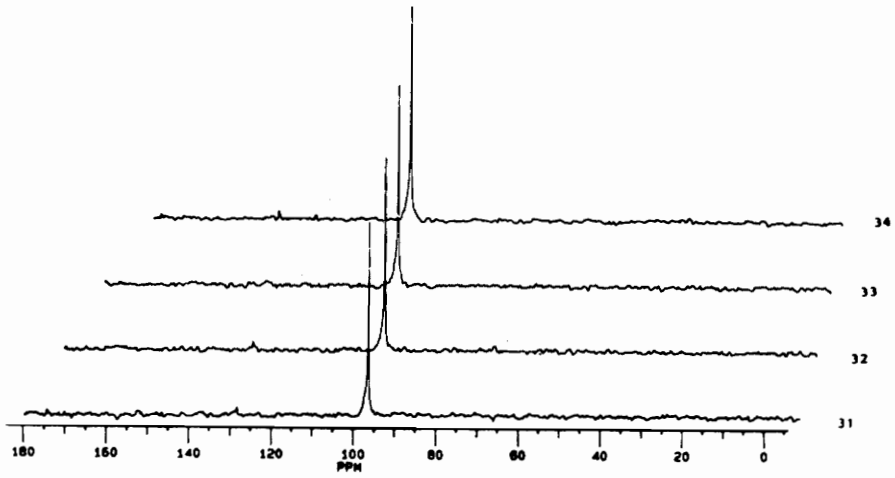

Figure 6.18 LC -^{13}C NMR (DNP), 1000 μL chloroform, 1500 μL tetrachloroethylene, 2500 hexafluorobenzene, 3000 μL benzene, 1500 hexachloroethane, 2.5 mL/min, 5 scans/file, 19 sec/file, with CCl_4 as the mobile phase.

from file #'s 23 - 34. Despite the large injection volume and despite the six equivalent carbons of benzene, a relatively weak NMR signal is observed due to a modest dipolar DNP enhancement and/or to the presence of a three-spin effect which further reduces the DNP enhancement.

The next experimental LC - ^{13}C DNP experiment is illustrated in Figure 6.19 which reveals the resulting NMR spectra following an injection of 800 μL chloroform, 1200 μL tetrachloroethylene, 1600 μL trichloroethylene, and 1300 μL 1,1,1-trichlorotrifluoroethane onto the column at a slower flow rate of 2.3 mL/min. Each file consists of 10 scans with 31 seconds per file. The elution of both trichloroethylene and 1,1,1-trichlorofluoroethane can be observed as early as file #3. Trichloroethylene is observed from file #3 to file #13 - a time span of approximately of 5 - 6 minutes while 1,1,1-trichlorotrifluoroethane extends from file #3 to #8. Tetrachloroethylene emerges in file #6 and remains until file #9. Finally, chloroform elutes at file #9 and can be observed as late as file #18 - a time span of 5 minutes which serves as an indication of the sensitivity of the LC - ^{13}C NMR apparatus.

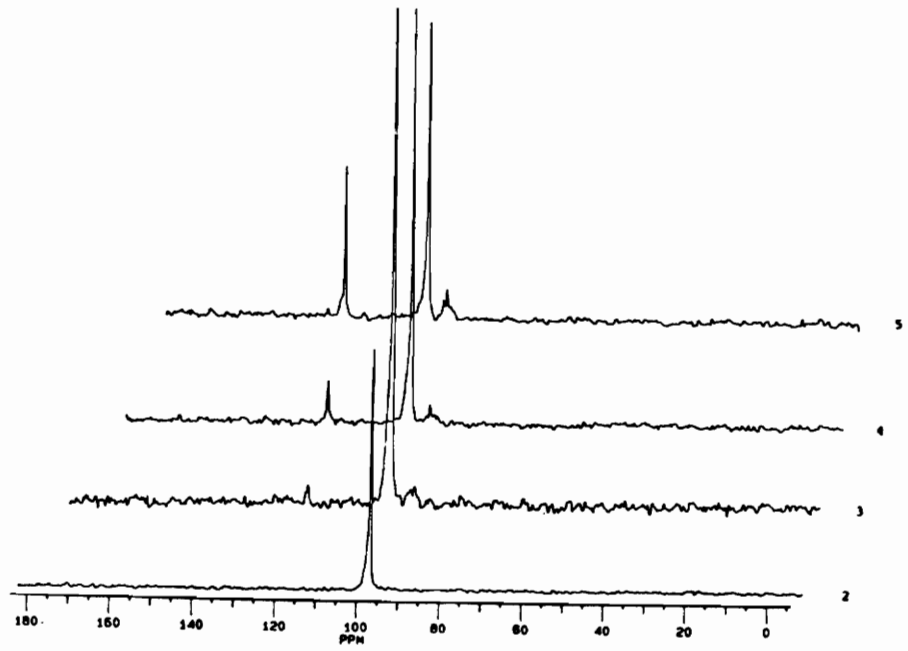

Figure 6.19 LC -^{13}C NMR (DNP), 800 μL chloroform, 1200 μL tetrachloroethylene, 1600 μL trichloroethylene, 1300 μL 1,1,1-trichlorotrifluoroethane, 2.3 mL/min, 10 scans/file, 31 sec/file, with CCl_4 as the mobile phase.

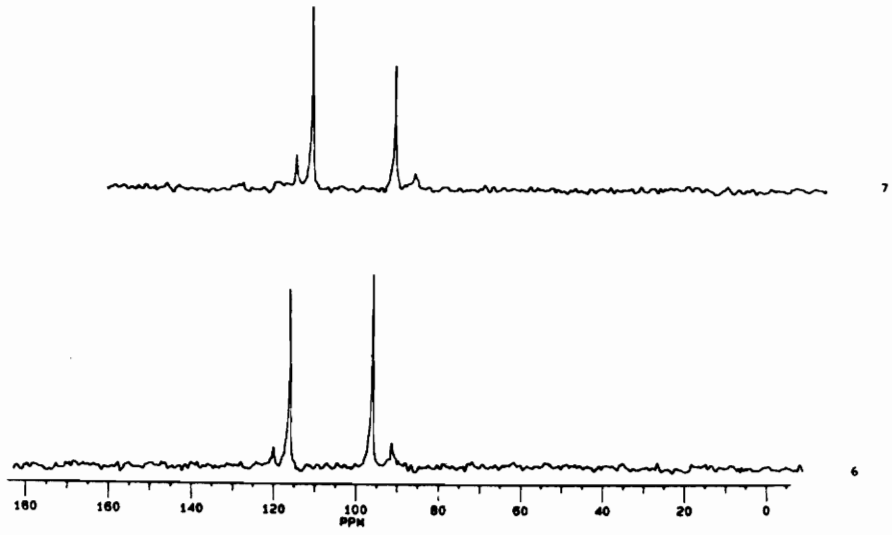

Figure 6.19 LC -^{13}C NMR (DNP), 800 μL chloroform, 1200 μL tetrachloroethylene, 1600 μL trichloroethylene, 1300 μL 1,1,1-trichlorotrifluoroethane, 2.3 mL/min, 10 scans/file, 31 sec/file, with CCl_4 as the mobile phase.

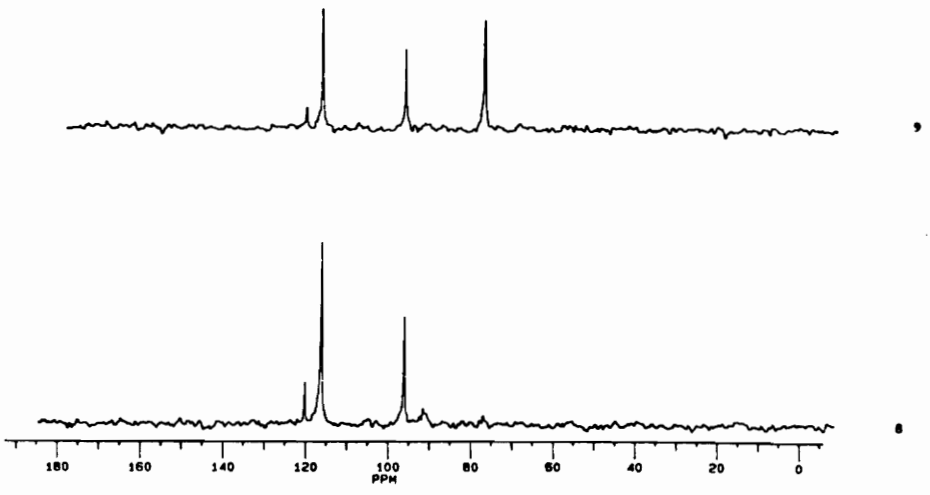

Figure 6.19 LC -^{13}C NMR (DNP), 800 μL chloroform, 1200 μL tetrachloroethylene, 1600 μL trichloroethylene, 1300 μL 1,1,1-trichlorotrifluoroethane, 2.3 mL/min, 10 scans/file, 31 sec/file, with CCl_4 as the mobile phase.

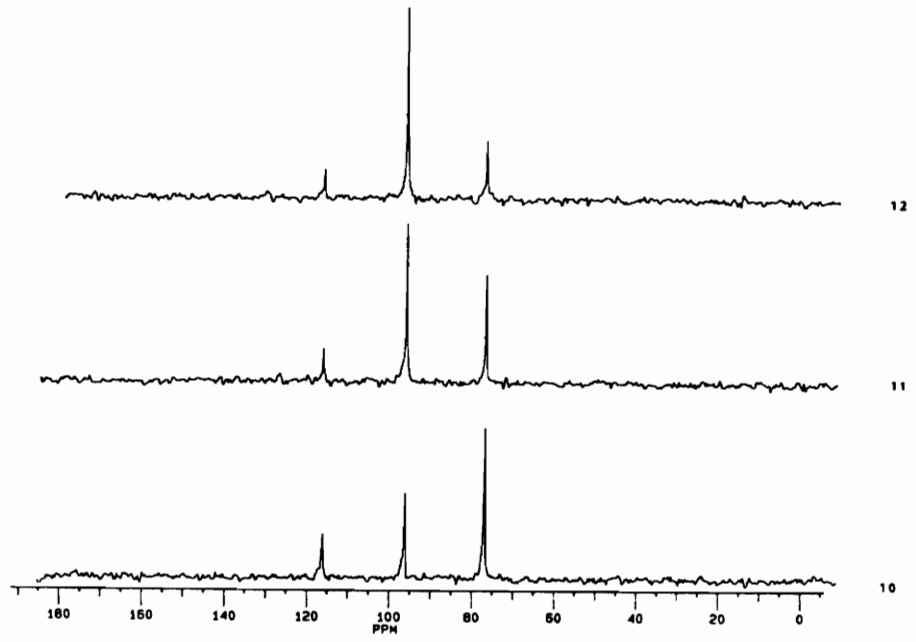

Figure 6.19 LC -^{13}C NMR (DNP), 800 μL chloroform, 1200 μL tetrachloroethylene, 1600 μL trichloroethylene, 1300 μL 1,1,1-trichlorotrifluoroethane, 2.3 mL/min, 10 scans/file, 31 sec/file, with CCl_4 as the mobile phase.

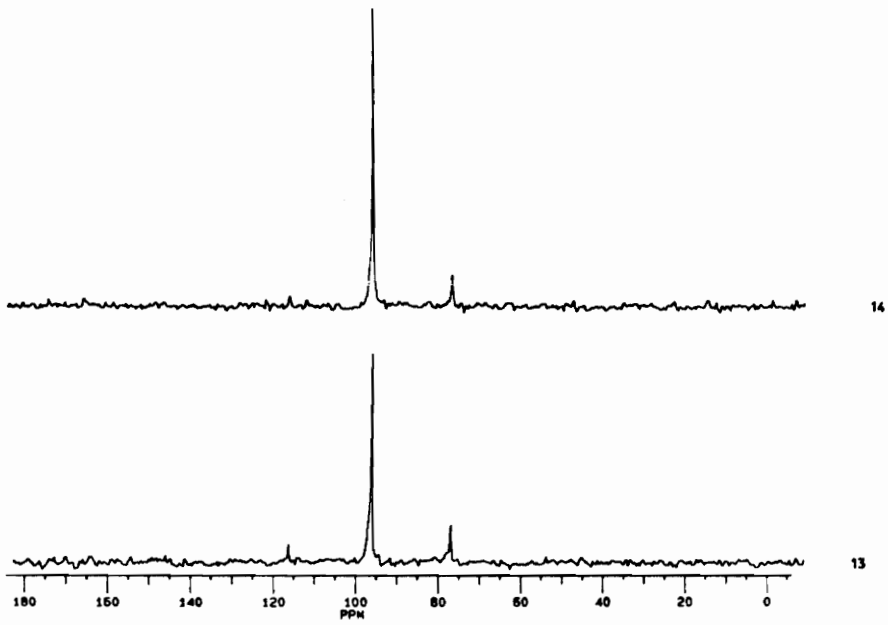

Figure 6.19 LC -^{13}C NMR (DNP), 800 μL chloroform, 1200 μL tetrachloroethylene, 1600 μL trichloroethylene, 1300 μL 1,1,1-trichlorotrifluoroethane, 2.3 mL/min, 10 scans/file, 31 sec/file, with CCl_4 as the mobile phase.

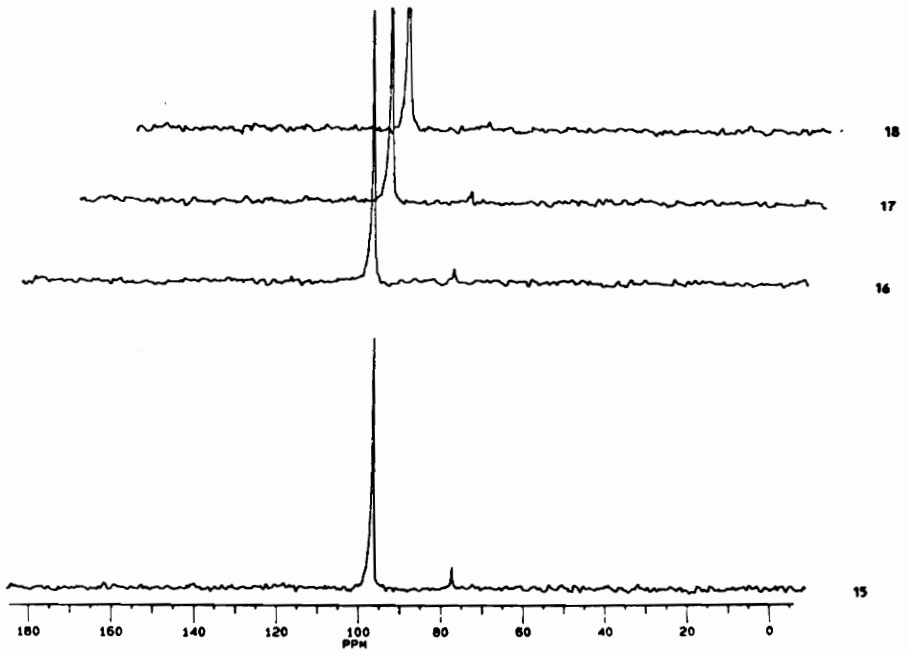

Figure 6.19 LC -^{13}C NMR (DNP), 800 μL chloroform, 1200 μL tetrachloroethylene, 1600 μL trichloroethylene, 1300 μL 1,1,1-trichlorotrifluoroethane, 2.3 mL/min, 10 scans/file, 31 sec/file, with CCl_4 as the mobile phase.

The ^{13}C NMR spectra for yet another LC - ^{13}C DNP experiment is illustrated in Figure 6.20. In this case, an injection of 500 μL chloroform, 750 μL tetrachloroethylene, 1000 μL trichloroethylene, 1000 μL 1,1,1-trichlorotrifluoroethane, 1000 μL 1,1,2-trichloro-1,2,2-trifluoroethane, 1300 μL hexachloroethane, 1500 μL chlorobenzene, and 1500 μL 1,3,5-trichlorobenzene was performed at a slightly higher flow rate of 3.5 mL/min. Each file consists of 10 scans with a time per file of 31 seconds.

Chloroform elutes first at file #12 and remains until file #20. The two aromatics (chlorobenzene and 1,3,5-trichlorobenzene) elute between file #'s 14 - 16. Hexachloroethane elutes next and is detected in file #16. The two freons (1,1,1-trichlorotrifluoroethane and 1,1,2-trichloro-1,2,2-trifluoroethane) both elute in file #17. Although both aromatic compounds exit the column at similar times and are not separated from a chromatographic standpoint, they are readily distinguished in the chemical shift domain utilizing NMR (DNP) detection. The remaining haloalkenes (trichloroethylene and tetrachloroethylene) are observed in file #'s 17 - 19.

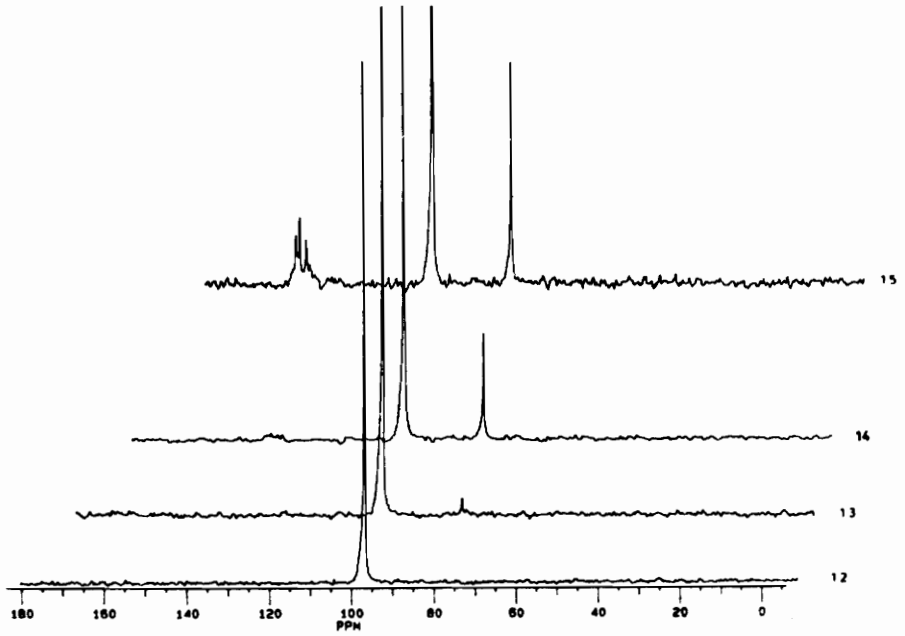

Figure 6.20 LC -^{13}C NMR (DNP), 500 μL chloroform, 750 μL tetrachloroethylene, 1000 μL trichloroethylene, 1000 μL 1,1,2-trichloro-1,2,2-trifluoroethane, 1000 μL 1,1,1-trichlorotrifluoroethane, 1300 μL hexachloroethane, 1500 μL 1,3,5-trichlorobenzene, 1500 μL chlorobenzene, 3.5 mL/min, 10 scans/file, 31 sec/file, with CCl_4 as the mobile phase.

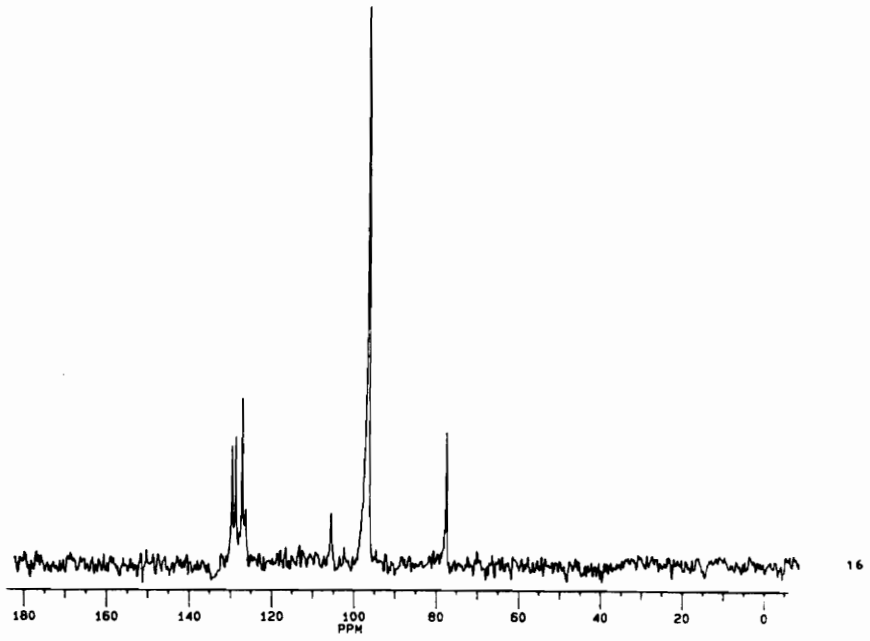

Figure 6.20 LC -^{13}C NMR (DNP), 500 μL chloroform, 750 μL tetrachloroethylene, 1000 μL trichloroethylene, 1000 μL 1,1,2-trichloro-1,2,2-trifluoroethane, 1000 μL 1,1,1-trichlorotrifluoroethane, 1300 μL hexachloroethane, 1500 μL 1,3,5-trichlorobenzene, 1500 μL chlorobenzene, 3.5 mL/min, 10 scans/file, 31 sec/file, with CCl_4 as the mobile phase.

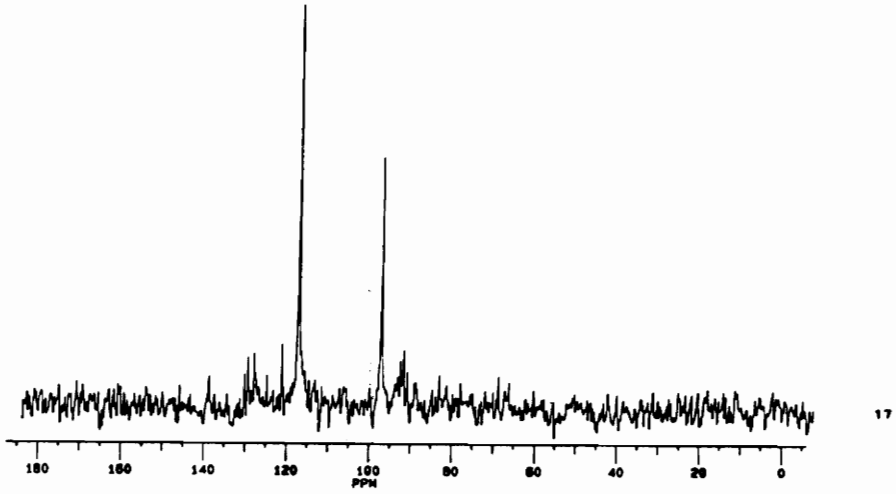

Figure 6.20 LC -^{13}C NMR (DNP), 500 μL chloroform, 750 μL tetrachloroethylene, 1000 μL trichloroethylene, 1000 μL 1,1,2-trichloro-1,2,2-trifluoroethane, 1000 μL 1,1,1-trichlorotrifluoroethane, 1300 μL hexachloroethane, 1500 μL 1,3,5-trichlorobenzene, 1500 μL chlorobenzene, 3.5 mL/min, 10 scans/file, 31 sec/file, with CCl_4 as the mobile phase.

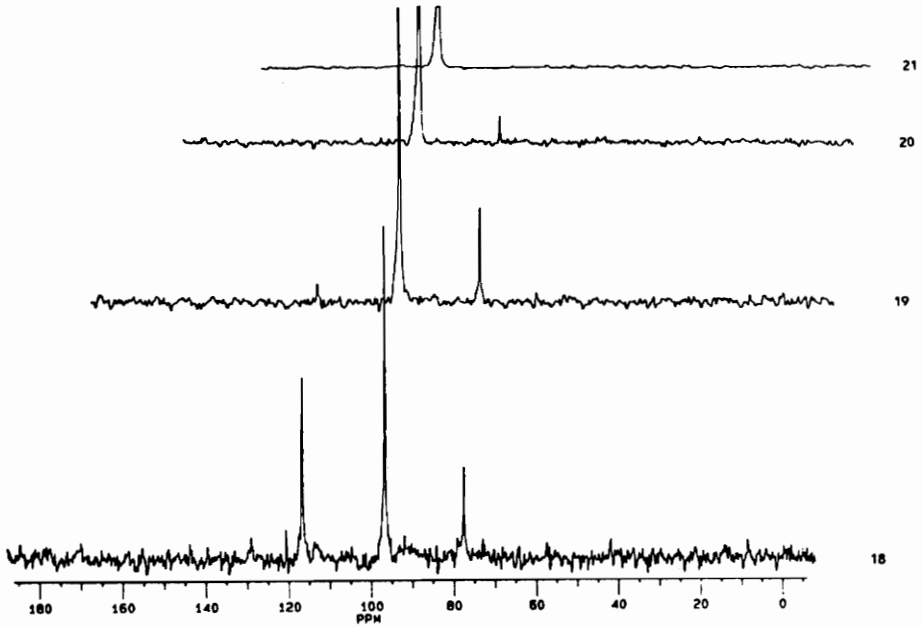

Figure 6.20 LC -^{13}C NMR (DNP), 500 μL chloroform, 750 μL tetrachloroethylene, 1000 μL trichloroethylene, 1000 μL 1,1,2-trichloro-1,2,2-trifluoroethane, 1000 μL 1,1,1-trichlorotrifluoroethane, 1300 μL hexachloroethane, 1500 μL 1,3,5-trichlorobenzene, 1500 μL chlorobenzene, 3.5 mL/min, 10 scans/file, 31 sec/file, with CCl_4 as the mobile phase.

6.3 Continuous-flow ^{13}C NMR (DNP) recycle experiments.

6.3.1 Introduction.

Continuous-flow NMR for ^{13}C nuclei has been utilized in the investigation of reaction pathways,[55-56] in quantitative studies,[65] in DEPT (Distortionless Enhanced Polarization Transfer) experiments,[66] and in studies of biological metabolites[67] in flowing systems. The reason for this dearth of information regarding flow ^{13}C NMR experiments is primarily due to the insensitivity of these nuclei arising from a low natural abundance relative to ^{1}H NMR.

Previous work on continuous-flow carbon-13 nuclear magnetic resonance spectroscopy has employed both enriched[56-58] and natural abundance[55,59-62] samples. The use of ^{13}C labelled samples enables an improvement in signal-to-noise due to a recovery of a factor of $\approx$ 100 from a natural abundance viewpoint.

The presence of flow in the NMR experiment requires several considerations. First, there is a potential loss in signal enhancements from a suppressed

nuclear overhauser effect (NOE). Second, broadening of the NMR signal with a concomitant reduction in peak intensity will occur at high flow rates. Another factor to consider in the flow experiment is obtaining sufficient preequilibration of the magnetization in the magnetic field prior to observation with a r.f. pulse (scan). To optimally satisfy this criterion, a time of 3-5 T_1 between each scan should be alloted in order to obtain full premagnetization build-up. However, relaxation times (T_1) for carbon nuclei are typically on the order of seconds to minutes which corresponds to relatively long build-up times. Thus, there is a lengthy delay between scans in the ^{13}C NMR experiment, and experimental time is thereby increased. However **when flow is involved** and after excitation of ^{13}C nuclei with a r.f. pulse, the sample volume can then be flushed from the detector cell, and fresh ^{13}C spins can enter the detector region for observation. Thus, the lengthy delays of seconds to minutes between scans normally employed in static NMR experiments are obviated. Quaternary carbons typically possess the largest T_1 values and the most inefficient relaxation mechanisms, and the long delays between scans and lengthy experimental times for static NMR experiments are often accentuated with quaternary ^{13}C nuclei. With

flow, however, quaternary carbons benefit the most since they are flushed from the detector cell as a function of flow rate. In addition, more scans per unit time can be taken, and this is the primary advantage of performing continuous-flow, recycle experiments. The presence of dynamic nuclear polarization (DNP) serves to augment the otherwise weak or non-existent ^{13}C NMR signal intensities. In summary, with the recycle DNP experiments, **more scans can be taken per unit time with increased sensitivity** relative to the static experiment and relative to flow recycle ^{13}C NMR experiments where DNP is not utilized.

6.3.2 Objectives.

The primary objectives of the recycle DNP experiments are to demonstrate (1) shorter experimental times relative to those obtained in the static mode and (2) increases in ^{13}C signal intensity, at least for certain classes of compounds. Secondary objectives include demonstrating the influence of increased free radical concentration in solution as well as the effect

of flow rate on the resulting ^{13}C NMR spectra when utilizing the liquid-liquid intermolecular transfer (LLIT) experiment.

6.3.3 SLIT recycle experiments.

The solid-liquid intermolecular transfer (SLIT) recycle experiments involve a mixture of halogenated and non-halogenated compounds (Test Mixture "A") as manifested in Table 6.1. Carbon tetrachloride was present as the solvent in a ratio of approximately 5 : 1 (v/v) with the remaining compounds; whereas the aromatic compounds were at concentrations of ≈ 20 % (v/v). Finally, the halogenated alkanes, alkenes, and aromatics were present in the lowest concentrations with chloroform present at only 0.36 % (v/v). In summary, most of the aromatics (benzene and chlorobenzene) were present in relatively large amounts in order to demonstrate whether or not the weak dipolar dominated and scalar dominated signals could be observed with DNP. In constrast, 1,3,5-trichlorobenzene, hexachlorobenzene, chloroform, hexachloroethane, trichloroethylene, and

tetrachloroethylene were present in only trace amounts in order to demonstrate the potential impact for DNP enhancements of NMR signal intensities.

Figure 6.21 shows the resulting NMR spectrum from Test Mixture "A", which represents 896 scans at a flow rate of 3.5 mL/min with an elapsed experimental time of only 56 minutes. The presence of a nuclear Overhauser effect (NOE) would probably not be observed since radicals are present. In this case, the presence of a NOE was not wanted in order to investigate whether or not a nuclear Overhauser effect (yielding a "+" influence on peak height) was reducing the signal intensity of dipolar dominated NMR signals (yielding a "-" influence on peak height).

To exhibit enhancements in NMR signal intensity from the presence of a NOE, the dominant relaxation pathway for "excited" ^{13}C nuclei must originate from a dipole-dipole mechanism. In the absence of a nuclear-electon relaxation mechanism (i.e. in the absence of a radical), ^{13}C nuclei bearing a hydrogen typically possess a dipole-dipole relaxation mechanism as the dominant one and therefore NOE enhancements are then possible. For quaternary ^{13}C nuclei (e.g. the solvent CCl_4) that possess no attached hydrogens, a NOE enhancement can not occur.

TABLE 6.1

TEST MIXTURE "A"

FOR SLIT AND LLIT EXPERIMENTS

SOLVENT IS CARBON TETRACHLORIDE

Compound	Concentration (M)
chloroform	0.0447 M
trichloroethylene	0.0694 M
hexachloroethane	0.0714 M
hexachlorobenzene	0.0761 M
1,3,5-trichlorobenzene	0.123 M
tetrachloroethylene	0.234 M
chlorobenzene	0.471 M
benzene	1.34 M

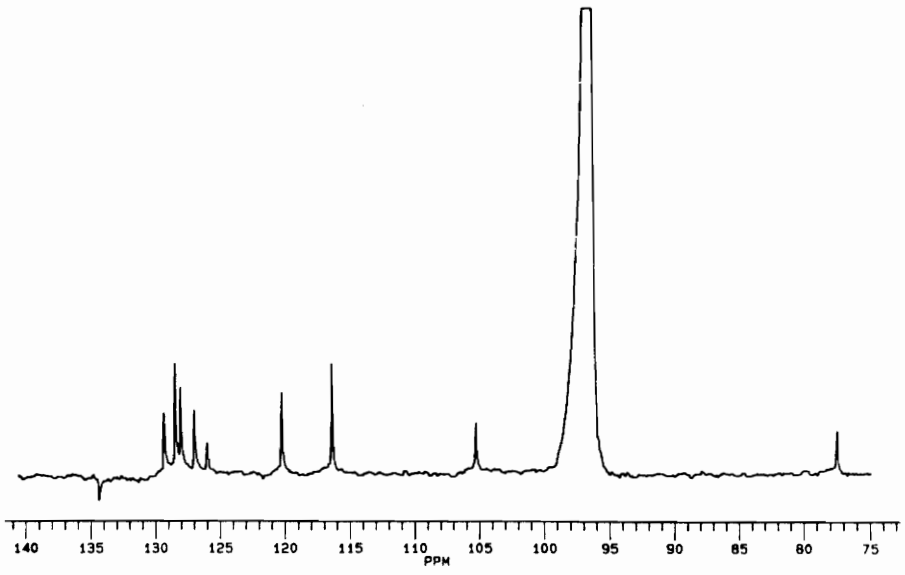

Figure 6.21 **Solid-Liquid Intermolecular Transfer (SLIT) experiment for Test Mixture A.** ^{13}C **NMR spectrum with DNP from recycling the mix for 896 scans at a flow rate of 3.5 mL/min with an elapsed time of 56 min. Data collection was obtained with the nuclear Overhauser effect. (with NOE)**

Of the eight compounds present in the mixture, only ^{13}C NMR signals for the hexachlorobenzene molecule could not be observed. However, signals for chloroform, hexachloroethane, trichloroethylene, tetrachloroethylene, benzene, chlorobenzene, and 1,3,5-trichlorobenzene were observed. Note that for chlorobenzene, all ^{13}C NMR signals were observed (**both** scalar and dipolar dominated signals). In this case, dipolar dominated signals were observed with the SLIT experiment despite the fact that SLIT experiments are generally not favorable for yielding dipolar dominated signals.

In order to investigate the possibility of a nuclear Overhauser effect on the resulting spectrum, the decoupling power was gated on **only** during acquisition of the FID so that build-up of the NOE would be at a minimum. Experimental conditions remained constant except for suppression of NOE's. Figure 6.22 (896 scans, 56 minutes) represents the resulting ^{13}C NMR spectrum without the NOE, and it is observed that only a minimal improvement of only 5 - 10% in the signal-to-noise ratio occurs with the NOE. As expected, suppressed NOE's occur in the presence of the radical.

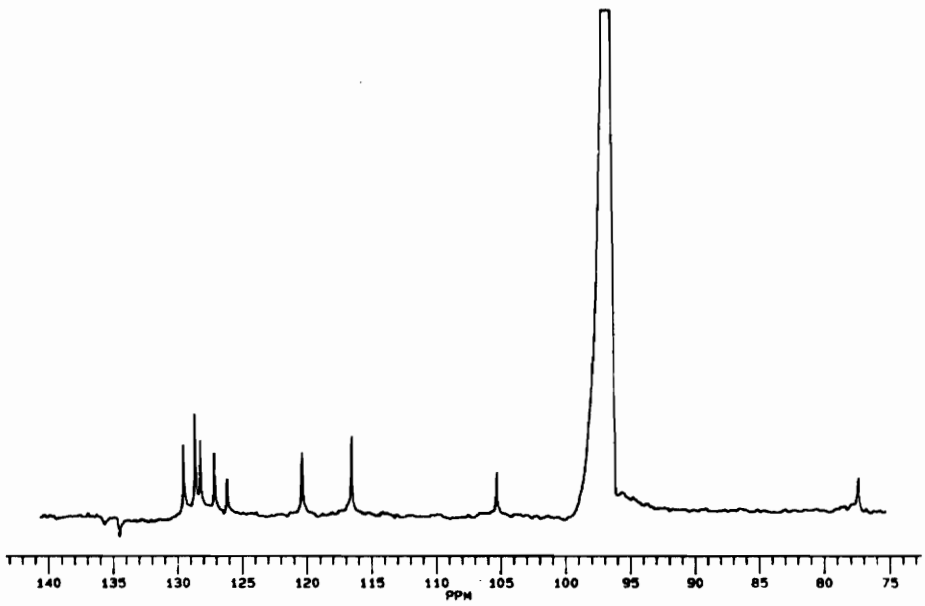

Figure 6.22 Solid-Liquid Intermolecular Transfer (SLIT) experiment for Test Mixture A. ^{13}C NMR spectrum with DNP from recycling the mix for 896 scans at a flow rate of 3.5 mL/min with an elapsed time of 56 min. Data collection was obtained with no nuclear Overhauser effect. (no NOE)

Next, a corresponding flow ^{13}C NMR spectrum was obtained **without utilizing DNP** for signal enhancement. Figure 6.23 illustrates the resulting ^{13}C NMR spectrum **without DNP** from recycling the test mix for 56 minutes (896 scans) at a flow rate of 3.5 mL/min. Experimental NMR parameters remained constant to ensure that an equivalent number of scans were obtained for an equivalent analysis time. The spectrum in Figure 6.23 (without DNP) demonstrates a significant reduction in signal-to-noise relative to earlier spectra where DNP was utilized. Note that only those compounds present in large quantities (benzene, chlorobenzene, and the solvent CCl_4) can be observed with the exception of one of the signals from 1,3,5-trichlorobenzene but with the poorest signal-to-noise ratio. Otherwise, none of the compounds present in trace amounts can be observed. The solvent peak exhibits a lower signal-to-noise ratio and is most likely due to the fact that CCl_4 has only one equivalent carbon with no attached proton and therefore enhancements from a NOE can not exist. An insufficient build-up of the premagnetization from too rapid a flow rate and from too small a preequilibration volume could occur for this compound due to its relatively large relaxation time (T_1). It is also possible that the signal intensity of the solvent peak

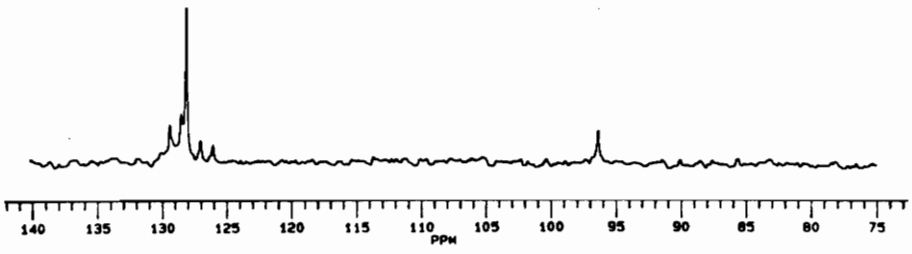

Figure 6.23 Solid-Liquid Intermolecular Transfer (SLIT) experiment for Test Mixture A. ^{13}C NMR spectrum **without DNP** from recycling the mix for 896 scans at a flow rate of 3.5 mL/min with an elapsed time of 56 min. Data collection was obtained with the nuclear Overhauser effect. (with NOE)

is reduced due to an insufficient time delay between scans. Benzene and chlorobenzene **do** possess attached protons and exhibit a NOE provided that the flow rate is not too rapid to permit sufficient preequilbration. The high signal-to-noise of benzene is most likely due to the presence of a NOE and due to the existence of **six** equivalent carbons - whose NMR signal coalesces into a large singlet.

At a flow rate of 3.5 mL/min with a detector cell volume of 150 μL, the sample bolus is mathematically flushed from the flow cell every 2.57 seconds. The delay between scans for the spectra was 3.50 seconds and was set for 1 second longer than the flush time to avoid scanning too rapidly (i.e. applying a r.f. pulse to ^{13}C nuclei which are still "excited" from the previous pulse and have not had sufficient time to "relax" and return to equilibrium).

To demonstrate the potential power of DNP for signal enhancement, the test mixture was recycled for **only 3½ minutes** (56 scans) at a flow rate of 3.5 mL/min as illustrated in Figure 6.24. Even after this brief time period, the compounds present in trace amounts were still observed with the exception of hexachlorobenzene which was never observed with the SLIT experiment. Trichloroethylene,

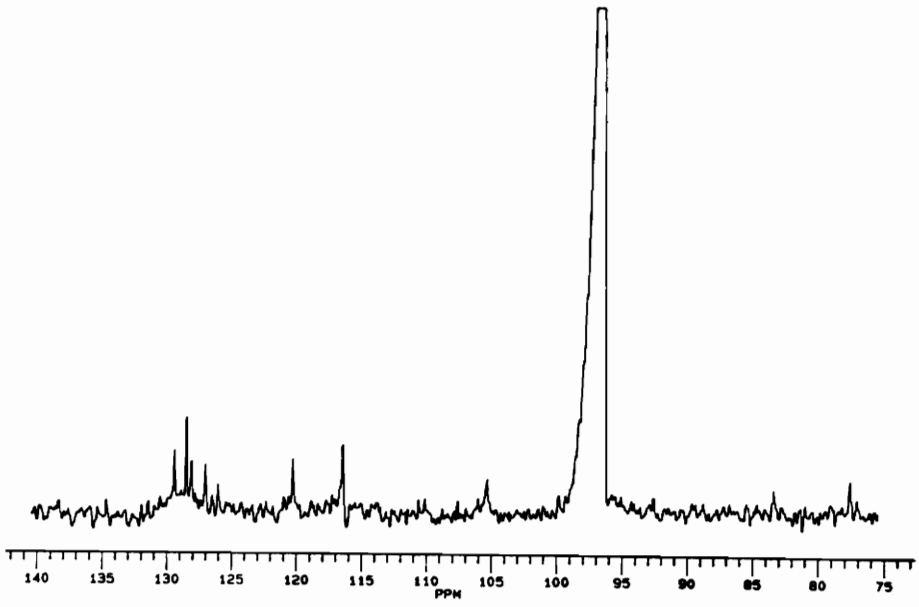

Figure 6.24 Solid-Liquid Intermolecular Transfer (SLIT) experiment for Test Mixture A. ^{13}C NMR spectrum with DNP from recycling the mix for just 56 scans at a flow rate of 3.5 mL/min with an elapsed time of **only 3½ min.**

tetrachloroethylene, hexachloroethane, chloroform, and 1,3,5-trichlorobenzene ^{13}C NMR signals were observed - albeit with a poor S/N. Yet another indication of the power of DNP is evident by noting the intense CCl_4 solvent peak which is quite large for only 3½ minutes of experimental time. Again, the detector cell flush time was 2.57 seconds with a delay between r.f. pulses of 3.50 seconds.

6.3.4 LLIT recycle experiments.

As a brief introduction to the LLIT experiment,[48-50] a free radical (e.g. TEMPO) is dissolved in a solution containing analytes, with the radical being present in both the low field where DNP occurs and the high field where NMR detection is performed. This is unlike the SLIT experiment where the radical is immobilized in the low field region and therefore is absent in the high field magnet. The primary variables to control in the LLIT experiment for obtaining maximum DNP signal enhancements are (1) flow rate, (2) radical concentration in solution, and (3) magnitude of the low field (B_o^L) strength.

In the presence of a free radical, the ^{13}C relaxation times (T_1) are reduced. The shorter this "new" relaxation time, the faster the flow rate must be in the LLIT experiment to transfer the polarized bolus to the high magnetic field for detection. Thus, the transfer time (amount of time the sample bolus resides between the low and high field) must be very short to avoid losing DNP enhanced NMR signals from those compounds with too short a relaxation time. Thus, for certain compounds (e.g. $CHCl_3$), the flow rate must be extremely rapid. However, if the flow rate is too rapid, then a potential reduction in the NMR signal intensity arising from a lack of premagnetization build-up and/or broadening of the signal at half-height will occur.

The second variable to control in the LLIT experiment is the concentration of free radical in solution. By manipulating the radical concentration, scalar and/or dipolar enhancements can either be increased or decreased to the extent that the NMR signal for certain compounds can be suppressed. For example, the relaxation time of chloroform is quite short in the presence of TEMPO, and the flow rate should therefore be high. At significantly high radical concentrations, the ^{13}C NMR signal for

chloroform will **not be observed**; whereas at very low radical concentrations the signal can be observed. It should be noted that as the concentration of radical decreases, there is a concomitant reduction in the magnitude of the DNP enhancement.[48]

A third variable to consider in the LLIT experiment is the magnitude of the microwave B_1 field. DNP enhancements are dependent on the extent of saturation of the electron spins, and optimization of this variable permits better polarization transfer from the electron to the nuclear spin.

It should be noted that the presence of radicals in the LLIT experiment will automatically suppress NOE's.

Figure 6.25 is the resulting ^{13}C NMR spectrum for a LLIT experiment with experimental conditions being optimized for compounds such as chloroform with the shortest ^{13}C relaxation times (T_1). Thus, a high flow rate and a low radical concentration of 0.00102 M TEMPO was employed. Recyling the test mixture at a flow rate of 5.2 mL/min with 896 scans for an elapsed time of 69 minutes was performed. The most obvious feature of the spectrum is the poor signal-to-noise ratio of all the compounds in general and is most likely due to a combination of the rapid flow rate and the low

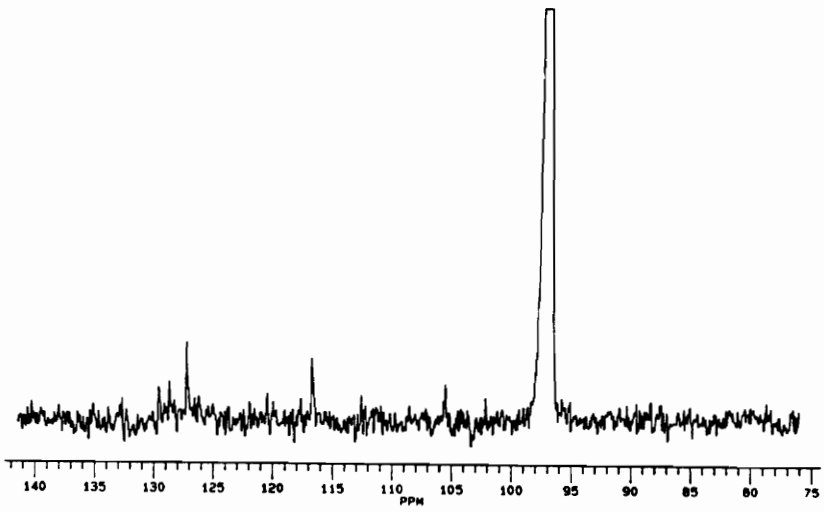

Figure 6.25 Liquid-Liquid Intermolecular Transfer (LLIT) experiment for Test Mixture A. ^{13}C NMR spectrum with DNP from recycling the mix for 896 scans at a flow rate of **5.2 mL/min** with an elapsed time of **69 min.** Concentration fo the free radical in solution is 0.00102 M TEMPO.

concentration of radical in solution. Enhancements are significantly reduced at low radical concentrations. The chloroform peak was **not** observed even under these conditions. However, other compounds present in trace amounts such as hexachloroethane, trichloroethylene, and tetrachloroethylene **do exhibit** NMR signals which can be detected. Of the compounds present in large amounts, chlorobenzene can be observed. However, benzene is **not** observed and is possibly due to the presence of a three-spin effect.

To determine whether the chloroform signal was not being observed due to transfer losses, the flow rate for the next SLIT experiment was increased from 5.2 mL/min to 7.2 mL/min. Figure 6.26 reveals the resulting spectrum after 896 scans, and none of the compounds exhibit signals with a sufficient signal-to-noise ratio which would imply that the poor signal-to-noise arises from a lack of premagnetization build-up before sampling with a r.f. pulse and **not** from a loss in DNP since the solvent peak has a relatively high signal-to-noise ratio.

A summary of the effect of flow rate on the resulting DNP enhanced NMR signals for a given free radical concentration is illustrated in Figure 6.27.

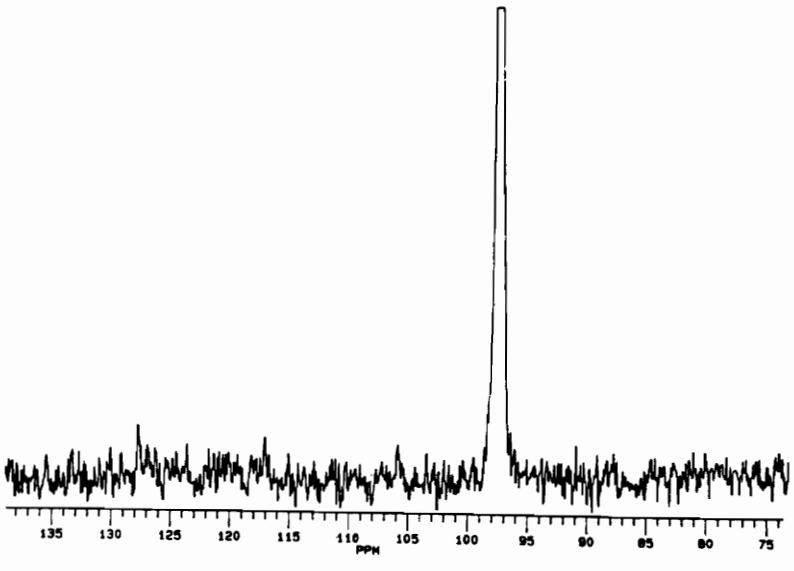

Figure 6.26 Liquid-Liquid Intermolecular Transfer (LLIT) experiment for Test Mixture A. ^{13}C NMR spectrum with DNP from recycling the mix for 896 scans at a flow rate of **7.2 mL/min** with an elapsed time of **40 min.** Concentration of the free radical in solution is 0.00102 M TEMPO.

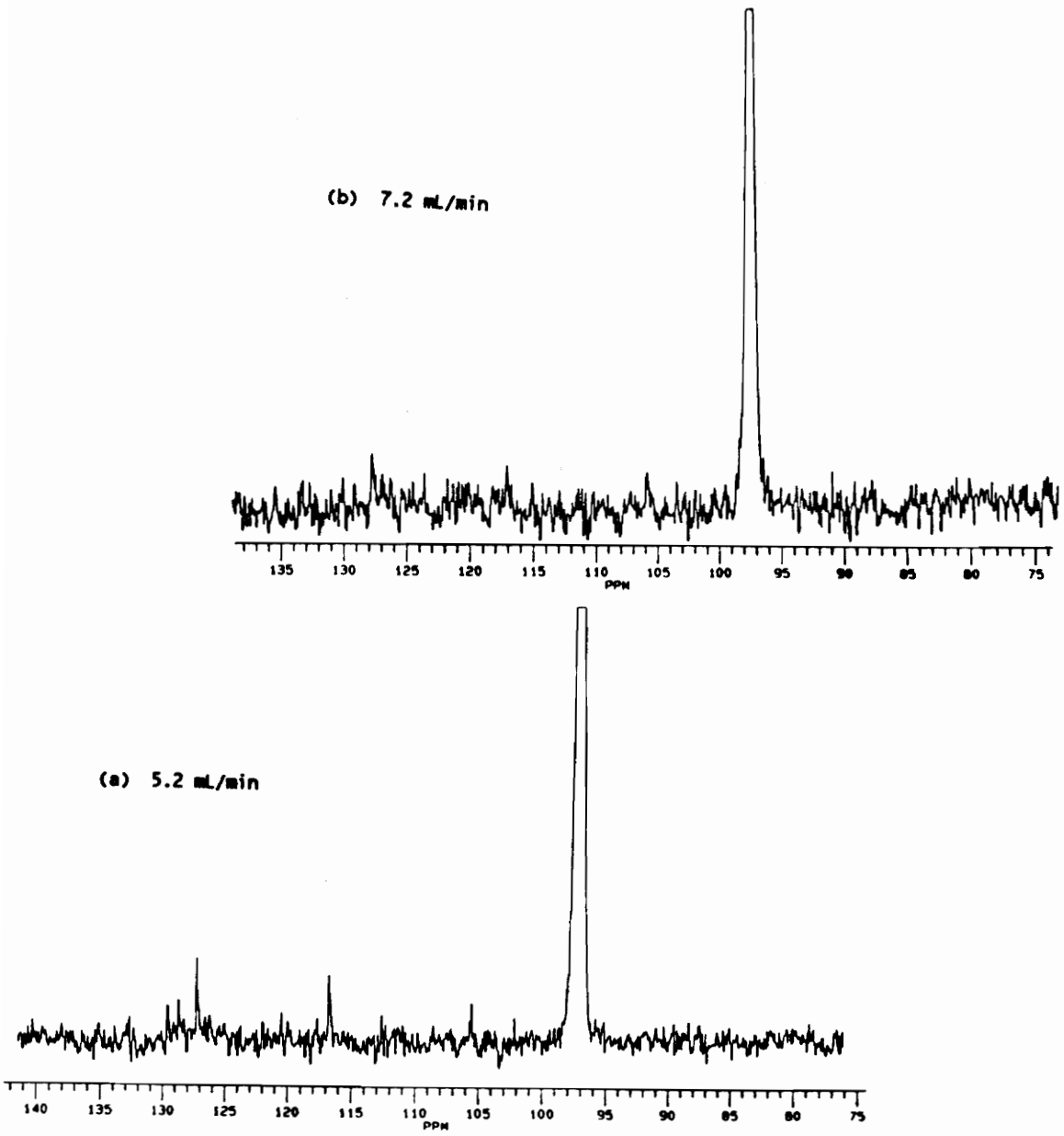

Figure 6.27 Liquid-Liquid Intermolecular Transfer (LLIT) experiment for Test Mixture A. ^{13}C NMR spectrum with DNP from recycling the mix for 896 scans at a flow rate of (a) 5.2 mL/min and (b) 7.2 mL/min. Concentration of the free radical in solution is 0.00102 M TEMPO.

Next, the concentration of TEMPO was increased from 0.00102 M to 0.00201 M with a flow rate of 5.2 mL/min as illustrated in Figure 6.28. In effect, a comparison between Figure 6.25 and Figure 6.28 can be made with the only variable being a factor of 2 increase in the radical concentration. Figure 6.28 reveals a significant improvement in signal-to-noise versus Figure 6.25. Benzene, chlorobenzene, 1,3,5-trichlorobenzene, and trichloroethylene exhibit increases in signal-to-noise whereas hexachloroethane and tetrachloroethylene (fully substituted alkanes and alkenes) show **no significant improvement** in signal-to-noise with the factor of two increase in radical concentration. As expected, the NMR signal of chloroform is still not observed because of the known short relaxation time and poor transfer efficiency from the low to the high field.[48]

In the next LLIT experiment, the concentration of radical was increased from 0.00201 M TEMPO to 0.00378 M TEMPO with a small reduction in flow rate from 5.2 mL/min to 4.5 mL/min as in Figure 6.29. The resulting spectrum does not reveal a significant improvement in signal-to-noise with the exception of the carbon signal from positions #'s 2,4,6 of 1,3,5-trichlorobenzene, with the exception of the

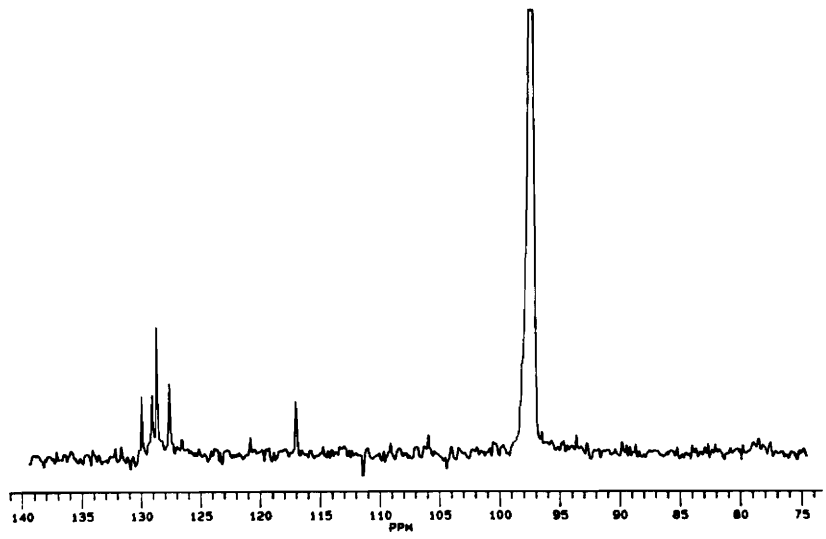

Figure 6.28 Liquid-Liquid Intermolecular Transfer (LLIT) experiment for Test Mixture A. ^{13}C NMR spectrum with DNP from recycling the mix for 896 scans at a flow rate 5.2 mL/min with an elapsed time of 58 min. Concentration of the free radical in solution is 0.00201 M TEMPO.

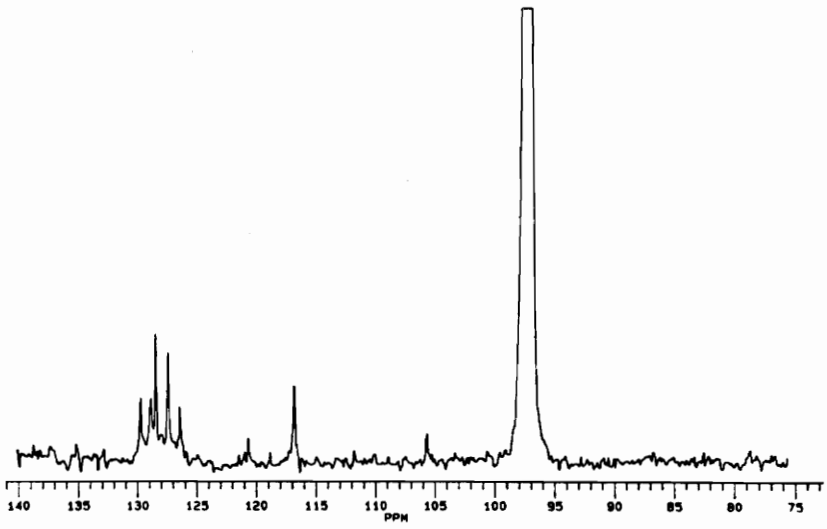

Figure 6.29 Liquid-Liquid Intermolecular Transfer (LLIT) experiment for Test Mixture A. ^{13}C NMR spectrum with DNP from recycling the mix for 896 scans at a flow rate of 4.5 mL/min with an elapsed time of 51 min. Concentration of the free radical in solution is 0.00378 M TEMPO.

hexachloroethane NMR signal, and with the exception of one of the carbon signals from position #4 of chlorobenzene. Overall, there is not a significant change in signal-to-noise.

As the concentration of radical increases to 0.0105 M TEMPO, **significant improvements in signal-to-noise were observed.** Figure 6.30 reveals the resulting ^{13}C NMR spectrum of the test mixture for 896 scans and is representative of only 56 minutes in experimental time. This spectrum reveals (1) increases in signal-to-noise of all compounds with the exception of benzene, and (2) more importantly, the emergence of several ^{13}C NMR signals which were not previously observed at lower radical concentrations. For example, the signal from carbon nuclei at position #'s 1,3,5 of trichlorobenzene as well as the carbon atoms at position #1 of chlorobenzene can now be observed. In addition, the emergence of the hexachlorobenzene signal at 132.5 ppm is now detected with the LLIT experiment albeit with a relatively low signal-to-noise ratio. However, note that the hexachlorobenzene signal was never observed with the SLIT recycle experiment. The benzene signal is no longer observed under these particular conditions and is most likely due to the transition of an otherwise positive signal to the

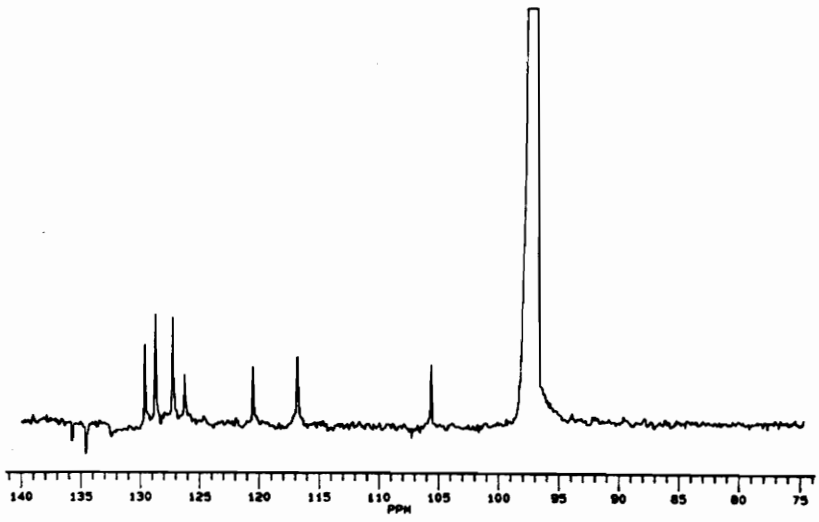

Figure 6.30 Liquid-Liquid Intermolecular Transfer (LLIT) experiment for Test Mixture A. ^{13}C NMR spectrum with DNP from recycling the mix for 896 scans at a flow rate of 5.2 mL/min with an elapsed time of 54 min. Concentration of the free radical in solution is 0.0105 M TEMPO.

negative, emission signal of a dipolar dominated signal of an opposite sign (+ to -). In addition, the NMR signals of hexachloroethane and tetrachloroethylene experience large enhancements.

Another LLIT experiment was performed where the radical concentration was increased from 0.0105 M TEMPO to 0.0179 M TEMPO with the flow rate being held constant at 5.2 mL/min. Figure 6.31 reveals the resulting carbon NMR spectrum which **demonstrate yet another significant increase in the signal-to-noise ratio.**

Compounds whose signals exhibit the largest improvements in signal-to-noise are 1,3,5-trichlorobenzene, chlorobenzene, hexachlorobenzene, benzene, tetrachloroethylene, and hexachloroethane. Benzene, which was not observed and at a null in the previous spectrum, is now observed as a large negative signal at 128.5 ppm since the dipolar dominated contribution the the NMR signal is now larger and more negative. At this point, all compounds in the test mixture are observed under these conditions with the lone exception of chloroform - whose DNP enhanced NMR signal is not expected to be observable at high radical concentrations.

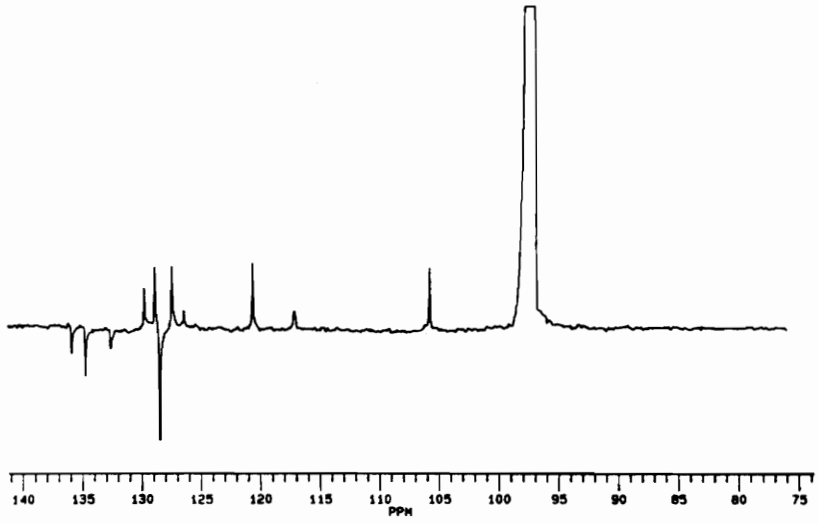

Figure 6.31 Liquid-Liquid Intermolecular Transfer (LLIT) experiment for Test Mixture A. ^{13}C NMR spectrum with DNP from recycling the mix for 896 scans at a flow rate of 5.2 mL/min with an elapsed time of 54 min. Concentration of the free radical in solution is 0.0179 M TEMPO.

To demonstrate the potential power of utilizing DNP for recycle ^{13}C NMR experiments, only **11½ minutes** (192 scans) of experimental time was necessary to obtain the ^{13}C NMR spectrum of Figure 6.32. Although the signal-to-noise is poorer, NMR signals can still be observed for 1,3,5-trichlorobenzene, chlorobenzene, hexachlorobenzene, benzene, tetrachloroethylene, trichloroethylene, and hexachloroethane. Thus, compounds present in both large quantities and trace amounts are still observable. As previously discussed, chloroform is not detectable.

A summary of the influence of free radical concentration on the resulting DNP enhanced NMR signals at a fixed flow rate is summarized in Figure 6.33.

6.3.5 Summary.

In summary, all eight compounds in the test mixture were observed when both SLIT and LLIT experiments were employed. The **SLIT** recycle experiment revealed seven of the eight compounds in the test mix with the lone exception being hexachlorobenzene whereas the **LLIT** recycle experiment also detected seven of the eight compounds in the test mix - but this time with the exception of chloroform.

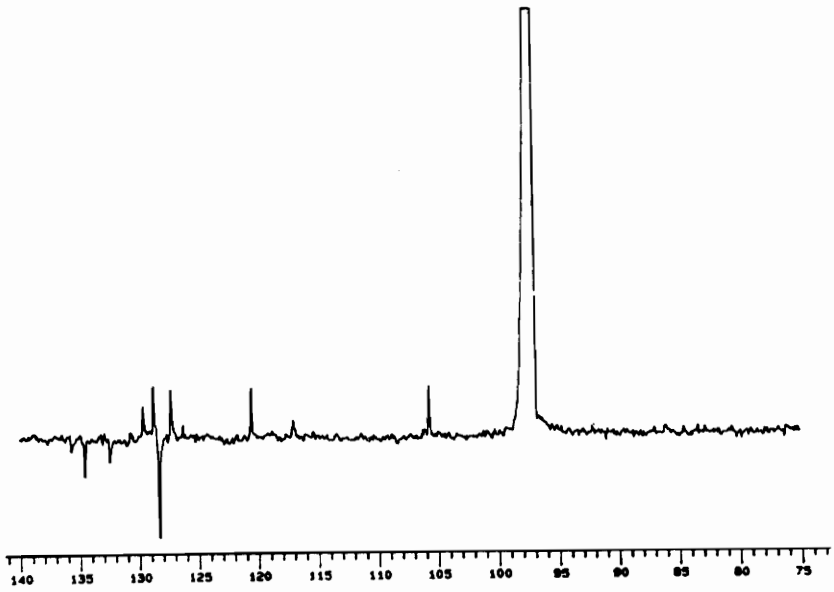

Figure 6.32 Liquid-Liquid Intermolecular Transfer (LLIT) experiment for Test Mixture A. ^{13}C NMR spectrum with DNP from recycling the mix for **192 scans** at a flow rate of 5.2 mL/min with an elapsed time of **only 11½ min.** Concentration of the free radical in solution is 0.00179 M TEMPO.

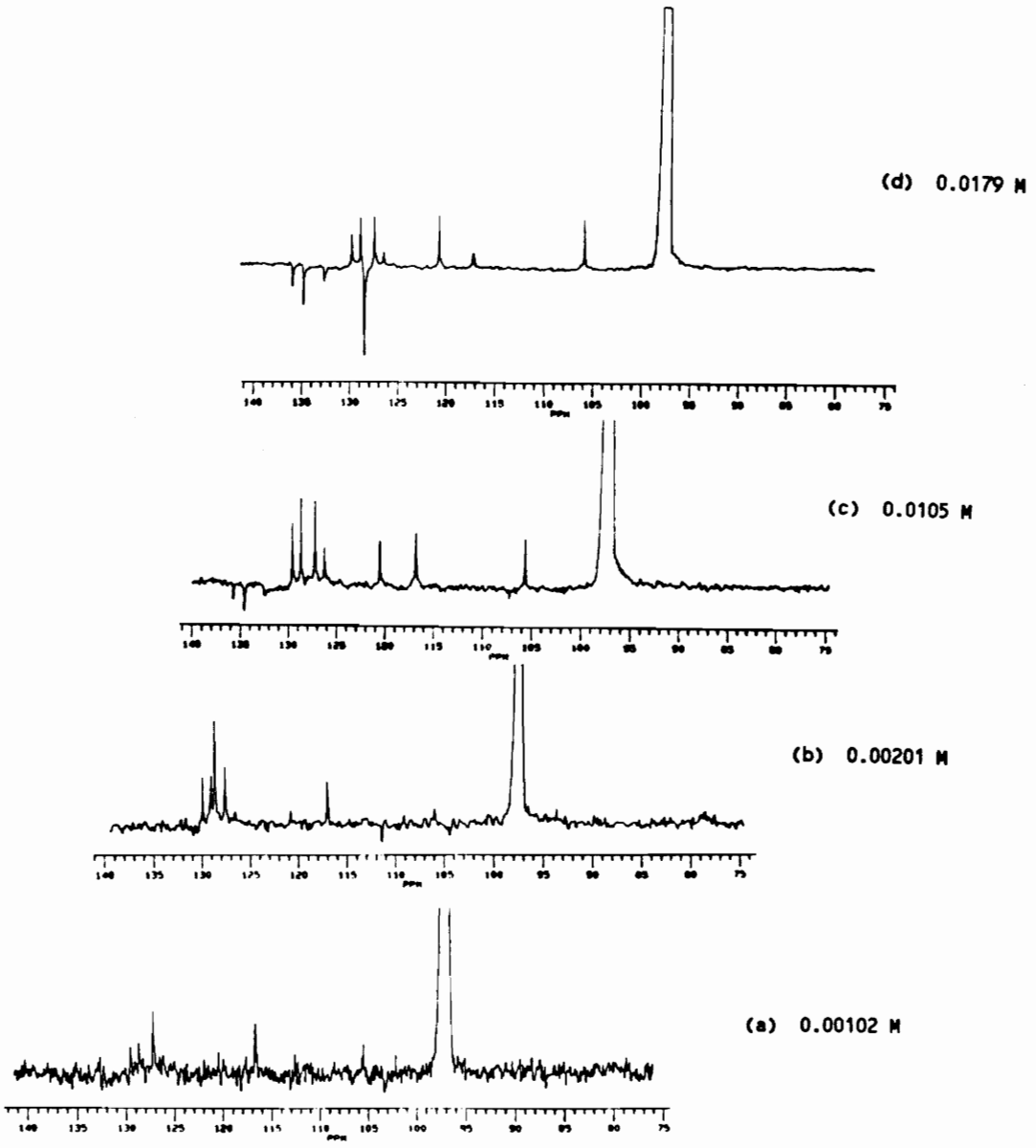

Figure 6.33 Liquid-Liquid Intermolecular Transfer (LLIT) experiment for Test Mixture A. ^{13}C NMR spectrum with DNP from recycling the mix for 896 scans a at a flow rate of 5.2 mL/min at the following concentrations of TEMPO: (a) 0.00102 M, (b) 0.00201 M, (c) 0.0105 M, and (d) 0.0179 M.

The **SLIT** experiment would typically favor scalar dominated NMR signals while the intensity of dipolar dominated signals was significantly diminished. In contrast, **LLIT** experiments were, in general, more amenable to both dipolar and scalar dominated enhancements. However, the LLIT experiment does not appear to be favorable for scalar dominated enhancements for ^{13}C nuclei (e.g. $CHCl_3$) with too short a relaxation time, (T_1).

CHAPTER 7: FUTURE DEVELOPMENTS

7.1 Obtaining larger signal enhancements.

7.1.1 Higher field strength.

The transition from lower to higher magnetic field strengths would be expected to yield an increase in signal-to-noise. The maximum theoretical gain in signal height is proportional to the 7/4 power of the magnetic field strength. Thus, a change from a magnetic field strength of 4.7 T to 9.4 T would theoretically result in a relative gain in signal-to-noise by a factor of 3.4 over existing DNP enhancements.

7.1.2 Instrumental design.

Contributions from improvements in instrumental design could further assist ^{13}C NMR as a LC detector and could shorten experimental time for both the SLIT and LLIT recycle

experiments by providing a higher signal-to-noise ratio in a shorter amount of time. Installation of a solenoid coil with the addition of shim coils could yield improvements[62] by a factor of 4 over the conventional Helmholtz coil design. Another improvement in signal-to-noise by factors of 2 - 4 could be obtained by cooling the NMR detection coil to liquid helium temperatures but thermally isolating the sample cell.[64] Further improvements in signals by factors of 4 - 10 could be obtained by utilization of state-of-the-art electronics in our NMR spectrometer and home-built flow probe which are approximately 10 years old at this point. In addition, placement of the chromatographic column inside the bore of the low field magnet would yield an improvement in signal-to-noise by premagnetizing the carbon nuclei being separated while still inside the column. This strategic placement of the chromatographic column could obviate the need for a large, dead volume preequilibration region and consequently reduce band broadening and thereby improve the efficiency of the chromatographic separation.

7.1.3 Dual microwave cavity.

Further improvements in signal-to-noise could be expected with the addition of a dual microwave cavity.[48]

With a dual cavity, experiments involving the SLIT technique could yield a higher signal-to-noise since more SPIN (Silica Phase Immobilized Nitroxide) radical would be exposed to the microwave field and interact with the sample so that potentially larger DNP enhancements by at least a factor of 2 could then be expected.

7.1.4 Inverse detection.[68-72]

The employment of inverse detection would serve to further increase gains in signal-to-noise. Inverse polarization transfer experiments ($^{13}C \rightarrow {}^{1}H$) utilize detection of ^{13}C nuclei via the ^{1}H channel and are more sensitive by a maximum theoretical factor of $(\gamma_H/\gamma_C)^{3/2}$ when compared with experiments with direct observation of the ^{13}C nucleus (without NOE). Potential enhancements of up to a factor of ten could be expected. The coupling of improvements in signal-to-noise arising from inverse detection with the enhancements from utilizing DNP would significantly improve the sensitivity of ^{13}C NMR detection. However, inverse detection does depend on molecules with attached hydrogens at the carbons of interest.

7.1.5 Summary.

In conclusion, a combination of the aforementioned methods for attaining a higher signal-to-noise ratio coupled to the large enhancements which DNP has been shown to provide would have yielded a significant reduction in detection limits and injection volumes in the LC - ^{13}C NMR experiments performed in this thesis. In this case, LC - ^{13}C NMR would approach the sensitivity of LC - ^{1}H NMR separations. In addition, both the SLIT and LLIT recycle experiments would have experienced a further reduction in experimental time. It is anticipated that additional improvements by one to two orders of magnitude are clearly feasible.

REFERENCES

1. Suryan G., Proc. Indian Acad. Sci, Sec. A, 15, 153, (1951).

2. Forsen S. and Rupprecht J., J. Chem. Physics. E, 2, 292, (1969).

3. Arnold, D. and Burichart L., J. Applied Physics, 42, 938, (1971).

4. Hayward R. et al., Mol. Phys., 23, 1083 (1972).

5. Grover et al., J. Appled Phys., 42, 938, (1971).

6. Stejskal E., J. Chem Phys., 43, 3597, (1965).

7. Singer J., Science, 130, 1652 (1959).

8. McCormick W., Rev. Sci. Instrum., 40, 346, (1969).

9. Morse O. et al., Science, 170, 440, (1970).

10. Suryan G., Proc. Indian Acad. Sci, Sec. A, 15, 153, (1951).

11. Forsen S. et al., J. Chem Phys. E, 2, 292, (1969).

12. Zhernovoi A., NMR in a Flowing Liquid, New York, (1965).

13. Fyfe C. et al., J. Magn. Reson., 23, 377, (1976).

14. Fyfe C. et al., J. Am. Chem. Soc., 101, 951, (1979).

15. Fyfe C. et al., J. Am. Chem. Soc., 101, 956, (1979).

16. Grimaldie J. et al., J. Am. Chem. Soc., 94, 7641, (1972).

17. Albert K. et al., Z. Naturforsch, 39c, 859, (1984).

18. Watanabe N. et al., Proc. Jpn. Acad., 54, 194, (1978).

19. Bayer E. et al., J. Chromatogr., 186, 497, (1979).

20. Haw J. et al., Anal. Chem., 52, 1135, (1980).

21. Haw J. et al., Anal. Chem., 53, 2327, (1981).

22. Haw J. et al., Anal. Chem., 53, 2332, (1981).

23. Haw J. et al., JEOL News, 18A, #2, 58, (1982).

24. Haw J. et al., Anal. Chem., 55, 22, (1983).

25. Dorn H.C., Anal. Chem., 56, 747A, (1984).

26. Bayer E. et al., J. Chromatogr., 186, 497, (1979).

27. Bayer E. et al., Anal. Chem., 54, 1747, (1982).

28. Buddruss et al., Organic Magn. Reson., 13, #2, 153, (1980).

29. Buddruss et al., Anal. Chem., 55, 1611, (1983).

30. Albert et al., J. Chromatogr., 463, 355, (1989).

31. Albert et al., Anal. Chem., 61, 772, (1989).

32. Grenier-Loustalot M.F. et al., Analusis, 18, 200, (1990).

33a. Clore G. et al., J. Magn. Reson., 54, 170, (1983).

33b. Hore P.J., J. Magn. Reson., 55, 283, (1983).

33c. Bayer et al., J. Chromatogr., 186, 497, (1979).

34. Zhernonoi A., NMR in a flowing liquid., Consultants Bureau, New York, (1965).

35. Albert et al., Trends in Anal. Chem., 7, #8, 288, (1988).

36. Fyfe et al., J. Magn. Reson., 23, 377, (1976).

37. Albert et al., Magn. Reson. in Medicine, 11, 309, (1989).

38. Laude et al., Anal. Chem., 56, 2471, (1984).

39. Albert et al., J. Chromatogr., 463, 355, (1989).

40. Buddruss et al., Organic Magn. Reson., 13, #2, 153, (1980).

41. Haw et al., JEOL News, 18A, #2, 58, (1982).

42. Dorn et al., Anal. Chem., 56, 747A, (1984).

43. Bayer et al., Anal. Chem., 54, 1747, (1982).

44. Atta-ur-Rahman, One and 2-D NMR Spectroscopy, Elsevier, Amsterdam, (1989).

45. Dorn et al., Appl. Magn. Reson., 2, 9, (1991).

46. Tsai et al., Appl. Magn. Reson., 1, 231, (1990).

47. Dorn et al., J. Magn. Reson., 79, 404, (1988).

48. Tsai K.H., Dissertation, Virginia Tech, (1990).

49. Gitti R., Dissertation, Virginia Tech, (1991).

50. Gu J., Dissertation, Virtinia Tech, (1992).

51. Hausser K. et al., Adv. Magn. Reson., 3, 79, (1968).

52. Dwek R. et al., Ann. Rev. NMR Spectroscopy, 2, 293, (1969).

53. Natusch D. et al., Mol. Phys., 11, 421, (1966).

54. Hausser K. et al., J. Chem. Phys., 61, 204, (1964).

55. Albert K. et al., Magn. Reson. Chem., 25, 919, (1987).

56. Albert K. et al., Z. Naturforsch., 39c, 859, (1984).

57. Bayer E. et al., J. Chromatogr., 312, 91, (1984).

58. Albert K. et al., Magn. Reson. Medicine, 11, 309, (1989).

59. Albert K. et al., J. Chromatogr., 346, 17, (1985).

60. Laude D. et al., Anal. Chem., 57, 1286, (1985).

61. Laude D. et al., Anal. Chem., 57, 1281, (1985).

62. Zhang Y. et al., J. Magn. Reson., 87, 46, (1990).

63. Glass T.E. et al., J. Magn. Reson., 51, 527, (1983).

64. Styles P. et al., J. Magn. Reson., 60, 397, (1984).

65. Laude D. et al., Anal. Chem., 57, 1286, (1985).

66. Albert K. et al., J. Chromatogr., 346, 17, (1985).

67. Albert K. et al., Magn. Reson. in Medicine, 11, 309, (1989).

68. Ernst, Bodenhausen, Wokaun, Principles of NMR in One and Two Dimensions, in vol. 14, The International Series of Monographs in Chemistry, Clarendon Press, Oxford, 1990.

69. Bermel W., Bruker Reports, 30.

70. Martin, G. et al., J. Natural Products, 54, (1), pp. 1-70, (1991).

71. Bax A. et al., J. Magn. Reson., 67, 565, (1986).

72. Bax A. et al., J. Am. Chem. Soc., 108, 2093, (1986).

APPENDIX 1

TABLE OF CHEMICAL SHIFTS

Chloroform.....77.5 ppm

Carbon tetrachloride.....96.5 ppm

Hexachloroethane.....105.5 ppm

Tetrachloroethylene.....120.6 ppm

Trichloroethylene.....116.7 ppm

.....not observed at 124.2 ppm

1,1,1-trichlorotrifluoroethane.....

.....multiplet 133.5, 128.0, 122,4, 116.7 ppm

.....multiplet 97.4, 96.5, 95.5, 94.6 ppm

1,1,2-trichloro-1,2,2-trifluoroethane.....

.....multiplet 130.5, 129.8, 124.5, 123.8 ppm

.....multiplet 119.5, 118.6, 117.8, 113.5, 112.7, 112.0 ppm

Benzene.....128.5 ppm

Chlorobenzene.....134.5, 129.9, 128.8, 126.6 ppm

1,3,5-Trichlorobenzene.....135.8, 127.5 ppm

Hexachlorobenzene.....132.5 ppm

Hexafluorobenzene.....doublet 141.1, 136.1 ppm

VITA

Steven Alan Stevenson was born one of seven children on June 17, 1968 in Clearlake Highlands, California and raised as the son of a school teacher and housewife. He graduated from Angelo State University, San Angelo, Texas where a B.S. degree was received in the spring of 1990. Upon graduation, he departed to Blacksburg to continue an education in Analytical Chemistry at Virginia Polytechnic Institute and State University where he will receive a M.S. degree in the fall of 1992.